24

Geological subsurface models of the Netherlands

Jan Stafleu, Freek S. Busschers, Michiel J. van der Meulen, Maryke den Dulk, Jan L. Gunnink, Denise Maljers, Jan H. Hummelman, Jeroen Schokker, Ronald W. Vernes, Jelte Stam, Willem Dabekaussen, Johan H. ten Veen, Hans Doornenbal, Romée Kars & Renée de Bruijn*

*Corresponding author: jan.stafleu@tno.nl

ABSTRACT

TNO – Geological Survey of the Netherlands, builds and maintains a suite of 3D national subsurface models. Down to a depth of about 7 km, DGM-deep maps Carboniferous to Neogene seismo-stratigraphic horizons, using exploration data that energy and mining companies must submit to the Survey under the Mining Act. Down to about 500 m, the country is covered by the layer-based models DGM and REGIS II. DGM maps the geometries of Neogene to Quaternary lithostratigraphic units. REGIS II further subdivides DGM into hydraulically parameterized hydrogeological units and is essential to regional groundwater flow models. Down to a depth of 50 m below mean sea level (NAP), the multi-purpose GeoTOP model maps both lithostratigraphy and lithology of the shallow subsurface in a detailed 3D voxel model. A fourth set of models addresses the Quaternary stratigraphic record of the North Sea down to a depth of ca. 30 m below the seabed.

This chapter describes input data and interpretation, modelling approaches and the general application of each of the models. An assessment of model uncertainties is included because the models are constructed using point and/or line observations each of which has a specific spatial density and quality. Next, the effects of the key registry of the subsurface (BRO) on the modelling approach with a focus on quality control is described. Later, the visualization of the models on web portals and in stand-alone software packages is described and is followed by a number of case studies presenting innovative methods. The chapter concludes with perspectives for systematic modelling in the Netherlands.

<< Artist impression showing several Dutch 3D subsurface models (not to scale). The top part of the figure shows a voxel model based on boreholes. At greater depths, lithostratigraphic surfaces and seismostratigraphic horizons are based on boreholes and seismic data.

DOI: 10.5117/9789463728362_ch24

Introduction

TNO – Geological Survey of the Netherlands (TNO-GDN) focuses on the sustainable use and management of the subsurface in the Dutch on- and offshore. One of TNO-GDN's primary tasks is to map the architecture and properties of the subsurface, and to make this data available to the public domain. For the deeper subsurface the management and utilization of information is governed by the Mining Act (Rijksoverheid, 2002), while for the shallow subsurface a new key registry was implemented in 2015 (Van der Meulen et al., 2013; Rijksoverheid, 2015). This key registry is a national database for subsurface data and information, which the Dutch government bodies are obliged to use when making policies or decisions related to the subsurface.

From about the year 2000 onward, following a long history of systematic mapping since the 1960s, TNO-GDN and its predecessor *Nederlands Instituut Toegepaste Geowetenschappen van TNO* (NITG-TNO), replaced its analogue geological mapping projects by digital subsurface modelling procedures (see Van der Meulen et al. (2013) for an overview). Modelling is primarily carried out using borehole and seismic data and, depending on depth, at different resolutions. At present, TNO-GDN runs three subsurface mapping programmes with four national models in total which are all data-driven and stochastic in nature (Stafleu et al., 2019) (Fig. 24.1):

- Down to a depth of ca. 10 km, the Digital Geological Model for the deep subsurface (DGM-deep) programme maps Carboniferous to Neogene seismostratigraphic horizons, using exploration data that energy and mining companies must submit to GDN under the Mining Act.
- Down to a depth of ca. 500 m, the Digital Geological Model for the shallow subsurface (DGM) and the Regional Groundwater Information System II (REGIS II) programmes map the geometries and hydrological characteristics of the Neogene, Pleistocene and Holocene stratigraphic record (Gunnink et al., 2013a). The lithostratigraphic DGM is used for applications requiring geological information. Its primary purpose is to serve as the framework for the REGIS II model, which subdivides DGM lithostratigraphic units into hydraulically parameterized hydrogeological units (Vernes & Van Doorn, 2005; Vernes et al., 2021). REGIS II is the *de facto* hydrogeological standard used in groundwater flow models and other assessments for Dutch water and environmental authorities.
- Down to a depth of 50 m below NAP (Dutch Ordnance Datum, approximately mean sea level - MSL), the GeoTOP programme maps the lithostratigraphy and lithology of the Neogene, Pleistocene and Holocene stratigraphic record in a 3D voxel model (Stafleu et al., 2011a, 2021a). Lithological variation within the lithostratigraphic layers is mapped in great detail. GeoTOP is a multi-purpose model supporting a number of applications involving the shallow subsurface, for example the planning of large infrastructural works, land subsidence predictions, groundwater flow studies and site-response assessments of induced earthquakes. GeoTOP currently covers ca. 70% of the surface area of the Netherlands. In areas where GeoTOP is not yet available, the less detailed voxel model NL3D (Van der Meulen et al., 2013) can be used. Another example of a 3D voxel model with national coverage is TNO-GDN's aggregate resources model (Van der Meulen et al., 2025, this volume).

A fourth set of models addresses the Pleistocene and Holocene stratigraphic records of the North Sea to a depth of ca. 30 m below the seabed. These models are more application oriented than the ones mentioned above. Sand resource models such as DIS (Maljers-Oosterwijk et al., 2014; TNO-GDN, 2022a) and TILES (Hademenos et al., 2019; Van Lancker et al., 2019) are constructed for sand extraction purposes and cover a zone of up-to ca. 12 km seaward of the coastline.

3D modelling at TNO-GDN is primarily data-driven, placing it on the implicit end of the modelling spectrum (Stafleu et al., 2019). In implicit models, geological concepts such as the layering sequence and layer contact types are implemented in specialized modelling software (e.g. Isatis®, Petrel®) and automated modelling workflows (Russell et al., 2019). Furthermore, implicit modelling relies on computer algorithms (e.g. kriging, indicator simulation) to model layer boundaries (tops and bases) and layer properties (e.g. lithology, hydraulic conductivity). It is a complex approach involving many steps that have to be completed each time the model is recreated using new data or new geological insights (Fig. 24.2). However, the emphasis on data and computer algorithms does not imply that explicit geological knowledge is not used. Interpretation of boreholes, wells and seismic data as well as mapping of the spatial extent of geological units still strongly relies on the manual implementation of geological concepts by geologists, as is the case in explicit geological modelling (Russell et al., 2019). This is even the case for the development of automated stratigraphic interpretation routines for GeoTOP, where geologists with programming skills implement geological concepts in Python-code.

The next section describes input data and interpretation, modelling approaches and general application of each of the four models. An assessment of quantification of the model uncertainties is included because the models are constructed using point and/or line observations that each have a specific spatial density and quality, and also

because predictions are made using a flow of different stochastic (interpolation) algorithms. The effects of the key registry of the subsurface on the modelling approach with a focus on Quality Control (QC) is described in the third section of this chapter. Subsequently, the presentation of the models on the different web portals and by using stand-alone software packages is described, followed by a number of applications in which innovative methods were used that will be implemented in future updates of the models. The chapter concludes with perspectives for systematic modelling in the Netherlands.

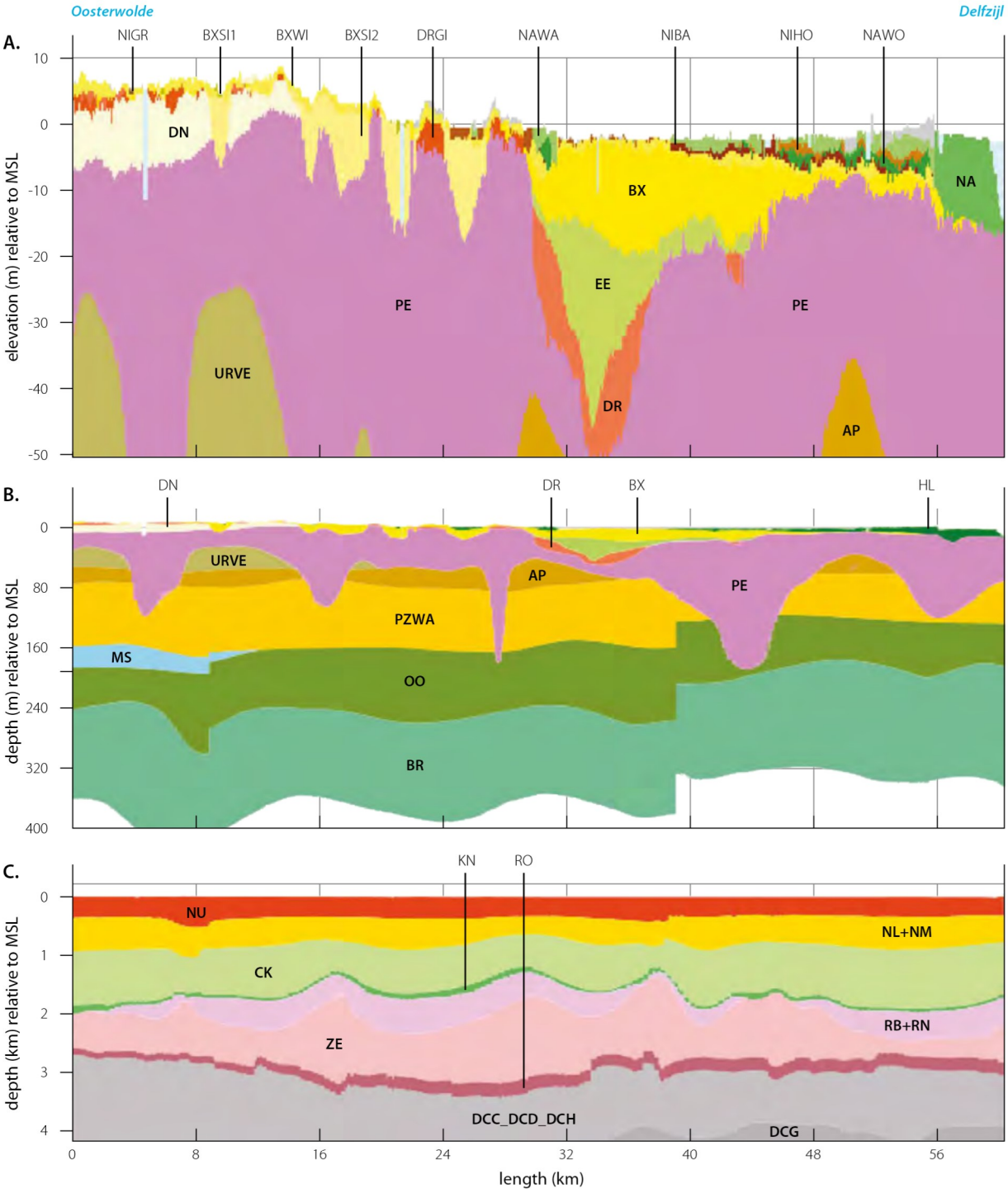


Figure 24.1. *Stratigraphic cross-sections through three of the four national subsurface models in the Groningen area (north-eastern Netherlands). a) GeoTOP; b) DGM; c) DGM-deep. The cross-sections were created using the DINO-web portal (www.dinoloket.nl/en). The abbreviations for groups, formations and members are explained on the portal and in Kruiver et al. (2017b, their Table 1). Modified after Kruiver et al. (2017b).*

The national models

DGM-model for the deep subsurface

The deep mapping programme was the first systematic modelling effort undertaken by the Geological Survey of the Netherlands. In 1985, the Survey was commissioned to compile a consistent, regional-scale petroleum geological framework. Geological horizons, ranging from Permian to Neogene in age, were mapped, the results of which were first published on paper and later became the constituents of a stacked layer model now referred to as DMG-deep (Figs 24.1c, 24.2; Duin et al., 2006; Kombrink et al., 2012; Van der Meulen et al., 2013). The model is based on 2D and 3D seismic survey data, combined with a variety of well data, and supported by biostratigraphic, petrophysical and geochemical analyses. Attribution of hydrocarbon and later of geothermal reservoirs relies on well data as well as burial history analysis and basin modelling techniques. The latter approach is used to predict maturation levels of source rock, as well as reservoir and seal properties (porosity, permeability, geothermal gradients). The general approach and workflow of the deep mapping programme correspond to those of the hydrocarbon exploration and production industry, but on a regional instead of a reservoir scale.

The modelling of the deep subsurface relies on the combined interpretation of seismic amplitude data and exploration well data (Fig. 24.2). Seismic surveys are ideal for observing the subsurface layer structure including faults at depths of up to several kilometres. A seismic dataset can either be acquired in 2D (cross-section) or 3D (cube) and the penetration depth depends largely on the acquisition parameters of the survey.

TNO-GDN hosts the national geophysical database that contains all seismic data acquired and made public under the Dutch Mining Act. Data delivered to TNO-GDN is so-called post-stack time migrated data, which is the first processing result obtained after stacking and migrating the signal data. In seismic data, depth is recorded in travel time between the generation of the wave at the source and the return of the reflected wave at the receiver. The true depth can only be obtained when the seismic velocity of the rock intervals is known. This velocity depends on many factors (e.g. lithology, fluid content and compaction) and generally increases with depth, but can vary significantly per layer. As velocity measurements are often sparse, the true depth is generally one of the biggest sources of uncertainty in seismic interpretation.

Whereas the seismic data provides information on geometries, well data (especially interpreted well stratigraphy or well tops) help to ground-truth the seismic interpretation by providing lithostratigraphic information in true depth. Depending on the stratigraphic level concerned, 600-3500 wells are available to constrain the seismic interpretation. A good seismic-to-well tie is essential for the interpretation of seismic reflectors that represent geological boundaries. Petrophysical well log data pertaining to sonic velocities and densities, i.e. the two quantities that define acoustic reflection strength, are commonly used to generate synthetic seismograms that can be compared with the real seismic data in order to establish an optimal seismic-to-well tie.

Over several decades, the Geological Survey executes such well-constrained seismic interpretations (TNO-NITG, 2004; Duin et al., 2006; Kombrink et al., 2012) for both nationwide and regional studies, on- and offshore. Over 95% of the publicly available 3D-surveys were used in the interpretation (Fig. 24.3) and all non-confidential wells were consulted. In general, every 10th to 20th inline and crossline in the 3D surveys is interpreted, correspond-

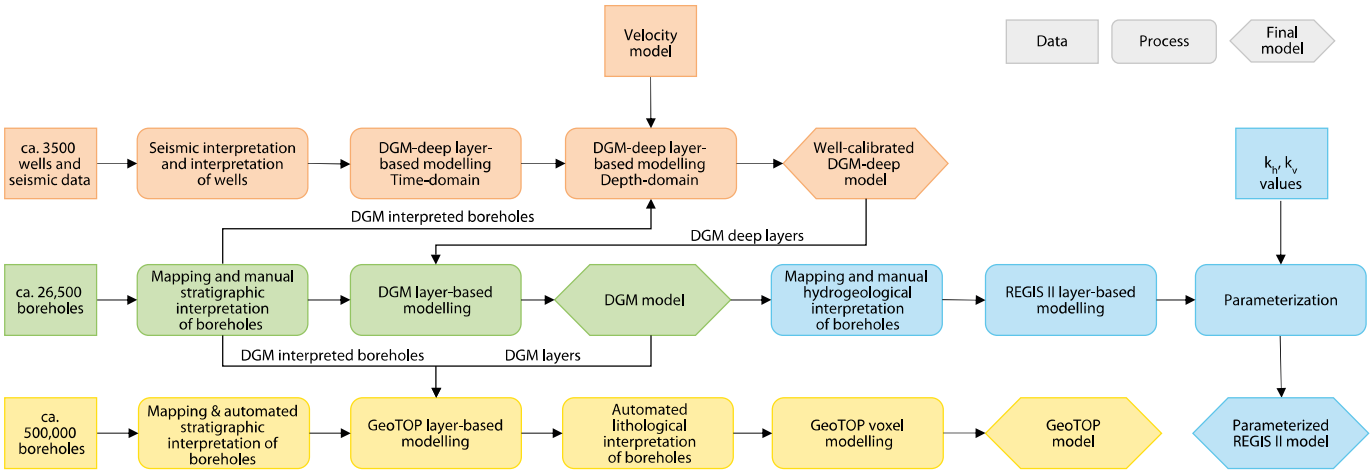


Figure 24.2. *Modelling approach for the four national subsurface models with the most important modelling steps involved. Also shown are the interdependencies between the models.*

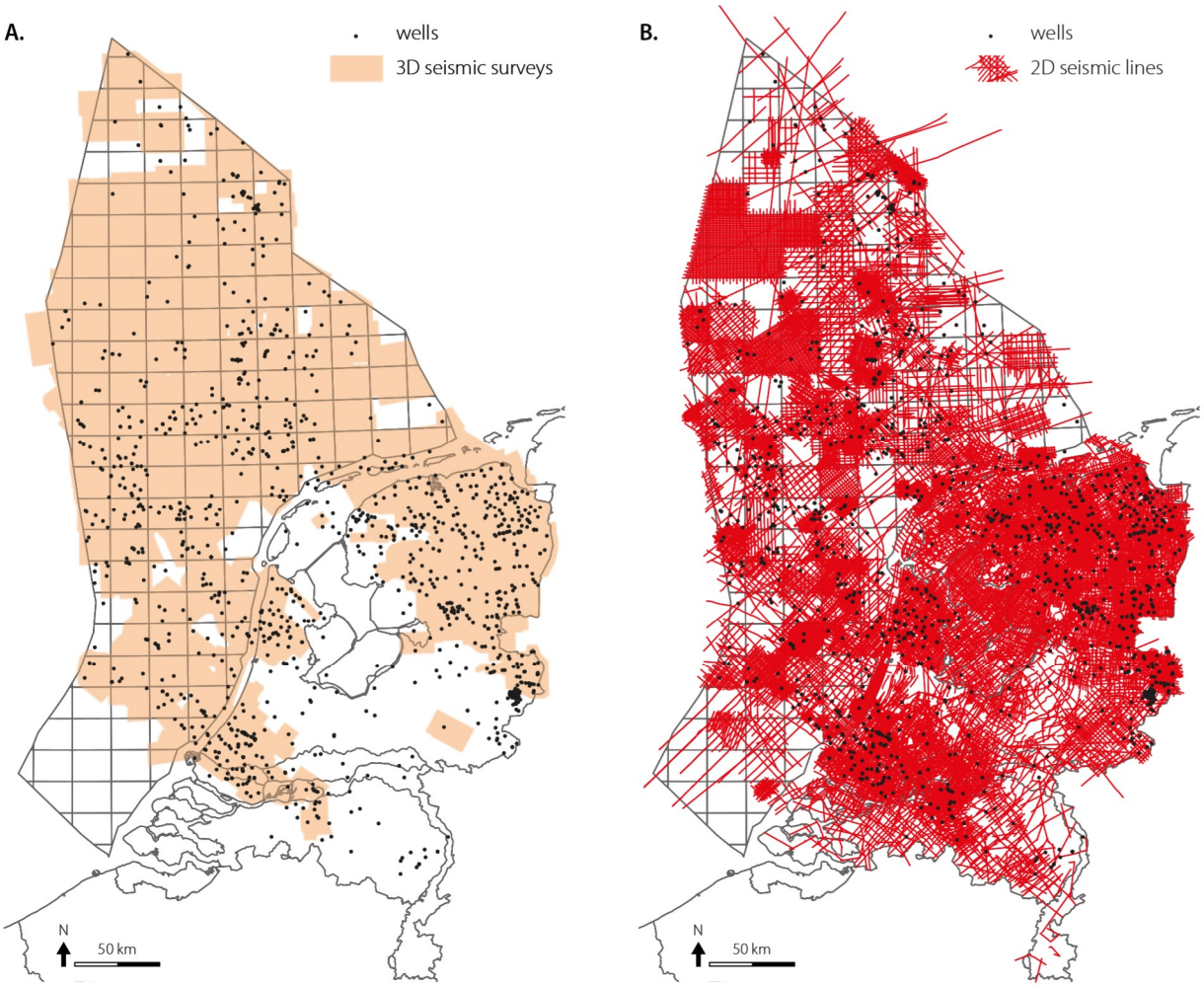


Figure 24.3. *Seismic and well coverage for the DGM-deep model.*

ing to a ca. 250 m resolution. 2D seismic data is used to fill in areas not covered by 3D seismic surveys. In some areas interpretations still originate from the early days of analogue ('paper') 2D seismic interpretations. The interpretations mainly focus on 13 stratigraphic levels that represent the (near) bases of the Paleozoic, Mesozoic, and Cenozoic lithostratigraphic groups (Fig. 24.4) as defined in the Stratigraphic Nomenclature of the Netherlands (TNO-GDN, 2022b). Faults that are evident in seismic data, i.e. faults that have a vertical offset larger than the seismic resolution, are interpreted as well.

Both the seismic interpretations and the well markers are used to produce the DGM-deep model, a stacked layer model of the deep subsurface of the Netherlands represented at 250 x 250 m grid resolution. In every new update of DGM-deep, newly available public data are incorporated. The latest 2019 version, DGM-deep v5, combines on- and offshore data into a single layer model (Fig. 24.4). Faults are modelled separately and are not part of the DGM-deep model. However, the ca. 6000 fault objects that result from the fault-modelling workflow (see Textbox 1) are implicitly used in the layer modelling process by taking into account the fault offset.

The applied modelling workflow initially produces time grids that are generated by interpolating seismic horizon picks using a convergent gridding algorithm in Petrel®. Subsequently, a conversion from the time domain to the depth domain is made using VELMOD 3.1, a velocity model built from well log and check-shot data (Van Dalfsen et al., 2005; Pluymaekers et al., 2017). After time-depth conversion, miss-ties between the generated depth grids and the well marker depths are analysed. Wells with high miss-ties, for instance those that are related to simplified model representations of complex geological features are filtered out. Subsequently, the remaining miss-tie values are interpolated with a kriging algorithm and the resulting well-residual grids are added to the depth converted grids to obtain a well-tied stratigraphic model, i.e. a model that acknowledges all selected well data (see also Kombrink et al., 2012).

In the southwest and easternmost part of the country, where Paleogene and Neogene units are close to the sur-

face, interpreted boreholes used for the DGM-model of the shallow subsurface are used to assist in the construction of the DGM-deep layer model. In these areas, the depth range of the North Sea groups is too shallow to be detected by exploration seismic data. The same applies to the southernmost part of the country where the Upper Cretaceous Chalk Group crops out or is at shallow depths.

A limitation of the modelling approach and the applied grid resolution is that structural complexity is poorly honoured, particularly around salt structures and reverse faults. For example, duplication of stratigraphy, as is the case near overhanging salt structures or reverse faults, is simplified to sub-vertical representations.

In the final modelling step, the model's uncertainty is addressed by calculating standard deviation grids resulting from stochastic simulations of those horizons that are based on seismic interpretation. DGM-deep uses assumptions of uncertainty in data quality as well as geological complexity that are incorporated in different model simulations by a stochastic simulation technique. Quantification of uncertainty in depth of the stratigraphic interfaces is based on the variation that is present between the different model runs (Fig. 24.5).

The DGM-deep model may be regarded as the national 3D geological map suitable for applications requiring geological information on the depth and distribution of consolidated rocks in the deeper subsurface (>1500 m). The lithostratigraphic layers in the model are linked to their

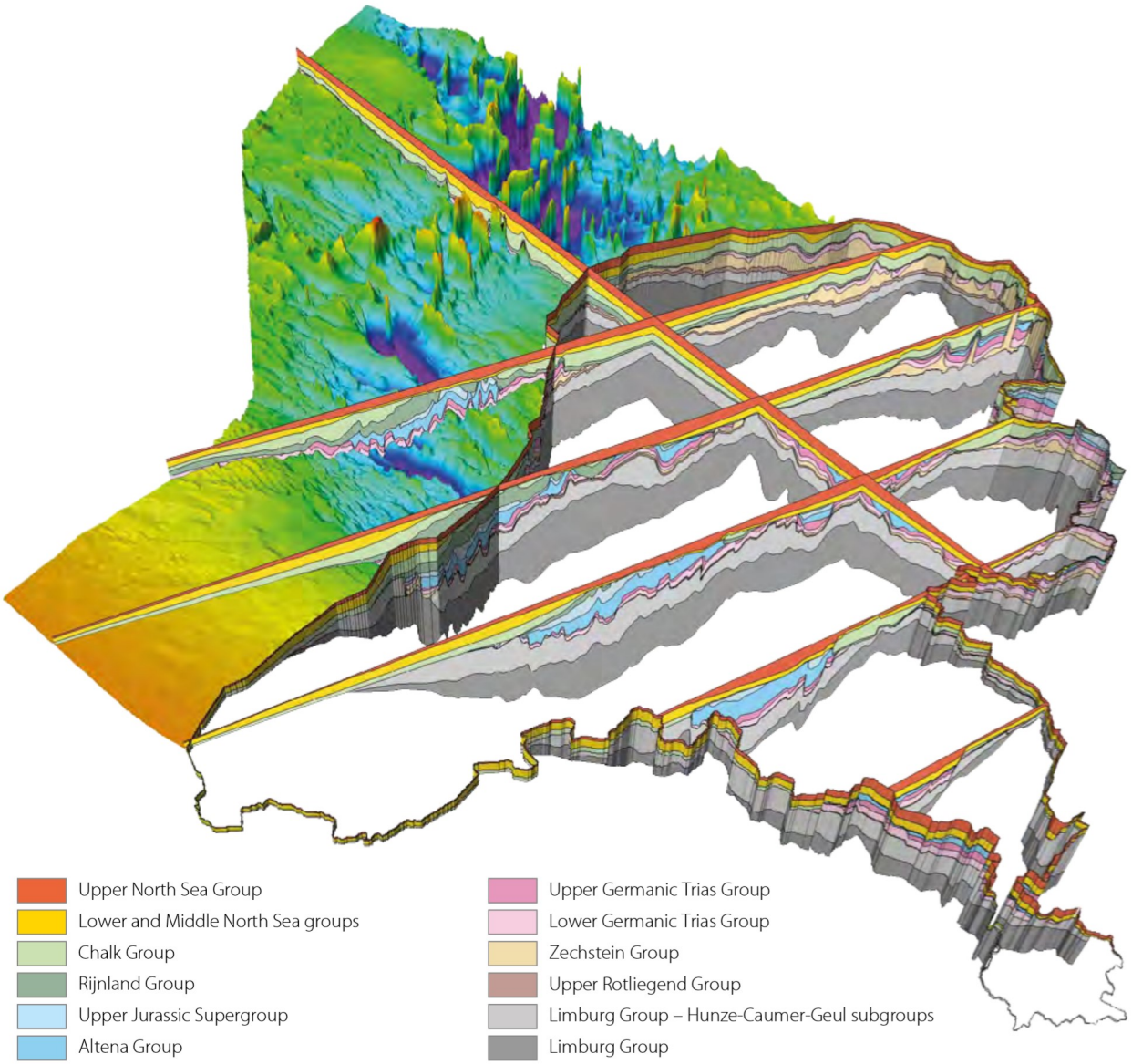


Figure 24.4. *Oblique view on the 3D layer model DGM-deep v5 (available at the DINO-web portal, www.dinoloket.nl/en), covering both the on- and offshore domains of the Netherlands. The visualized surface represents the top of the Zechstein Group in the offshore domain. Colour range indicates depth from shallow (red) to deep (purple).*

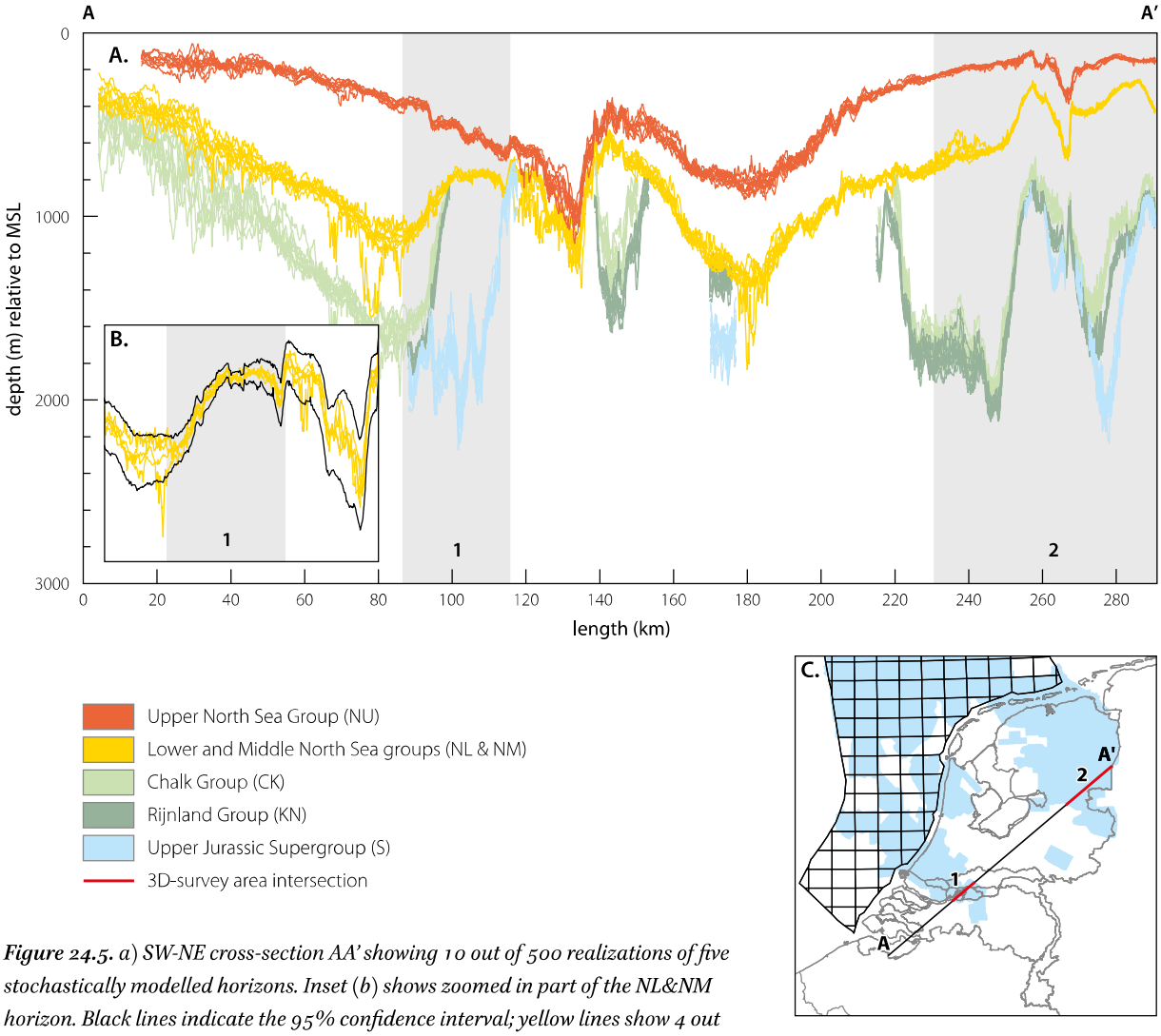


Figure 24.5. *a) SW-NE cross-section AA' showing 10 out of 500 realizations of five stochastically modelled horizons. Inset (b) shows zoomed in part of the NL&NM horizon. Black lines indicate the 95% confidence interval; yellow lines show 4 out of 500 individual realizations. c) Map showing the position of the cross-section AA' with the 3D-survey areas indicated in blue. Red horizontal lines at the top of the cross-section mark 3D-survey areas shown as grey intervals in a).*

definition and description in the Stratigraphic Nomenclature (TNO-GDN, 2022b; see the section about model visualization), allowing users to explore both layer geometry and general rock composition in their area of interest. The model also serves to understand the general geological evolution of the Netherlands, as the presence, thickness and distribution of the units is largely controlled by the main tectonic events (De Jager et al., 2025, this volume). Stratpiler (Kombrink et al., 2012) is a method to automatically extract structural elements from DGM-deep. It groups al possible stratigraphic sequences into specific classes that comply with the definition of highs, platforms and basins that pertain to a certain geological period.

The DGM-deep model does not contain information on individual reservoir- or aquifer layers and cannot be applied directly to study the multivarious potential of the deeper subsurface. The geothermal aquifer potential maps included in ThermoGIS v2.0, however, do include such information and the DGM-deep model was used as a basis for detailing it. The ThermoGIS model will be described in more detail in the section on innovative modelling methods and case studies; a comprehensive description of the construction of the model can be found on the NLOG website (www.nlog.nl/en/welcome-nlog).

DGM-model for the shallow subsurface

Systematic digital mapping of the shallow Dutch subsurface started in 1999 with the development of the Digital Geological Model (DGM; Figs 24.1b, 24.2; Stafleu et al., 2011b, 2019; Gunnink et al., 2013a). DGM is constructed using a set of ca. 26,500 consistently interpreted boreholes. It is a 3D stacked-layer lithostratigraphic model of the entire onshore part of the Netherlands down to a depth of ca. 500 m (with a maximum of 1200 m in the Roer Valley Gra-

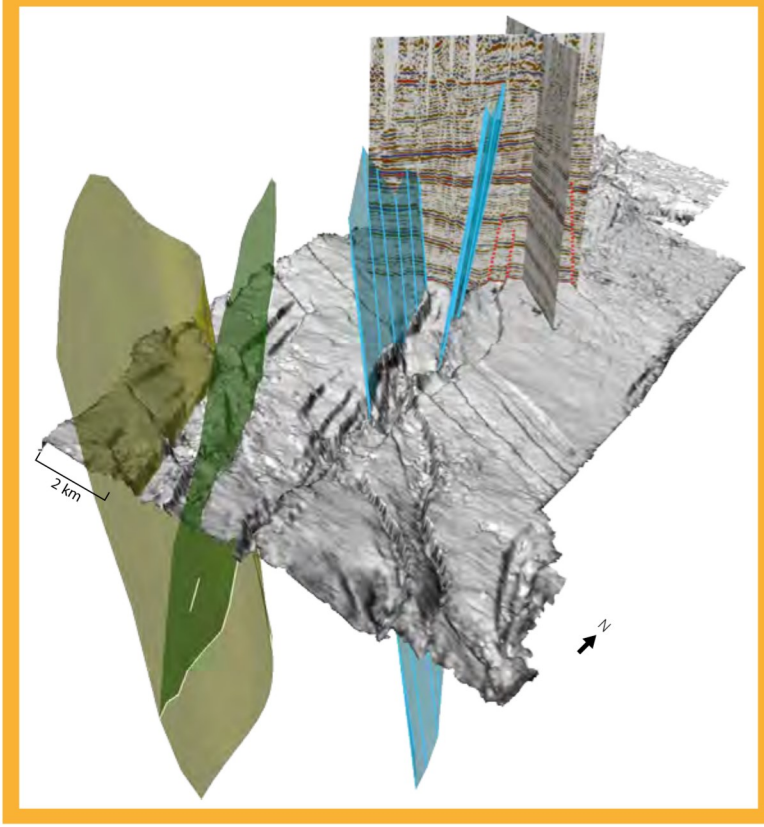
Faults

1

Whereas few faults are visible at the surface, at larger depths (>1 km), the subsurface of the Netherlands is characterized by structural complexity and a dense network of faults dominated by SE-NW orientations (see Ten Veen, 2021; De Jager et al., 2025, this volume). The different tectonic styles in the Netherlands are related to various tectonic phases including the Paleozoic assembly of the Pangea super-continent (Caledonian and Variscan orogenies), the Mesozoic rifting and break-up of Pangea (Cimmerian phases), and the interplay of Alpine collision and Atlantic rifting during the Late Cretaceous and Cenozoic. Consequently, many of the faults have been reactivated during various tectonic phases. At a larger scale, fault zones form tectonic boundaries between different geological domains. At a smaller scale the faults themselves strongly influence or determine the characteristics and kinematic behaviour of rock formations (e.g. fluid flow, tendency to generate earthquakes). In the Netherlands, evident and well-known faults are often linked to the occurrence of natural earthquakes in tectonically active regions. Yet certain subsurface activities (e.g. production and injection) may also trigger earthquakes in regions that are otherwise tectonically stable, induced seismicity in the Groningen gas field being the most renowned example. Furthermore, faults may also be related to other types of hazards such as migration of fluids and gas from deep formations towards shallower groundwater aquifers or the surface environment. Faults are thus a critical component of the TNO-GDN models.

In the deep subsurface, faults can be interpreted based on the offsets of seismic reflectors. Due to the resolution of the seismic data, offsets smaller than 10-20 m are not easily recognizable. At the seismic line, the interpreted fault is represented by a so-called fault stick. In 2D seismic lines the fault sticks are isolated features that in between the seismic lines need to be connected based on the interpreter's judgement. In 3D seismic data, multiple fault sticks can be combined into 3D fault surfaces and therefore fault interpretations can be made with higher confidence.

Based on the interpretation, a fault model is created that selects and groups fault sticks that belong to one fault. In this process, a geologically sensible solution is sought that, as much as possible, honours regional trends. In 3D, the ability to display the seismic amplitude data or seismic attributes horizontally (in time slices) or at geologically sensible surfaces provides adequate means to detect the true orientation and extent of the fault. Where available, fault information at or close to the surface (e.g. Van Balen et al., 2019, 2021) is also used to constrain the location of the modelled fault surface.



3D image of two intersecting seismic lines. Fault interpretations are made on the seismic lines and are represented by so-called 'fault sticks' (in red). The fault sticks are combined into fault planes (light blue planes) to produce a fault model. This involves selecting and (re) grouping fault sticks that belong to one fault and making the interrelationships between faults geologically consistent (green planes are faults). An edge-detection method using the variance (in grey scale) aids in highlighting faults and is here attributed to the base of the North Sea Supergroup surface.

The shallow subsurface (ca. <500 m depth) is not covered adequately by conventional seismic exploration data and very few shallow seismic datasets have been acquired. Therefore, in contrast to the DGM-deep model, faults for the DGM model of the shallow subsurface are inferred from sedimentary thickness and facies changes that emerge from correlation and interpolation of borehole data. To achieve a connection with the deeper subsurface, the uppermost stratigraphic level of the DGM-deep model, i.e. the base of the Upper North Sea Group, is used as a guiding surface for interpreting shallow faults. Contrary to the deep subsurface, in the shallow subsurface faults are represented as vertical planes. This oversimplification is rationalized by the fact that most faults steepen toward the surface. Moreover, this vertical inclination is hardly noticeable at the mapping scales used.

All modelled Dutch faults are collected in the European Fault Database that was developed in the context of the GeoERA-HIKE project (funded by the European Union's Horizon 2020 research and innovation programme) (Ten Veen, 2021). This database builds on a hierarchical classification system (Hintersberger et al., 2018) that ties the mapped faults to tectonic units and to larger- or smaller scale faults. It includes existing (upgraded) fault data and many previously unpublished faults and aligns with the observation that fault systems are segmented and consist of many individual faults. Geometrical fault objects can be retrieved from the GIS-database and, using a vocabulary, are linked to a concept giving it hierarchical and temporal context (Hintersberger et al., 2021). Currently, all modelled faults can be represented as 2D intersection lines with the main stratigraphic horizons (or the land surface) they transect. The database, for example, allows for simple selection of active faults in a certain area and provision of semantic information and fault attributes. The latter are still mainly limited to geometric aspects (length, strike, dip, surface area), fault type (e.g. normal, reversed), timing of fault activity (youngest stratigraphic surface affected) and observation/evaluation method (e.g. seismic interpretation, inferred modelling).

Apart from geological relevance, the fault database can be used to support hazard assessments (natural and induced seismicity, fluid pathways and seals, gas migration, ground motion and subsidence). Furthermore, the database has economic and environmental relevance as it provides the framework for the location of various resources.

ben). It consists of a series of layers, in which each lithostratigraphic unit is represented by rasters for top, base and thickness of the unit (cell size 100 x 100 m). Raster layers are stored in two different formats: Esri's non-proprietary ASCII grid format and ERDAS Imagine's proprietary binary grid format (which has a better performance in GIS applications). The lithostratigraphic units are modelled at formation level. The complex fluvio-deltaic Holocene deposits comprising four formations, six members and eight beds, are represented by one layer only.

The ca. 26,500 borehole descriptions used in DGM are selected from the DINO database (Fig. 24.6). This selection aims at a spatially even distribution of good quality borehole data penetrating the Quaternary and Neogene deposits. Shallow boreholes, which are those less than 10 m deep, are not used in DGM, except in the northern Netherlands where they were used for mapping of the hydrologically important glacial till deposits at the base of the Drente Formation. The selected boreholes are stratigraphically interpreted by manually assigning a lithostratigraphic classification (Westerhoff et al., 2003; TNO-GDN, 2022b). Subsequently, the base of each of the lithostratigraphic units in the boreholes is used for interpolation and modelling. The basic strategy for the lithostratigraphic interpretation is to work from nation-wide to regional-scale cross-sections that, in turn, constitute the geological framework for the final interpretation of individual boreholes. However, these cross-sections are not explicitly used in the interpolation process.

In addition to the interpretation of the boreholes, a map of major faults in the Cenozoic deposits is constructed. The map is a thorough revision of earlier publications, including maps based on seismic data acquired for the exploration of oil and gas. Additional seismic data came from high resolution surveys in the Roer Valley Graben, which is the most prominent tectonic feature in the shallow subsurface of the Netherlands. For every lithostratigraphic unit, the faults that influenced the base of the unit are selected and used as 'barriers' in the interpolation process.

The depths of the base of each lithostratigraphic unit as derived from the borehole data are interpolated to raster surfaces using the block-kriging algorithm (Goovaerts, 1997; Chilès & Delfiner, 2012) as implemented in the geostatistical software-package Isatis®. The top surface follows indirectly from the joined basal surfaces of overlying units when all units are stacked (see 'stacking the units' below). The base surface was chosen because this surface is formed by depositional processes that are linked to the unit itself, whereas the top surface is often a reflection of

younger erosive processes. Interpolation is assisted by additional information that includes: (1) maps with the maximum spatial extent of each lithostratigraphic unit; (2) trend surfaces showing geological structures (basins) or trends (dip direction and dip angle); (3) guiding points ('synthetic boreholes') inserted at locations with specific geological features like pinching out or incised channels. An important trend surface at the base of the model (formed by the Breda Subgroup in large parts of the country), is imported from the DGM-deep model. This trend surface is one of the interdependencies of the models as depicted in Fig. 24.2.

The last step in the modelling process consists of stacking the basal surfaces of each unit in a stratigraphically consistent way. In the stacking process, younger basal surfaces may intersect with older ones. In general three types of intersection are possible: (1) the upper unit has eroded the lower units. In this case the lower units are clipped by the upper unit; (2) the upper unit has been deposited against or on top of the relief of the lower unit without eroding the underlying unit. In this case the upper unit is clipped by the lower unit; (3) the intersection is an artefact of the interpolation process occurring between two conformable units. In this case the basal surfaces of the two units are adjusted in such a way that the intersection is removed. The choice of the type of intersection depends on the geological concept. The stacking process is performed within Isatis®, using grid-to-grid operations that are also available in standard GIS software. An impression of the resulting DGM model is shown in Figure 24.7.

The uncertainties in depth and thickness of the stratigraphic units in the DGM model are controlled by many factors (e.g. data quality, interpolation uncertainty). In the current DGM model, model uncertainty is quantified by applying cross-validation (Gunnink et al., 2010). In this approach a data point is left out and the depth of the base of the unit is estimated at that location by interpolation of the remaining data points. This is done sequentially for all datapoints. The difference between the true and the estimated depth at each location is used to quantify a 'regional' standard deviation. The regional uncertainty is lowered near data locations, by a factor derived from the kriging variogram. This method benefits from quantifying the overall magnitude of uncertainty by cross-validation, while retaining the influence of the variogram to determine fine scaled variation in uncertainty at locations in proximity to data points. An updated version of the method described above (Dabekaussen & Hummelman, 2021; Zehner et al., 2021) is currently in use for uncertainty calculations of layer-based modelling at TNO-GDN. The model uncertainty of the stratigraphic units is communicated as standard deviation maps, for example for the base of the Beegden Formation (Fig. 24.8).

DGM may be regarded as the national 3D geological map suitable for applications requiring geological information of the mainly unconsolidated sediments (sand, clay, peat) in the shallow subsurface. The lithostratigraphic layers in the model are linked to their definition and description in the Stratigraphic Nomenclature (TNO-GDN, 2022b) allowing users to explore both layer geometry and general sediment composition in their area of interest. However, the main purpose of the DGM model is to serve as a framework for the REGIS II and GeoTOP models described below.

REGIS II: hydrogeological model

Another important step in digital mapping was the development of the REGIS II hydrogeological model (Regional Groundwater Information System II; Vernes & Van Doorn, 2005; Van der Meulen et al., 2013; Vernes et al., 2021). The model uses the same borehole dataset as used in the DGM model. REGIS II further subdivides the lithostratigraphic

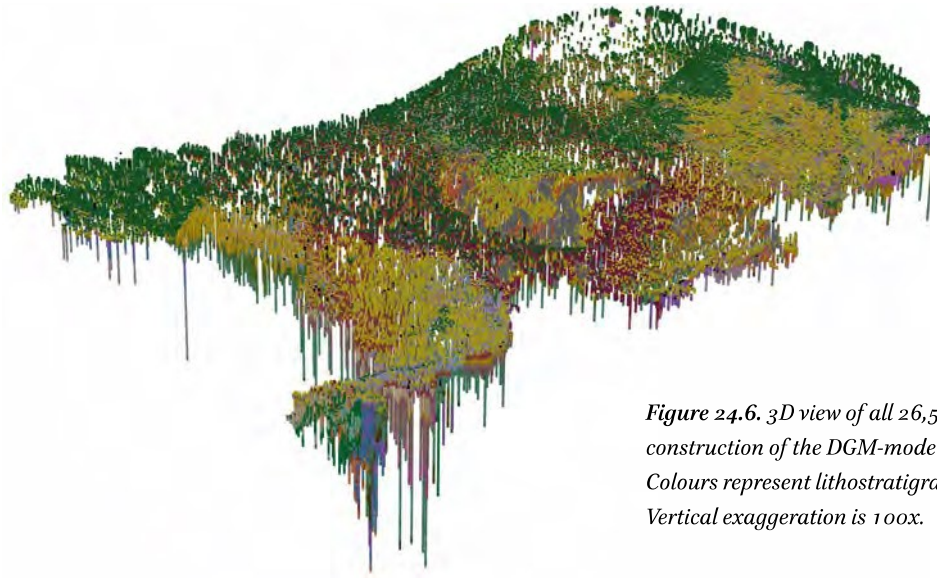


Figure 24.6. *3D view of all 26,500 boreholes used in the construction of the DGM-model of the shallow subsurface. Colours represent lithostratigraphic units at formation level. Vertical exaggeration is 100x.*

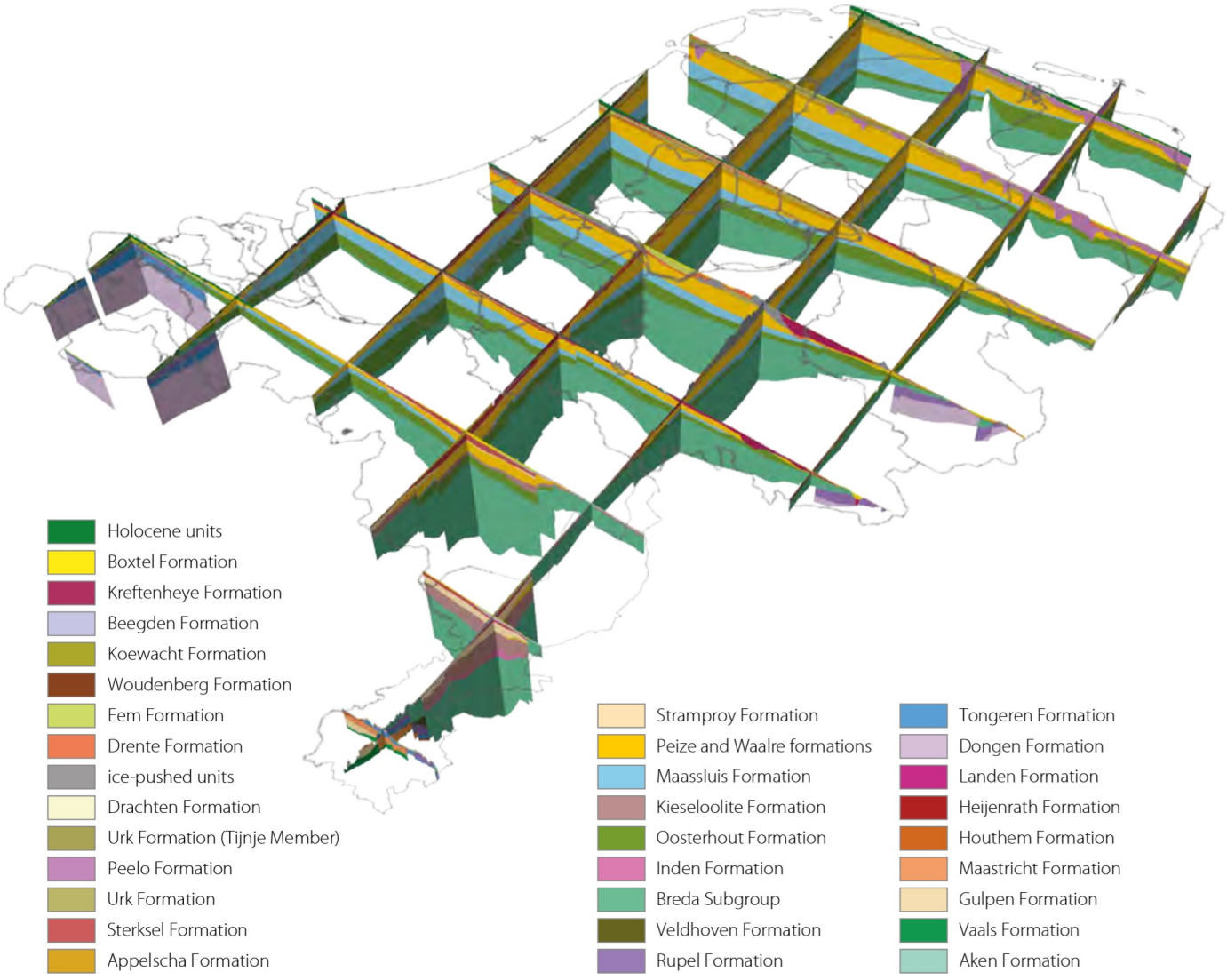


Figure 24.7. *Fence-diagram through the DGM model with an equidistance of 40 km showing the Neogene part of the North Sea Basin infill (Breda Subgroup and younger units) onlapping older Paleogene and Mesozoic formations along the basin shoulder. The Roer Valley Graben locally shows an increase in thickness of the Neogene units. The legend also contains units for other figures in this chapter that are not shown here. Vertical exaggeration is 45x.*

units of DGM into hydrogeological units (aquifers, aquitards and aquicludes). In addition, representative values of hydrological parameters (e.g. hydraulic conductivity) are calculated and assigned to the model hydrogeological units, making it suitable for groundwater flow modelling on a regional scale. Like DGM, REGIS II models the Holocene deposits as a single confining layer. REGIS II is widely used by regional authorities and water supply companies, for example in groundwater flow modelling studies. The reader is referred to Verweij et al. (2025, this volume) for an overview of the hydrogeological setting of the Netherlands.

The REGIS II model workflow uses the lithostratigraphic interpretation of boreholes and the layer-based DGM model as a starting point. The workflow then identifies hydrogeological units in the boreholes and follows with layer-based modelling and parameterization (Figs 24.2, 24.9). The hydrogeological units are interpreted and modelled within the lithostratigraphic units of DGM which remain unaltered during the process, making REGIS II and DGM fully consistent.

In the first step of the hydrogeological interpretation of the boreholes, each lithostratigraphic interval is subdivided into lithological classes: lignite, peat, clay, sandy-clay, clay with an unspecified sand content, fine sand, medium sand, coarse sand, sand with an unspecified grain size, glauconite sand, gravel, shells, chalk and marl, and sandstone and siltstone (Vernes et al., 2021). Stacked borehole intervals with similar lithological classes are aggregated. Subsequently, these aggregated intervals are manually in-

terpreted in terms of hydrogeological units. REGIS II distinguishes six types of hydrogeological units: sand, clay, peat, lignite, chalk and 'complex' (Vernes et al., 2021).

The modelling procedure for the tops and bases of the hydrogeological units is similar to that used in DGM for modelling of the lithostratigraphic units, with two main exceptions. First, the modelling of units within a DGM unit requires the interpolation of two surfaces rather than the base surface only. In most cases top and thickness are interpolated from the borehole data, after which the base is derived by simply subtracting the thickness from the top. In some cases, however, top and base are interpolated and thickness is derived. Second, in many cases it is difficult or even impossible to determine consecutive sandy hydrogeological units within a single geological unit. This is especially the case if these sandy units are not separated by a clayey, peaty or complex unit. Figure 24.10 illustrates this problem in a sandy DGM-unit in which two clay layers 'k1' and 'k2' are present. This problem is solved using a three-step approach where the units that are discriminated by their lithological contrast are modelled first (clayey units 'k1' and 'k2' in Fig. 24.10). The second step involves the construction of extrapolated horizons, which form the continuation of the top of a clayey unit within the extent of the DGM-unit (dashed lines in Fig. 24.10). The percentage thickness distribution of the sandy units at the top of the clayey, peaty and complex units is used to generate artificial data points to be used in the interpolation procedure of these extrapolated horizons. In the third step, the geometry of the sandy units ('z1', 'z2' and 'z3' in Fig. 24.10) is derived by combining the top and base of the clayey units with the extrapolated horizons.

As in DGM, the depths of the top and thickness (or top and base) observed in boreholes are interpolated to raster surfaces using the 'block-kriging' algorithm (Goovaerts, 1997; Chilès & Delfiner, 2012) in Isatis®. The interpolation process is assisted by maps showing the maximum spatial extent of each hydrogeological unit, trend surfaces and guiding points ('synthetic boreholes'). The modelling workflow ultimately subdivides the 34 DGM lithostratigraphic units into 125 hydrogeological units (Fig. 24.11).

The next step in the modelling workflow is the param-

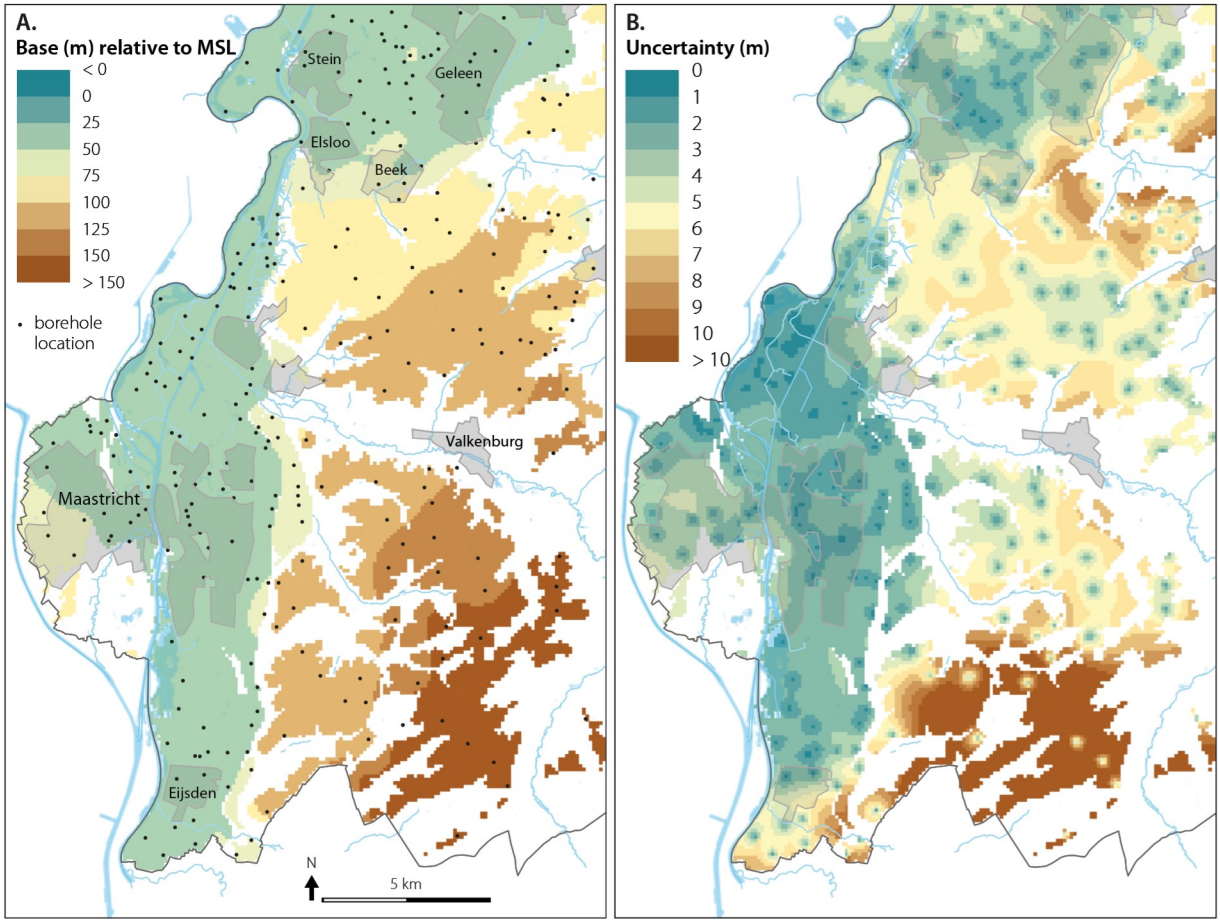


Figure 24.8. *Detail of the base Beegden Formation, showing (a) borehole locations and modelled depth in DGM, and (b) the cross-validation based uncertainty. Note how data proximity as well as local geological complexity influence the level of uncertainty (modified after Dabekaussen & Hummelman, 2021).*

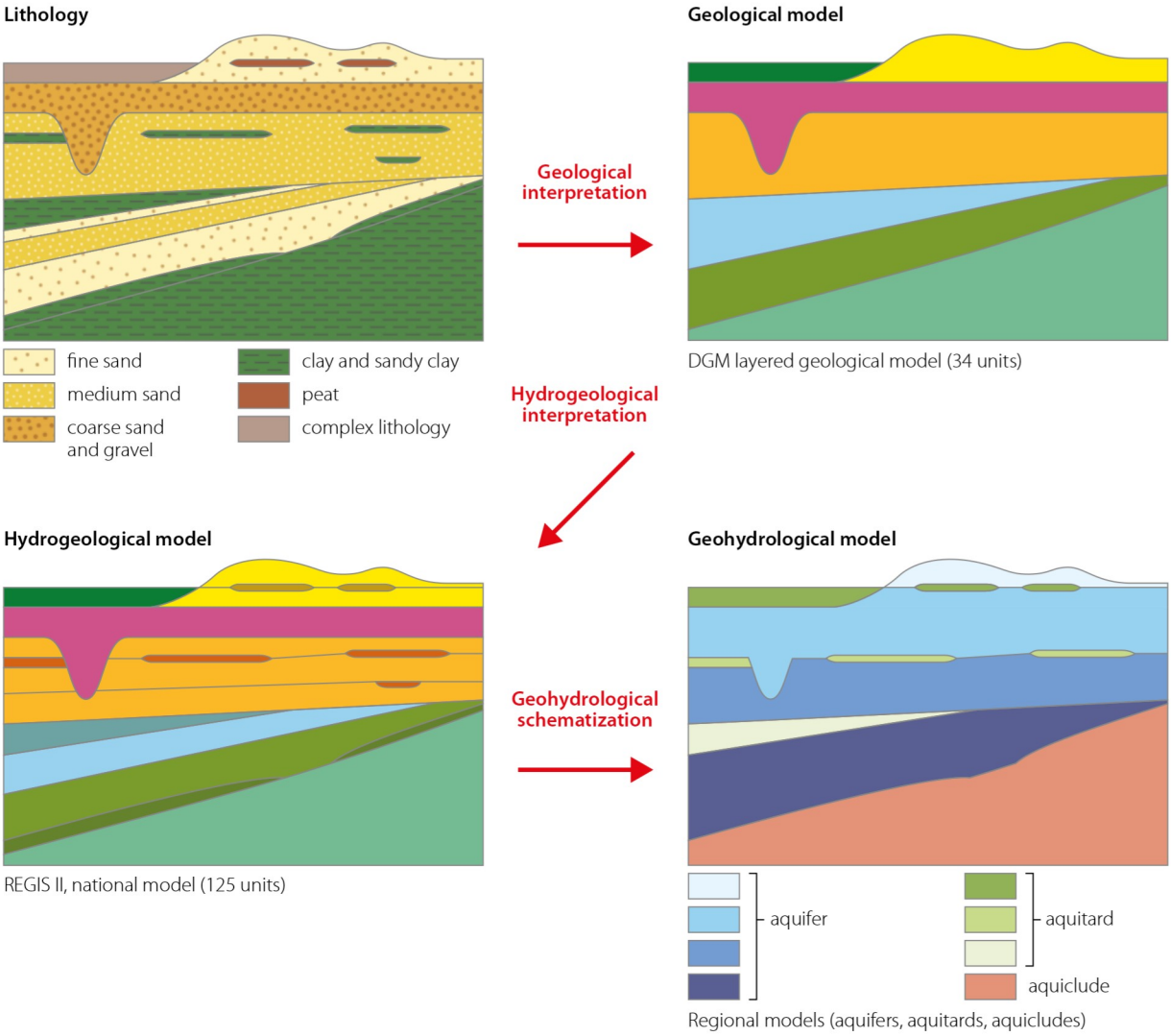


Figure 24.9. *The coupled DGM-REGIS II concept: geological interpretation of field observations creates a national lithostratigraphic model (DGM); hydrogeological interpretation of the DGM model produces the REGIS II national hydrogeological model; geohydrological schematization produces regional geohydrological models for national and regional authorities defining aquifers, aquitards and aquicludes (modified after Vernes & Van Doorn, 2005 and Van der Meulen et al., 2013, reprinted with permission).*

eterization of the hydrogeological units with hydraulic conductivity values in both the horizontal (k_h) and vertical (k_v) directions (Gunnink et al., 2013b; Vernes et al., 2021). Hydraulic conductivity measurements are only sparsely available, and therefore hydraulic conductivity is correlated with the lithological classes observed in the boreholes and subsequently interpolated to populate the entire volume of each hydrogeological unit.

The procedure involves four steps. In the first step, minimum and maximum hydraulic conductivity values for each combination of lithostratigraphic unit and lithological class are selected from a database comprising a mix of data obtained from measurements on samples taken from boreholes, selected pumping tests, literature and expert judgement. These values are then assigned to each combination of lithostratigraphic unit and lithological class in the boreholes. The second step groups the borehole intervals of the same lithological class within a hydrogeological unit and sums their thicknesses. The third step assumes the conductivities in the grouped lithological class intervals follow a log-normal distribution defined by the minimum (2.5 percentile) and maximum (97.5 percentile) values. Conductivities are then repeatedly (10,000 times) sampled. From the sampled conductivities, the weighted average conductivity at each borehole location is calculated, taking the thickness of each grouped lithological class interval into account. The arithmetic mean for horizontal and the harmonic mean for vertical hydraulic conductivity are used. From the 10,000 weighted average values, a single, upscaled conductivity value for the hydrogeological

unit at the location of the borehole is calculated. The last step uses the 'kriging with measurement error' algorithm to interpolate the upscaled values and the corresponding standard deviations to a hydraulic conductivity raster layer covering the entire hydrogeological unit (Fig. 24.12). By repeating this procedure for each hydrogeological unit, the entire model is parameterized.

The procedure outlined above results in upscaled hydraulic conductivity values and their corresponding standard deviations at each borehole location. The standard deviation is used in the interpolation of the borehole data to the hydraulic conductivity raster layer, by applying the 'kriging with measurement error' algorithm. As a result, each resulting hydraulic conductivity layer is accompanied by a standard deviation raster layer representing the model uncertainty (Hummelman et al., 2019; Vernes et al., 2021).

REGIS II's main field of application is groundwater management. The model is available online at www.dinoloket.nl and www.broloket.nl. These portals provide easy, free of charge access to the model, enabling a first analysis and evaluation of the hydrogeological configuration in a specific area through cross-sections, maps and synthetic boreholes. Consulting REGIS II is a first step in obtaining an estimate of subsurface conditions, for example at new drilling locations for monitoring or pumping wells.

Groundwater flow models are an important tool in groundwater management, the scale of which can vary from national to local. Given its regional scale, REGIS II provides the geometry and a first estimate of hydraulic conductivity ranges of the aquifers and aquitards in the Dutch national hydrological model LHM (*Landelijk Hydrologisch Model*; LHM, 2022) as well as for regional groundwater flow models like MIPWA (2022) and IBRAHYM (Vermeulen et al., 2007; Swierstra et al., 2018; nhi.nu/modellen/ibrahym). In addition, REGIS II is often used as a framework for local groundwater flow models where additional local data is used to get a more accurate estimate of the local hydrogeology. Spatial planning of activities in the subsurface requires hydrogeological information as well, for example to assess the potential for thermal energy storage systems, estimate the available fresh groundwater stocks, or regulate the maximum depth of thermal energy storage systems so as to protect groundwater reserves.

GeoTOP: voxel model of the upper tens of metres

GeoTOP is the latest national subsurface model developed at TNO-GDN. GeoTOP schematizes the shallow subsurface in millions of voxels of 100 x 100 x 0.5 m down to a depth of 50 m below mean sea level, which is the main zone of current Dutch subsurface activity (Figs. 24.1a and 24.2; Stafleu et al., 2011a, 2021a; Maljers et al., 2015). GeoTOP models all Holocene formations as well as several Holocene and upper Pleistocene members and beds as separate stratigraphic units by deploying virtually all borehole descriptions available in the national borehole database (ca. 495,000) complemented by ca. 125,000 auger holes of Utrecht University (Cohen, 2017). Each voxel in the model has multiple attributes: the lithostratigraphic unit the voxel belongs to (based on a detailed layer model), the 'most likely' lithological class that is representative for the voxel and the probability of occurrence for each of the lithological classes. Lithological classes are based on the average of 100 equiprobable model realizations. At present, GeoTOP

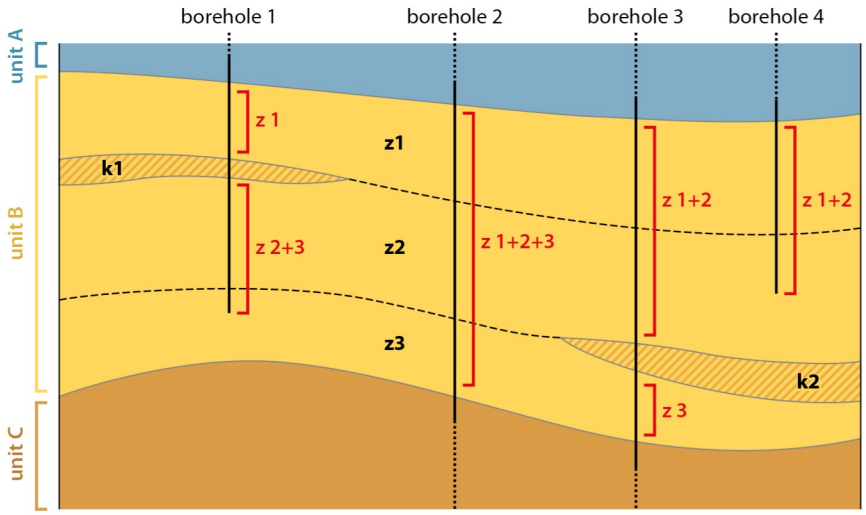


Figure 24.10. *Modelling of two clayey layers and three sandy layers within a single sandy DGM unit. In borehole 1, the topmost sandy layer 'z1' can be distinguished from 'z2' and 'z3' by the intercalating clayey unit 'k1'. In borehole 3, the lowermost sandy layer 'z3' can be distinguished from 'z1' and 'z2' by the intercalating clayey unit 'k2'. In the other boreholes, sandy layers 'z1', 'z2' and 'z3' are modelled by extrapolating the top of each clayey layer. Modified after Hummelman et al.* (2019).

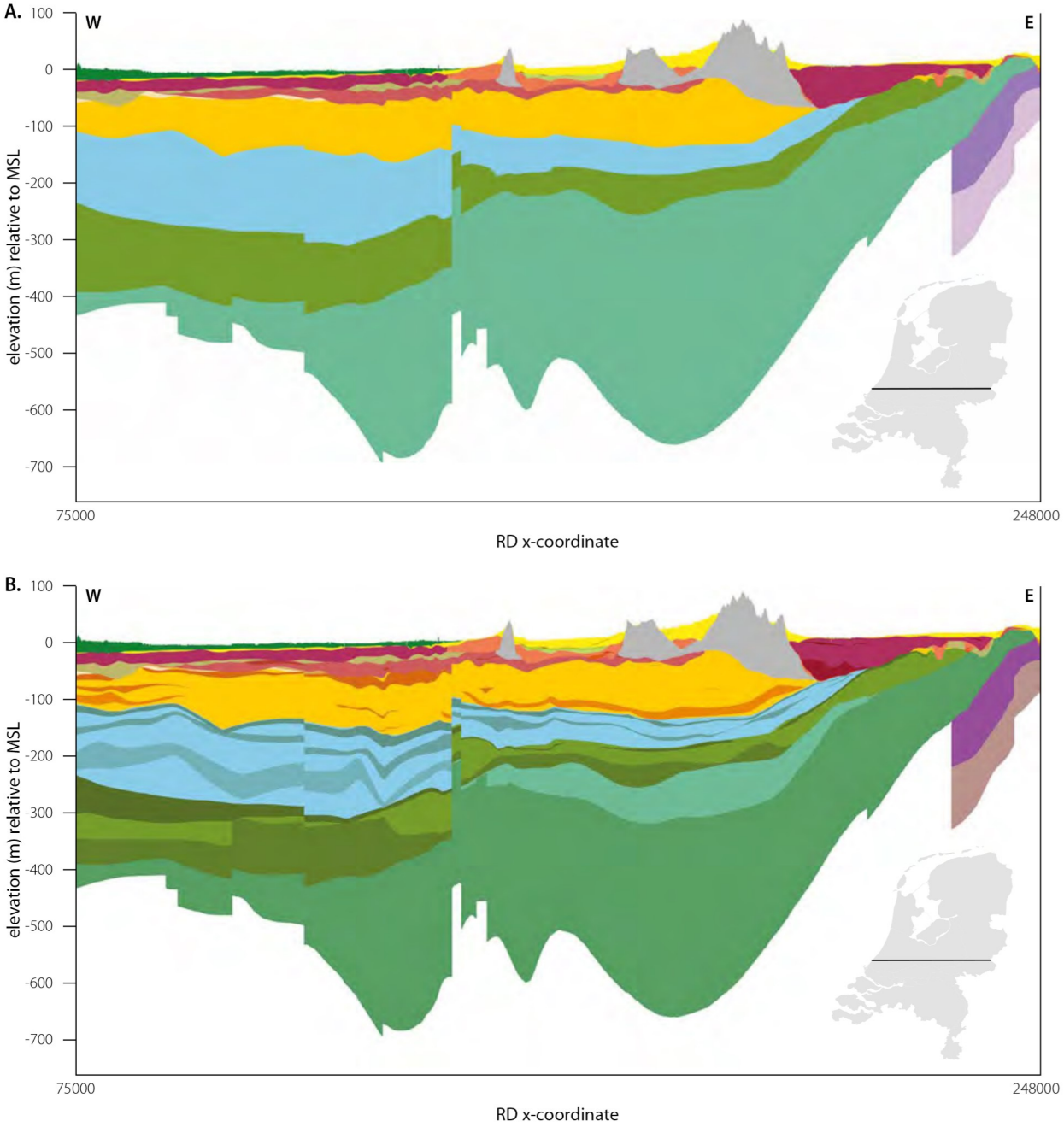


Figure 24.11. *Cross-sections through the DGM and REGIS II models: a) DGM model showing lithostratigraphic units (see Fig. 24.7 for legend); b) REGIS II model showing the subdivision in hydrogeological units. Clayey layers are shown in a darker shade of the corresponding lithostratigraphic unit.*

covers ca. 70% of the surface area of the Netherlands (including inland waters such as the Wadden Sea) using ca. 415,000 borehole descriptions from the two databases mentioned above.

Given the large number of boreholes, automated stratigraphic interpretation routines (Python scripts) were developed. These routines combine digital maps, stratigraphic rules (e.g. superposition) and lithological criteria (e.g. main lithology, admixtures, grain size and shell content, amongst other criteria) to determine the depth of the top and base of the lithostratigraphic units in borehole descriptions. This procedure delivers a uniform, consistent and reproducible set of interpreted boreholes (Fig. 24.13a).

An example of automated stratigraphic interpretation is the Basal Peat Bed. This thin layer of peat lies on top of the Pleistocene deposits, of which a trend surface is made based on manually labelled boreholes (including the 26,500 boreholes of the DGM model as well as other manually labelled boreholes in the national database). The procedure first selects those boreholes that are within the

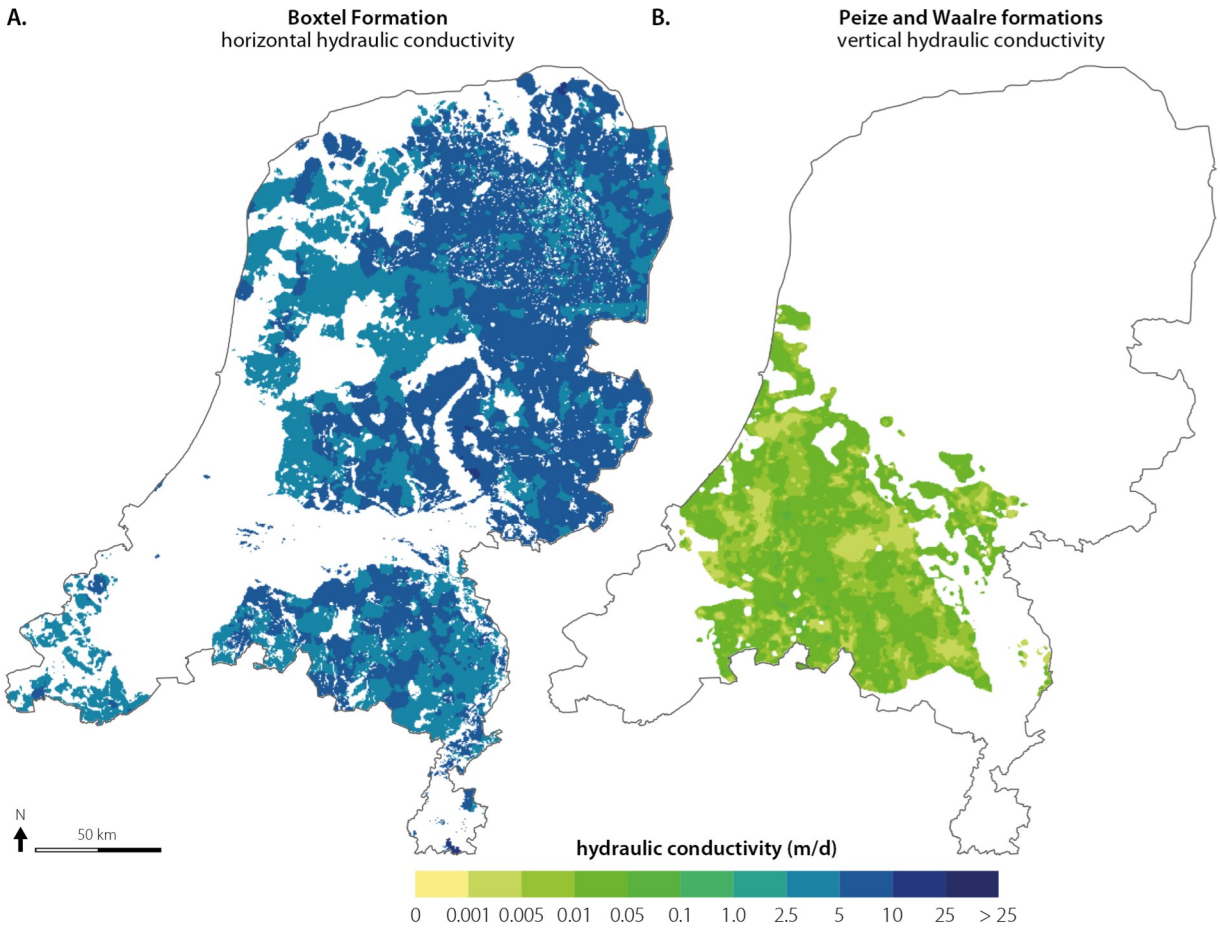


Figure 24.12. *Examples of hydraulic conductivity layers in the REGIS II model: a) sandy unit with horizontal hydraulic conductivity; b) clayey unit with vertical hydraulic conductivity.*

areal extent of the Basal Peat Bed and subsequently examines the description intervals of each borehole from bottom (the deepest interval) to the top (the interval at land surface). The following criteria are then used to identify intervals as part of the Basal Peat Bed:

- The lithology is peat or gyttja;
- The base of the interval is within a buffer of 2 m from the top Pleistocene trend surface;
- The lithology underlying the first interval found is (Pleistocene) sand, or a clay layer with a maximum thickness of 1 m.

The criteria are designed in this way to avoid misinterpretation of other Holocene peat deposits (e.g. the Hollandveen Member).

Another example comprises the small river valley deposits in the southern Netherlands (Boxtel Formation, Singraven Member). These Holocene infills contain peat, clay and clayey sand in an otherwise sandy Pleistocene environment (Fig. 24.14). However, the deeper parts of the infill may consist of fine to coarse grained sand that is difficult to distinguish from the underlying Pleistocene deposits. Therefore, additional criteria are needed. From manually labelled boreholes, the base of the unit is known to lie between 4 to 6 m below land surface. In most cases, the bottom of the unit is simply set at the deepest interval that satisfies this criterion (Fig. 24.14a). In the central part of the Roer Valley Graben however, a more sophisticated procedure can be followed. In this area, the river valleys eroded loam deposits of the Liempde Member (Boxtel Formation; Fig. 24.14b). In this case, the procedure sets the base of the river valley deposits at the deepest interval in a zone of 2 m below a trend surface based on labelled boreholes of the Liempde Member. After the base is determined, the top of the unit representing the Singraven Member is subsequently set at equal to the land surface or, if present, to the base of overlying anthropogenic deposits.

This second example shows that dependencies between the units exist, e.g. the Singraven Member can only be found after the procedures for anthropogenic deposits and the Liempde Member are completed. Fig. 24.14b also shows that defining hard criteria, such as a zone of 2 m, has some limitations: in a manual interpretation, a geologist would probably put the base of the Singraven Member an interval deeper than the automated procedure does.

The automated interpretation procedure works well in the shallow Holocene and upper Pleistocene units, where many good quality boreholes are available (Stafleu et al., 2021a). Furthermore, the shallow units often have sharp lithological contrasts and are therefore easily identifiable. The lithological contrasts between the generally sandy, fluviatile Pleistocene units at deeper levels are more subtle and hence less suitable for automated interpretation routines. The layer modelling of these units therefore relies on the same set of ca. 26,500 manually interpreted boreholes employed by DGM and REGIS II.

In the next modelling step, 2D interpolation techniques, implemented in the geostatistical software package Isatis®, are used to construct surfaces representing the bases of the stratigraphic units (Fig. 24.13b). The interpolation algorithms used (Sequential Gaussian Simulation in older model areas, block kriging in more recently constructed parts of GeoTOP; Goovaerts, 1997; Chilès & Delfiner, 2012) allow for the calculation of a mean depth estimate of each stratigraphic surface and its standard deviation. As in DGM, the interpolation is constrained by maps of the maximal areal extent of the units and is assisted with trend surfaces and guiding points. Subsequently, all surfaces are stacked according to their stratigraphic position, resulting in a consistent, integrated layer-based model with estimates of top and base of each stratigraphic unit (Fig. 24.13b). Top surfaces are derived from the bases of the overlying units.

The surfaces are then used to place each voxel in the model within the correct stratigraphic unit. If the midpoint of a voxel is situated below the top and above the base of a stratigraphic unit, the voxel is assigned to that particular unit. The surfaces of the layer model are also used to assign a stratigraphic unit to borehole intervals that remained uninterpreted in the interpretation step described above. These intervals are from the deeper units that were not part of the automated interpretation routines and do not form part of the 26,500 manually interpreted boreholes.

In the third step, the borehole descriptions are re-analysed and each interval is classified in one of six lithological classes: peat, clay, clayey sand & sandy clay, fine sand, medium sand, coarse sand & gravel. (Fig. 24.13c). Additional classes for gravel and shells are used for stratigraphic units that contain considerable amounts of these lithologies. No classification is applied to the anthropogenic deposits. The classification scheme follows the hydrogeological definition of REGIS II and is suitable for groundwater flow modelling amongst other applications. Compared to the stratigraphic interpretation, the classification is a

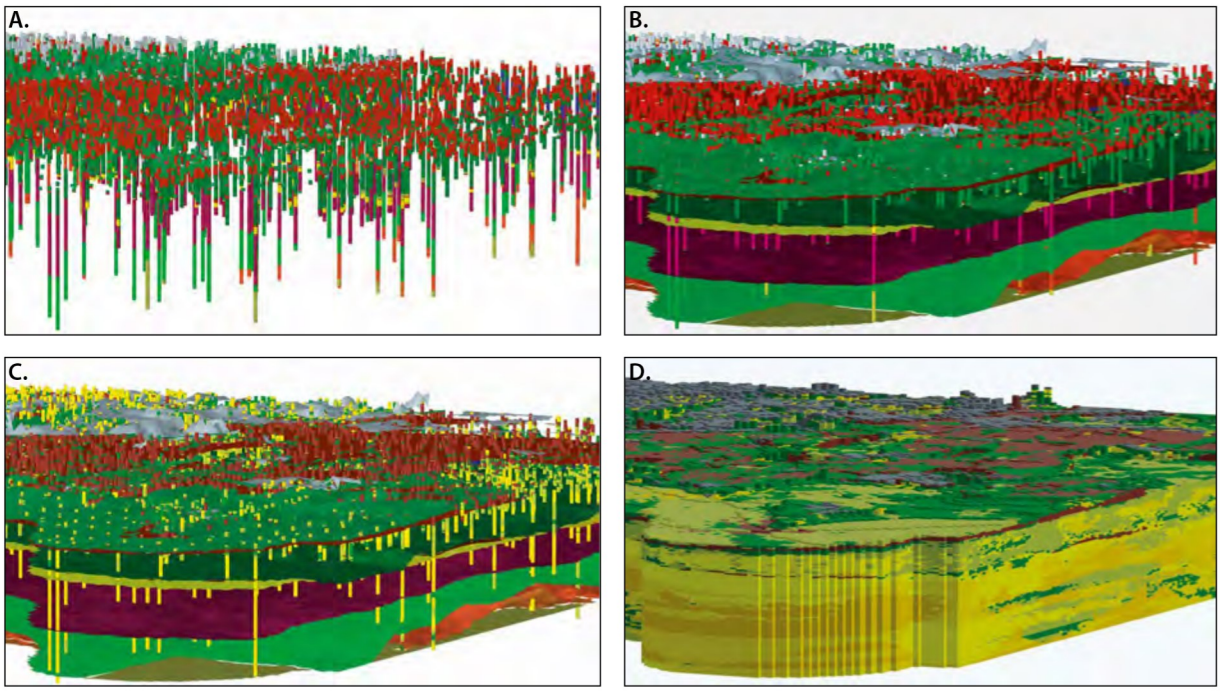


Figure 24.13. *The four main modelling steps in the construction of the detailed layer-based model underpinning the GeoTOP voxel model and the voxel modelling itself: a) automated stratigraphic interpretation of borehole descriptions into formations, members and beds; b) 2D interpolation of stratigraphic surfaces; c) subdivision of borehole descriptions into lithological and grain-size classes; d) 3D interpolation of lithological class for each stratigraphic unit separately. In (c) and (d), yellow colours indicate sand in three different grain-size classes, green colour is clay, light green colour is clayey sand and sandy clay, and brown peat. Reproduced from Stafleu et al. (2019).*

relatively simple procedure that is implemented in a single Python-script. Figure 24.15 shows examples of lithological class distributions observed in boreholes.

In the fourth modelling step, the voxels in the model are populated with estimates of lithological class. These estimates are calculated from the lithological classes observed in the boreholes using the stochastic simulation technique Sequential Indicator Simulation (Goovaerts, 1997; Chilès & Delfiner, 2012), in Isatis®. Because of the great diversity in composition and heterogeneity of the different stratigraphic units (Fig. 24.15), the simulation is performed for each stratigraphic unit separately.

The simulation results in 100 equally probable realizations of lithological class for each voxel in the model. From these 100 realizations, probabilities of occurrence of the lithological classes are calculated by simply dividing the number of times a particular lithological class is assigned to a voxel by the total number of realizations. In addition, a 'most likely' estimate of lithological class is determined (Fig. 24.13d). Along with the stratigraphic unit, the 'most likely' lithological class is the most used attribute of GeoTOP (Fig. 24.16).

The 100 different but equally probable realizations indicate the degree of uncertainty in the estimates of the lithological class. In the best case, all model runs result in the same value; in the worst case all possible values occur with the same frequency. For an individual voxel, as well as in a 1D vertical voxel stack, the probabilities can be displayed in a bar graph showing the probability distribution and hence the model uncertainty (Fig. 24.22). However, in 2D visualizations, for instance in a vertical cross-section through the voxel model, it is not possible to show all probabilities in a single view: the user will always be presented with one of the probabilities at a time. To solve this visualization problem, the concept of information entropy (Wellmann & Regenauer-Lieb, 2012) is used as a measure of uncertainty in GeoTOP (Stafleu et al., 2021a,b). The information entropy of a voxel is a single value ranging from 0 to 1 that can easily be calculated from each of the probabilities of the lithological classes. An entropy value of 0 represents no uncertainty (all model runs result in the same lithological class), whereas a value of 1 occurs when all lithological classes are equally likely. Values in between 0 and 1 account for both the number of lithological classes with a probability higher than 0 (the more classes, the higher the entropy) and the differences amongst the probabilities (the greater the differences, the lower the entropy).

Figure 24.17 shows the information entropy of the lithological classes in a fence diagram through a small part of the GeoTOP voxel model (Stafleu et al., 2021b). The diagram shows areas that are strongly influenced by single boreholes as vertical zones of low entropy. In addition, homogeneous stratigraphic units dominated by a single

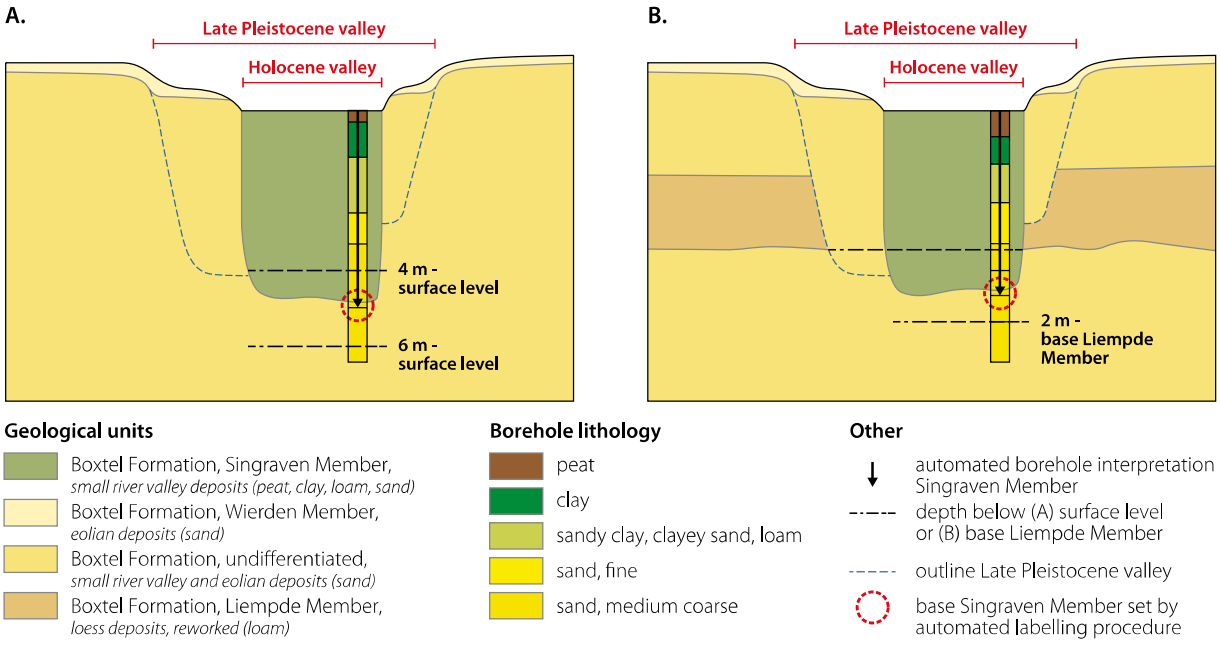


Figure 24.14. *Conceptual model illustrating the automated stratigraphic interpretation of a borehole in the small river valley deposits of the Singraven Member (Boxtel Formation): a) in most areas, the base of the unit is simply set at the deepest interval where the base is in between 4 and 6 m below land surface; b) in the Roer Valley Graben, a more sophisticated approach can be used involving a trend surface calculated on the basis of previously interpreted boreholes of the Liempde Member (Boxtel Formation).*

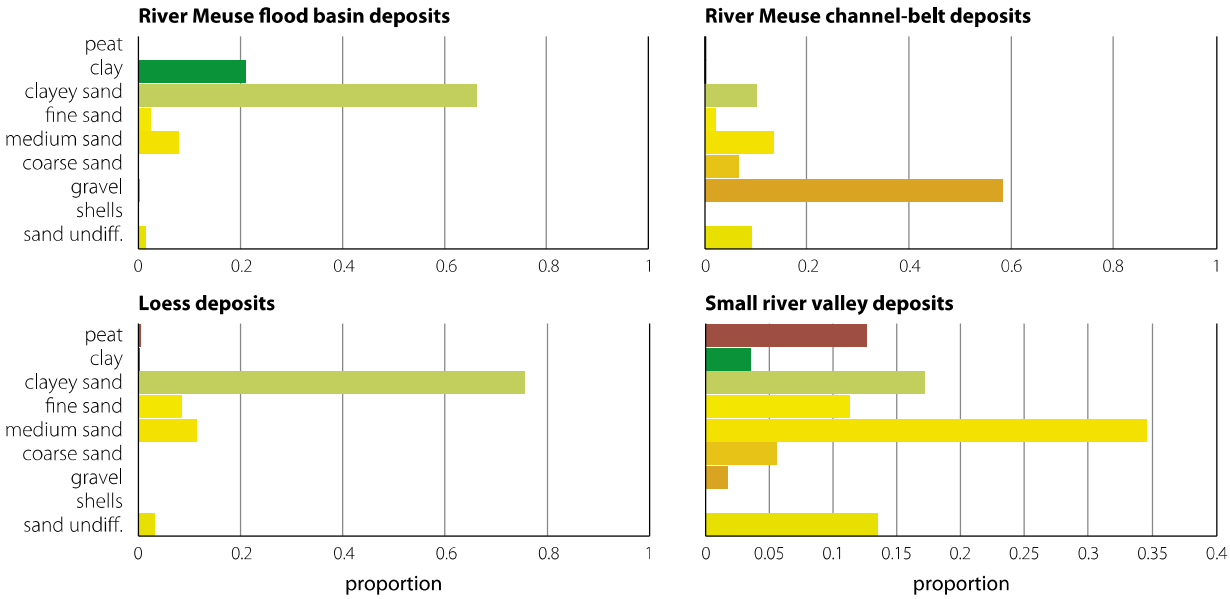


Figure 24.15. *Bar graphs of lithological classes in borehole intervals of four stratigraphic units in the GeoTOP model area of the southern Netherlands. Note the diversity in composition and heterogeneity. 'Sand undifferentiated' refers to sandy borehole intervals without grain-size information. In the voxel modelling, these intervals are only used to determine if a voxel is sandy or not.*

lithological class can be distinguished (e.g. 'Unit A' in Fig. 24.17, low entropy) from heterogeneous units ('Unit B', high entropy). In general, entropy increases with depth as data density decreases.

GeoTOP is a multi-purpose model supporting applications involving the shallow subsurface, including:

- Evaluations of subsurface geotechnical conditions in the planning stage of large infrastructure projects (Van der Meulen et al., 2013);
- Long-term predictions of land subsidence due to compaction of clay and oxidation of peat (Koster et al., 2018a,b; CAS, 2022; Fig. 24.20);
- Aggregate resource assessments (Van der Meulen et al., 2013; Maljers et al., 2015);
- Defining the lithological characteristics of Holocene channel belt systems (Stafleu & Busschers, 2017);
- Potential environmental impacts of dredging operations (Stafleu et al., 2021a);
- Generalized soil composition map of the upper 8 m, used to assess the suitability of the subsurface for sewage infrastructure (Dambrink et al., 2014; Fig. 24.27c);
- Groundwater flow studies (Van der Meulen et al., 2013);
- Site-response assessment of induced earthquakes (Kruiver et al., 2017a,b; Van Ginkel et al., 2022; see the section on innovative modelling methods and case studies).

In several of these applications, GeoTOP is first parameterized with appropriate property values, like hydraulic conductivity in groundwater flow studies (Gunnink et al., 2013b), shear-wave velocity in the risk-assessment of induced earthquakes (Kruiver et al., 2017a,b) and the organic matter content of peat in advanced land subsidence predictions (Koster et al., 2018a,b). The basic assumption in these three examples is that the spatial variation of the relevant subsurface properties strongly depends on the two main attributes of GeoTOP: the lithostratigraphic unit and the 'most likely' lithological class (Stafleu et al., 2021a). Assigning property values to the voxels in GeoTOP may be simple, by using a lookup-table with a property value for each combination of lithostratigraphic unit and the lithological class, or it may involve a more complex vertical voxel-stack analysis that accounts for depth as a third factor controlling the property value. Some properties (e.g. hydraulic conductivity) require upscaling from the scale of the measurements (samples taken from boreholes) to the scale of the model (individual voxels).

Sand resource models for the North Sea

For the North Sea, two models have been developed to map the offshore sand resources. The DIS model (*Delfstoffen Informatie Systeem*), developed by TNO-GDN and Deltares for the Department of Waterways and Public works (Rijkswaterstaat), schematizes the offshore subsurface in millions of 200 x 200 x 0.5 m blocks down to a depth of 12 m below the seafloor. The model stretches along the entire coast of the Netherlands, starts at a water depth of -20 m NAP (Dutch ordnance datum) and extends 12 Nautical miles offshore. The model and accompanying

documentation (in Dutch) is available from the DINOloket web portal (TNO-GDN, 2022a). A second model covers the Belgian and southern Netherlands part of the North Sea (BPNS/sNPNS). This model, developed as part of the Transnational and Integrated Long-term Marine Exploitation Strategies project (TILES) has a resolution of 200 x 200 x 1 m and extends down to a depth of -65 m NAP (Dutch ordnance datum) (Hademenos et al., 2019; Van Lancker et al., 2019).

The modelling approach contains the same four main steps as the GeoTOP model, but there are some differences. In addition to boreholes, seismic data are a major information source in the offshore domain and the modelling approach is using this datatype as described in detail by Hademenos et al. (2019). Step one consists of stratigraphic interpretation of both borehole and seismic data. In contrast to GeoTOP, the interpretation of both datasets is mainly performed manually. In step two, the 2D interpolation of stratigraphic surfaces follows the same principles as applied in GeoTOP. The third step, the subdivision of boreholes into lithological classes, is comparable to the procedure for GeoTOP, but the definition of the classes varies according to the application of the model. In addition to a varying grain-size class definition, classes for the concentration of fines (silt and clay) and shells and gravel (TILES only) are used. These additional classes are of interest when determining the overall sand quality. In the fourth step, 3D interpolation is completed for lithological, mud, shell and gravel classes for each stratigraphic unit separately.

Model-related uncertainty of the offshore aggregate resource models is estimated in the same way as in Geo-

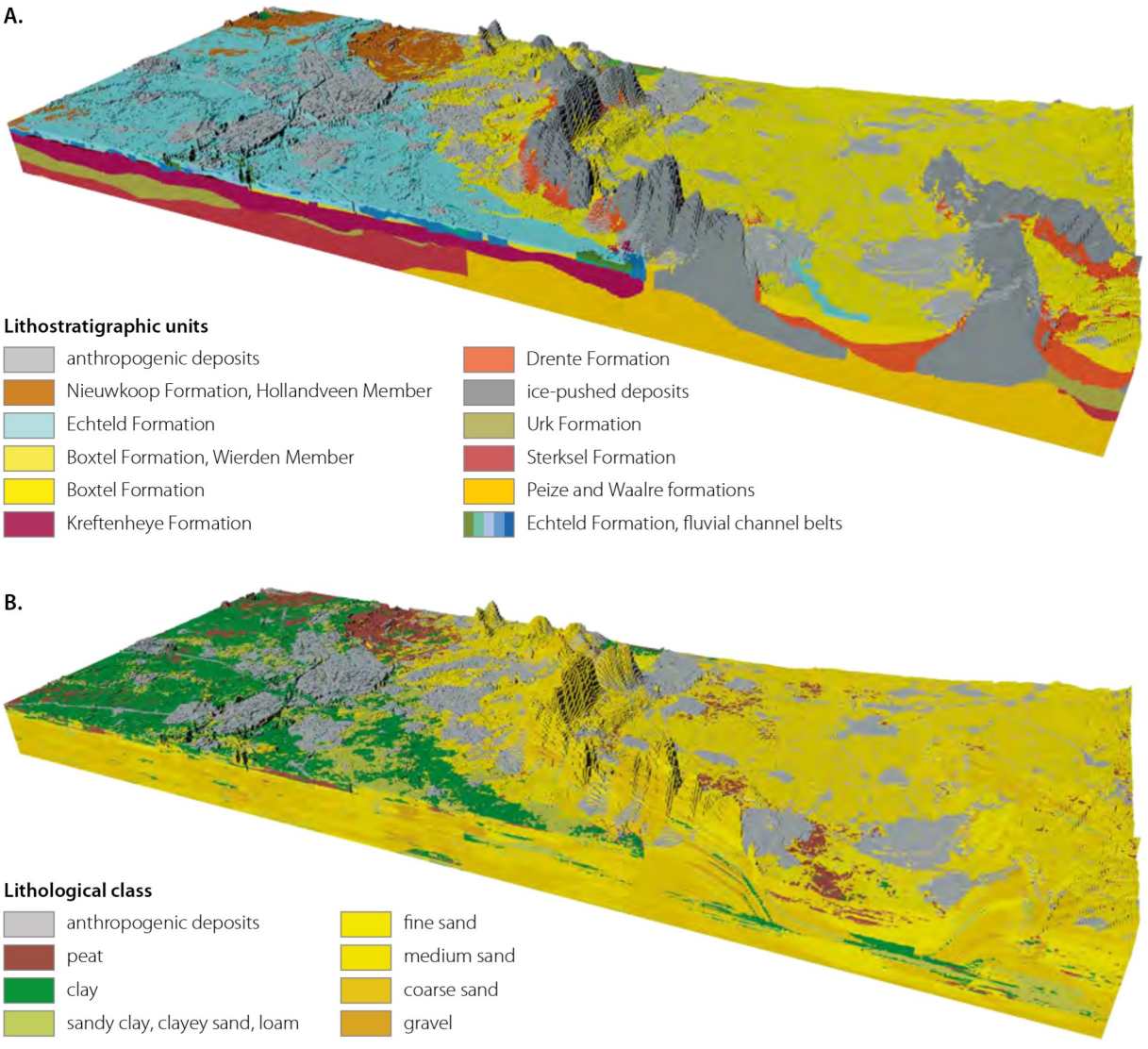


Figure 24.16. *GeoTOP 3D views of the Gelderse Vallei area in the central part of the Netherlands: a) lithostratigraphic units of Holocene and upper Pleistocene formations, members and beds; b) lithological classes. The displayed block measures 62 x 24 km; depth of the base is 50 m below MSL; vertical exaggeration is 75x. Modified after Stafleu & Dubelaar (2016).*

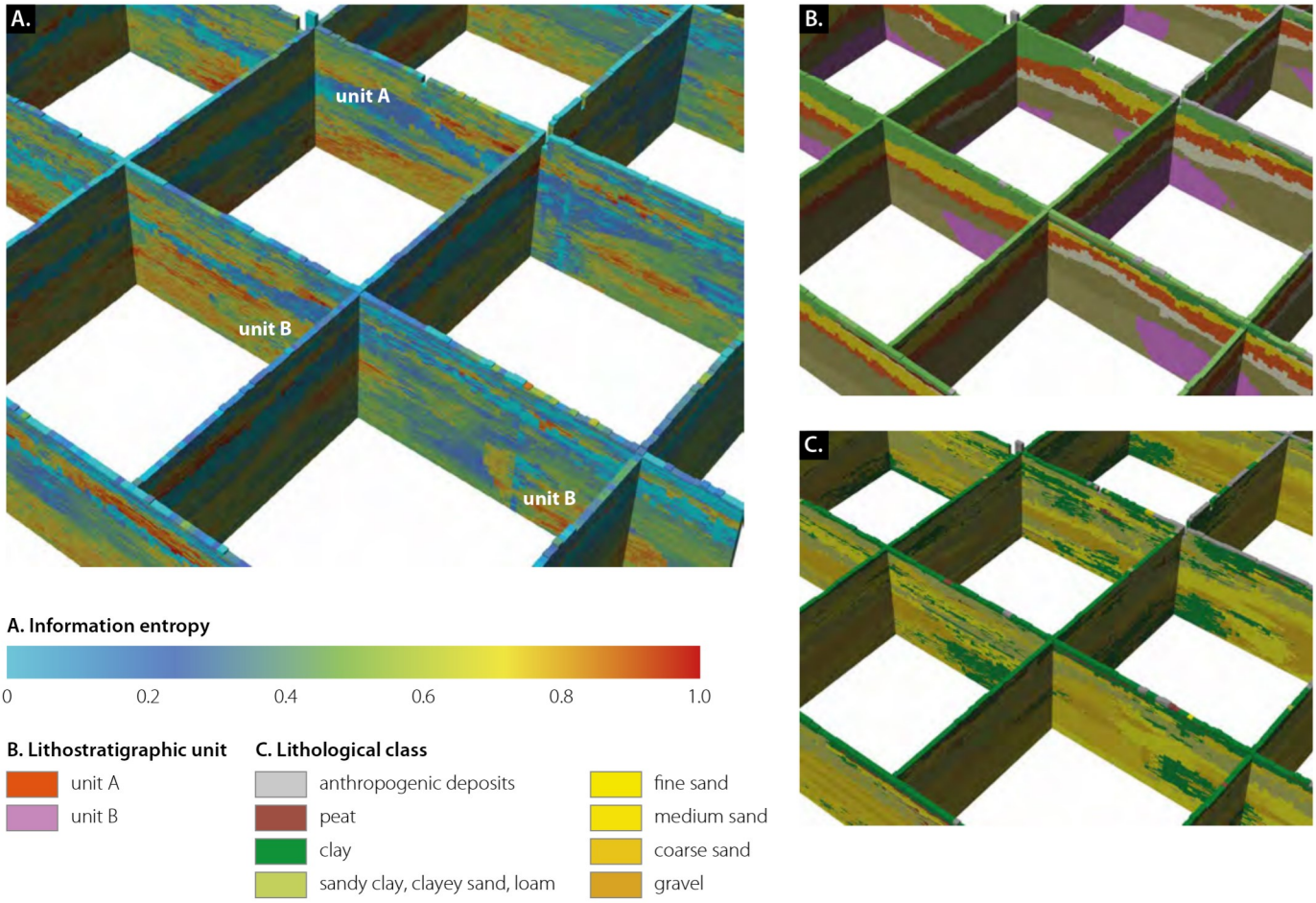


Figure 24.17. *a) Information entropy (representing model uncertainty) of lithological class in a fence diagram through part of the GeoTOP voxel model; b) stratigraphic units of the model; c) most likely lithological class. Unit A is dominated by a single lithological class (c) and has a low model uncertainty (a). Unit B is heterogeneous in its lithological composition (c) and has high model uncertainty values (a). Spacing of the fences is 4.5 km. Modified after Stafleu et al. (2021b).*

TOP. For the Belgian part of the TILES model, Kint et al. (2020) qualified and quantified data-related uncertainties for positioning, sampling and vintage. Uncertainty on positioning comprises navigational error, on-board and offdeck offsets and underwater drift. Sampling uncertainty arises from the suitability of the instruments to determine the lithological class. Vintage uncertainty is related to the change of the seabed since the moment of sampling. Parameters controlling vintage uncertainty are the age of the boreholes used and the sediment dynamics induced by environmental conditions and human activities (Kint et al., 2020). The three data uncertainties are interpolated and subsequently added as new properties in the voxel model, enabling users to visualize data uncertainty along with the modelled stratigraphy and lithology.

TILES and DIS are developed as decision support systems to enable sustainable management of the offshore sand resources. Both models are intended for regional use and they both show large scale patterns. Figure 24.18 for example shows that the probability to find medium grained sand is much higher further offshore compared to closer to the coast where fine grained sand is more prevalent. From a user's point of view, the greater value of medium grained sand must be weighed against the longer sailing time and higher fuel consumption involved in sand extraction further offshore.

The voxel models form the basis for a range of selection and visualization tools for use in policy development, for example to determine the influence of infrastructure on the short-term sand availability (Fig. 24.19).

Model quality control

In 2015, the Dutch parliament passed a new law, which puts subsurface data and information in the system of so-called key registries (*Basisregistraties*). The key registry of the subsurface (BRO, or *Basisregistratie Ondergrond*), managed by the Geological Survey of the Netherlands, holds subsurface data, including three of the four national

Anthropogenic deposits

2

In most urban areas the natural subsurface has been heavily disturbed by human activity and/or is covered by anthropogenic deposits (or: made ground). These areas do not only include city centres, with their often abundant subsurface archives related to historical urban development (e.g. Jayasena, 2020), but also modern residential and industrial areas, built on extensive sheets of filling sand (see photograph). Other examples include road and railway embankments that consist of natural aggregates or novel anthropogenic materials, coastal reinforcements and dikes, landscaped areas and landfills (see Van der Meulen et al., 2025, this volume) for an overview of the use of different sorts of aggregates over time).

In contrast to past geological maps, the 3D-subsurface model GeoTOP does provide information on the subsurface of urban areas and includes anthropogenic deposits as a separate stratigraphic unit (Schokker et al., 2015). The extent of these deposits has been derived from the Land Use Database of the Netherlands (LGN), a raster dataset in which the country has been subdivided into 39 land use classes. To ensure that highway embankments and dikes appear as continuous structures in GeoTOP, this raster dataset has been supplemented with spatial information from other sources (Stafleu et al., 2020).

However, the modelled thickness of anthropogenic deposits is generally not well constrained and GeoTOP does not give any information on the lithology of these deposits. Also, the composition and properties of the urban subsurface change rapidly over time, which means that data acquired before human interventions took place often do not reflect current subsurface conditions. Nonetheless, the demand for detailed subsurface information in the built environment is high and relates to anything from building stability and ground heat extraction to preserving cultural heritage and mitigating the effects of climate change (Van der Meulen et al., 2013). In preparation for the new Environment and Planning Act, major cities in the Netherlands are currently developing 3D spatial plans to optimize the use of subsurface space, thus potentially releasing valuable space above-ground.

To meet the growing demand for up-to-date, high-resolution subsurface information in urban areas, focus is on improved modelling of anthropogenic deposits. This includes:

- Improved spatial distribution and thickness modelling by incorporating additional data types, like cone penetration test data. To process this information, semi-automated interpretation routines are being employed, including artificial intelligence techniques like neural networks (e.g. Dabekaussen et al., 2020). Furthermore, in future GeoTOP releases of up-to-date information from the key registry BGT (*Basisregistratie Grootschalige Topografie*) will replace LGN data.
- Lithological characterization of anthropogenic deposits. This concerns both reworked natural deposits, as well as recycled non-natural materials (Dijkstra et al., 2019). To better recognize and characterize these deposits, both the lithological description standard (SBB 5.1; Bosch, 2000) and lithostratigraphic nomenclature (TNO-GDN, 2022b) will be updated and extended.



Subsurface disturbance beneath the campus of Vrije Universiteit Amsterdam: sewage and drinking water pipes crossing the local energy system, all embedded in 2 m of filling sand (photo: J. Schokker).

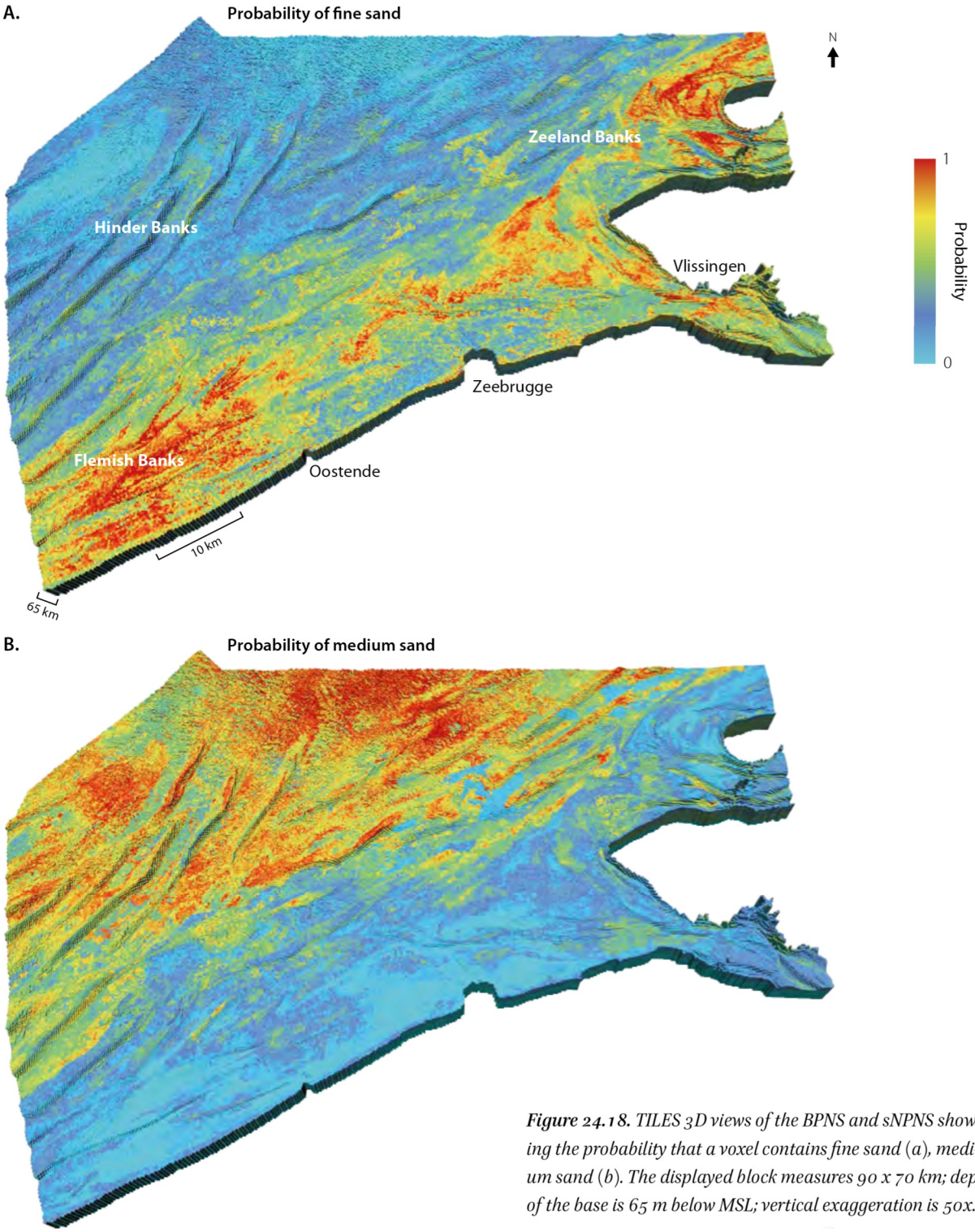


Figure 24.18. *TILES 3D views of the BPNS and sNPNS showing the probability that a voxel contains fine sand (a), medium sand (b). The displayed block measures 90 x 70 km; depth of the base is 65 m below MSL; vertical exaggeration is 50x.*

subsurface models (DGM, REGIS II and GeoTOP), as well as information on permits and underground infrastructure (Van der Meulen et al., 2013). Public bodies are legally required to consult both the data and the models in the key registry when making decisions related to the subsurface. If, for instance, a regional water authority would like to reinforce one of its dikes, they must first consult the BRO to check that subsurface data underneath the dike is already available. In addition, government agencies have a legal obligation to deliver all subsurface data they acquire and to report any errors they may discover in the data and models in the registry. These legal requirements are expected to lead to an increase in the use of the models. They also impose more stringent demands on the models in terms of their quality as well as in the update frequency, since the user community will expect the data they deliver

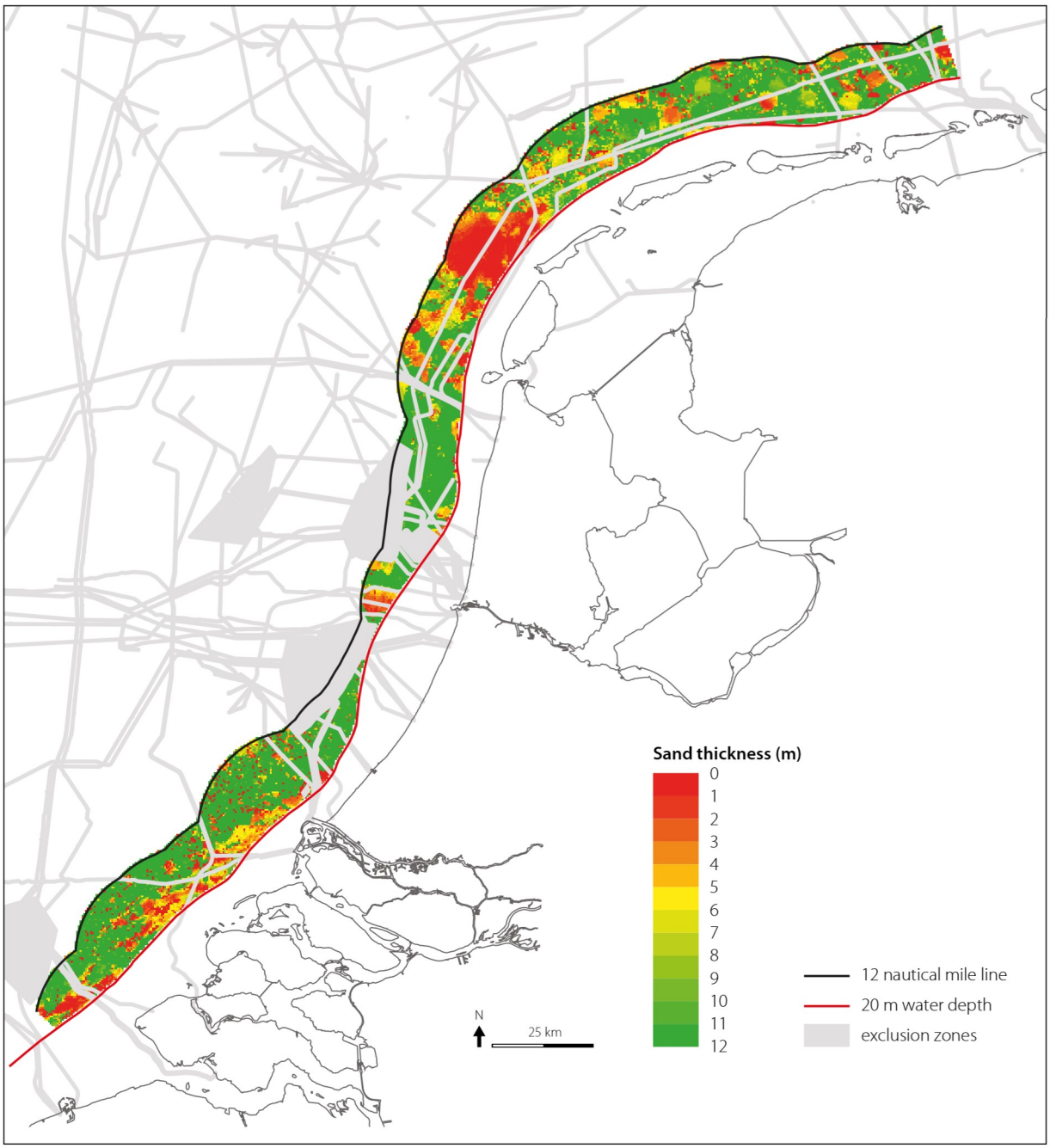


Figure 24.19. *Extractable sand in the upper 12 metres below the sea floor outside of exclusion zones (offshore infrastructure, e.g. wind farms, cables and pipelines) according to scenario B2. Modified after Maljers-Oosterwijk et al. (2014) updated using the DIS 2.1 dataset from the DINO web portal (TNO-GDN, 2022a).*

to be incorporated in the models as soon as possible (Van der Meulen et al., 2015).

Definitions of quality control usually break down into two elements: first, assessing the extent to which the model meets standards and requirements. This is the *intrinsic quality* of the model. The second element assesses *extrinsic quality*: does the model meet user requirements and expectations, or, in other words: is the model useful and fit for its purpose? Intrinsic and extrinsic quality do not necessarily coincide: a poor-quality model can still be useful, and a detailed, geologically plausible model can still be unfit for a particular application.

Feigenbaum (1991) illustrated the importance of quality control by looking at the costs related to good and poor quality. Good quality is about preventing errors or defects to occur at all, for instance by training staff, providing them with proper work instructions and by certification. In addition, good quality concerns appraisal which involves detecting errors via quality control or audits. Poor quality costs arise from having to do the work again, or to

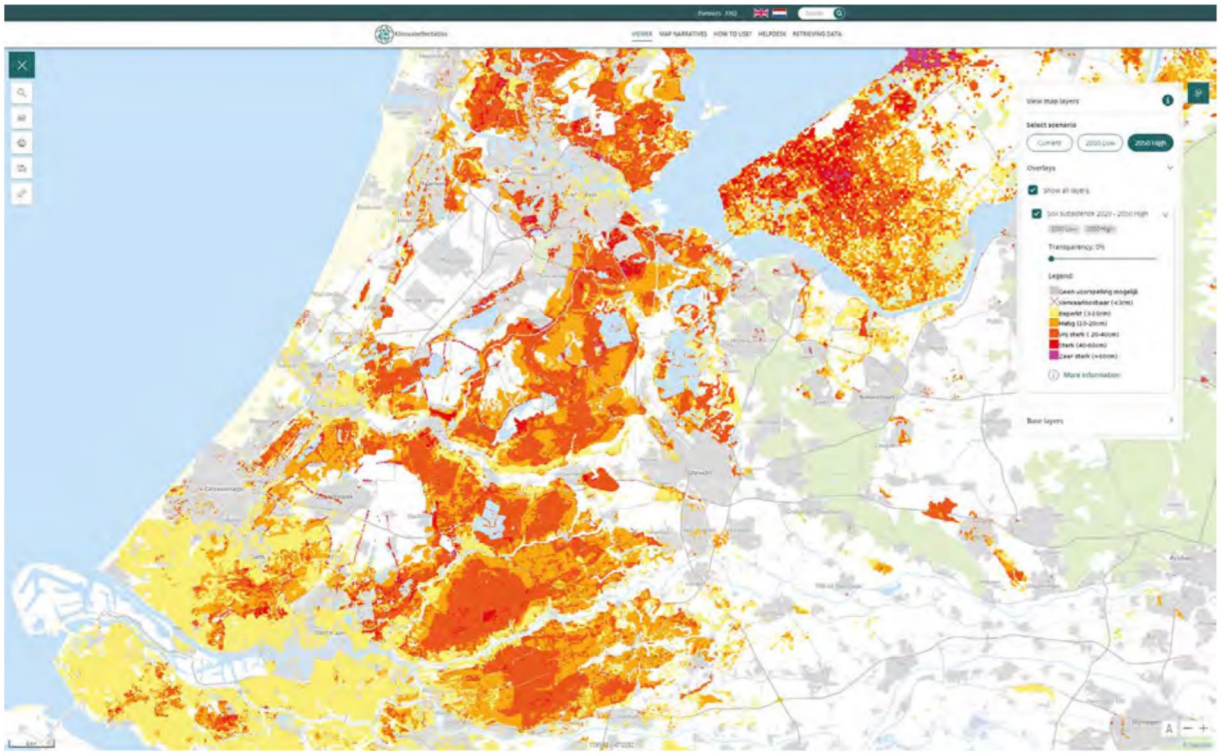


Figure 24.20. *Interactive map of predicted land subsidence due to the oxidation of peat in the western and central Netherlands. Screenshot taken from the online Climate Impact Atlas (CAS, 2022).*

correct it afterwards. It also comes from dealing with complaints from users and loss of reputation. The sum of the cost of good and poor quality is the total cost of quality. In general, larger investments in good quality lead to even larger savings in poor quality. Therefore, prevention and appraisal lead to a lower total cost of quality and hence lower total model production costs.

Intrinsic quality control

TNO-GDN started to implement a formal round of quality control (QC) of the national models in 2015. Expert geologists, who are not involved in the modelling process itself, inspect the models for defects. They are primarily focusing on intrinsic quality by systematically checking cross-sections, map views and 3D views of the final model. All defects, artefacts and geologically implausible configurations are reported to the modelling team who then address them. Examples of defects include, among others, errors in the mapped extent of geological units, pits and bumps in the layers caused by wrongly interpreted boreholes, faulted layers that are displaced in the wrong direction or have inconsistent displacement, implausible concentrations of a particular lithological class around bad quality boreholes, and artefacts at model area boundaries.

Creating a model is time-consuming and may take several years. This is because the modelling workflow (as outlined in the section on the national models) consists of many components, like drafting a conceptual model or design, mapping the extent of geological units, stratigraphic interpretation of boreholes and the actual modelling of layers and voxels. Defects in the final product may be rooted in one of the components that was created early in the modelling process, potentially one or two years earlier. For example, when an error is detected in the GeoTOP layer model, both the layer model and the voxel model will have to be corrected. Or even worse, if expert geologists disagree with the conceptual model being used, parts of the entire modelling process may have to be redone. Therefore, quality control should not be limited to the final product but should start early in the modelling process by assessing all major components. The modelling team should only start a new stage in the process if the current stage has been approved by the expert geologists. However, this staged approach in quality control makes the modelling process more time-consuming than it already was before QC was implemented. An alternative approach to detect defects early in the modelling process is to work in advance, i.e. to construct a preliminary final model from intermediate model components. For instance, when the modelling team is still working on maps and interpretations, the work-in-progress-result is used to create a first version of the layer model to see if the interpretations lead to implausible configurations. Or, if the team is still working on the layer model, a first draft of the voxel model can

be built to see if the subdivision in layers successfully captures the spatial distribution of lithology. Thus, working in advance provides the modelling team with invaluable feedback on the progress of their efforts. This 'fast forward modelling' puts a high demand on the turnaround time of the automated parts of the workflow (for example the interpolation processes implemented in Isatis® and Petrel®).

Another change imposed by the key registry of the subsurface is that users will expect more regular updates of the models. Modelling then becomes a process or a cycle rather than a project with a clear beginning and end. Quality control in turn will focus more on the changes made with respect to the previous version: are these changes reflecting new data and knowledge acquired since the last release, and do they correct for any errors reported by the user community? The focus of intrinsic quality control then shifts from geological plausible configurations to improvements made with respect to the previous version of the model. In other words, quality control will ensure that the new release results in a better model.

Extrinsic quality control

Due to the increasing size of the user community, we foresee another shift from evaluating intrinsic quality towards assessing the usability of the models in applications: will the model deliver the right answer to the users' needs? An example is the map in Fig. 24.20 indicating areas that are prone to land subsidence. The map is largely based on the GeoTOP voxel model and offers an entirely new look from the point of view of an application. Quite often defects in the model become apparent in an application, for instance a very unrealistic amount of subsidence that may have been overlooked by the expert geologist. In this way, applications help to find errors that arise from model configurations that are plausible, but nevertheless wrong. The key registry is another source of extrinsic quality control, as government agencies are required to report any errors they may encounter in the model when using it in their applications.

Model visualization

The models described in this chapter are disseminated free-of-charge via the DINO-web portal (www.dinoloket.nl/en/) in a number of ways, including an online map viewer with the option to create virtual boreholes and vertical cross-sections through the models, and as a series of downloadable GIS products. Full 3D visualization is supported by the freely downloadable SubsurfaceViewer® software, which allows users to download and visualize the models on their desktop computers. A recent development in model visualization is the capability of Esri's GIS-software to visualize large voxel-models such as GeoTOP in 3D. However, many users still prefer to work with the models in a 2D GIS environment. To serve these users, the models are delivered as 2D map products. These map products may be general, e.g. displaying the top, base or thickness of lithostratigraphic units, or they may be tailored to a specific application.

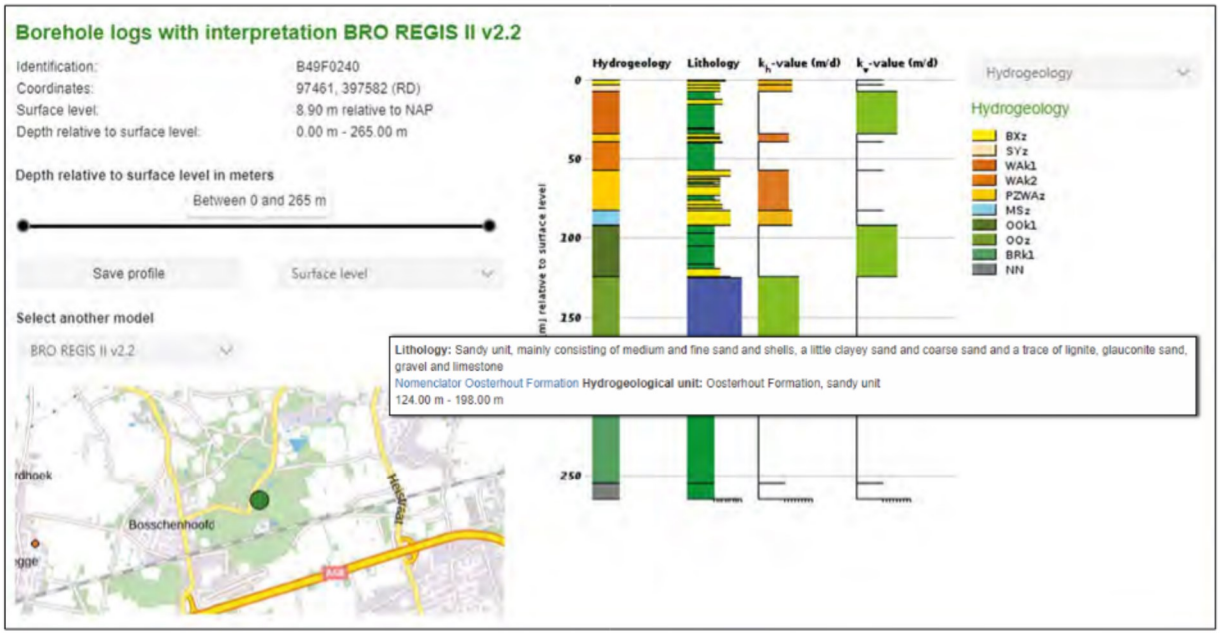


Figure 24.21. Borehole log with hydrogeological interpretation for the REGIS II model as displayed on the DINO web portal. The mouseover text offers a short lithological description of the hydrogeological layer as well as a link to the online Stratigraphic Nomenclature (TNO-GDN, 2022b) of the stratigraphic formation the unit belongs to.

Online viewer

The DINO web portal starts with a topographic map of the Netherlands. After selecting one of the models, a map of the extent of the model as well as the location of the boreholes used in the construction of the model is shown. The user can navigate through the map by zooming and panning or directly go to a location by using search-criteria such as borehole-ID's, (x,y)-coordinates or topographical names. Clicking on a borehole location opens a panel revealing the *borehole log* including the interpretation that is relevant for the selected model (Fig. 24.21). By hovering the mouse over the borehole intervals, the user is presented with short descriptions on the lithology and the interpreted units. In the case of stratigraphic units, a link to the full description of the unit in the online Stratigraphic Nomenclature (TNO-GDN, 2022b) is provided (see Fig. 24.21).

A simple point-and-click tool allows the user to create a *synthetic or virtual borehole* at any location in the model. For the DGM and DGM-deep models, the synthetic borehole shows the vertical succession of geological units at the selected location. In case of REGIS II, hydrogeological units are complemented with vertical plots of conductivity (k_h and k_v) as well as transmissivity of the sandy units and hydraulic resistance of the clayey layers (Fig. 24.21). A synthetic borehole through GeoTOP corresponds to a vertical voxel-stack where voxels are colour-coded with the two main attributes (stratigraphy and lithological class) as well as the probabilities of each lithological class (Fig. 24.22). As with the borehole logs, mouseover texts provide short explanations and, if applicable, a link to the Stratigraphic Nomenclature.

Another tool allows the user to create *vertical cross-sections* at any location similar to those shown in Fig. 24.11. A cross-section through the GeoTOP model offers the opportunity to select and display any of the attributes of the model.

Lastly, *maps* of the (hydro)geological units can be viewed. A map view is accessed via the cross-section by hovering over the appropriate unit. A mouseover text appears, including links to the different maps: depth to base for DGM-deep; top, base and thickness for the three shallow subsurface models and additional maps of hydraulic properties and the associated uncertainties for REGIS II. The map is zoomed in on the location of the cross-section, but the user may zoom or pan to other areas. If applicable, fault trajectories are plotted on top of the maps of the shallow subsurface models.

SubsurfaceViewer®: the 3D geological map

Detailed stratigraphic-lithological models such as GeoTOP may be regarded as 3D geological maps, complementing or replacing their 2D predecessors (Stafleu et al., 2021a).

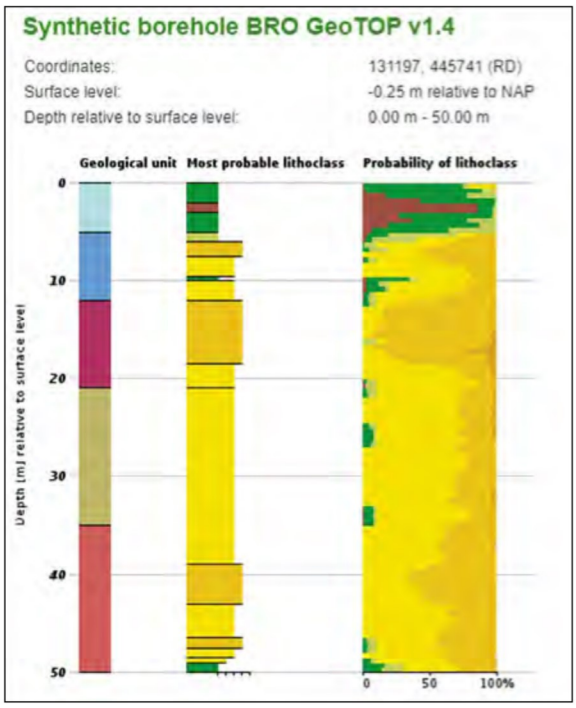


Figure 24.22. *Synthetic borehole or vertical voxel-stack taken from the DINOloket web portal showing the vertical succession of voxels at a location selected by the user. The rightmost plot shows areas with a high probability and hence low uncertainty (peat layers close to land surface, coarse sand at ca. 15 m), as well as a zone of high variability in lithological class (from 5 to 12 m). For legend of the lithological classes see Fig. 24.16.*

Schokker et al. (2015) used a case study in Amsterdam to demonstrate how 3D visualizations of DGM and GeoTOP create a better understanding of the distribution, thickness and interrelation of the geological units than seen on 2D maps. The SubsurfaceViewer® software, developed by INSIGHT Geologische Software GmbH (Sobisch, 2011), allows for full 3D visualization. The software is offered as a free download on the DINO web portal (www.dinoloket.nl/en) along with predefined cut-outs (usually blocks of 20 x 25 km) of the DGM, REGIS II and GeoTOP models (Stafleu et al., 2013, 2021a). DGM-deep is delivered in two parts: onshore and offshore. The SubsurfaceViewer® includes both a classical map view, a cross-section view and an interactive 3D view (Fig. 24.23). In addition, the SubsurfaceViewer® offers displays of borehole logs as well as synthetic boreholes. Boreholes, cross-sections, geological layers and voxels can all be visualized in 3D, and users can query the voxel model by selecting lithostratigraphic units, lithological classes, and/or probabilities.

NetCDF: 3D arrays

From a computational perspective, both the layer-based raster models and the voxel models may be regarded as

3D-arrays with numbers representing geological units or other attributes. NetCDF (Network Common Data Form; Unidata, 2022) is a data format that supports the creation, access, and sharing of array-oriented scientific data. The online viewer described above draws from NetCDF-files of the models, allowing real-time construction of synthetic boreholes and vertical cross-sections. NetCDF-files of REGIS II and GeoTOP are published on the GDN's OPeNDAP-server (www.dinodata.nl/opendap), allowing users to select an area of interest and download that part of the model as a NetCDF file. The file can then be used as input for software, e.g. in Python-scripts (for users with programming skills) or in off-the-shelf software. An example of the latter is ArcGIS Pro® (Esri, 2020) which has NetCDF-based voxel-functionality, allowing full interactive 3D visualization of GeoTOP (Fig. 24.24). The voxel-functionality includes selections, slicing, the creation of vertical cross-sections and adjusting the vertical exaggeration.

2D map products

GDN's standard model delivery consists of a downloadable dataset (zip-file) with the individual components of the model. The dataset of DGM-deep comprises a set of raster maps in two different ascii-formats: Esri's Ascii-grid and ZMap Plus, the latter format is commonly used in oil and gas Exploration. The layer-based models of DGM and REGIS II, as well as the underlying layer-based model of GeoTOP, are delivered as rasters in Erdas Imagine format, which performs better in desktop GIS software than Ascii-grids. The geometry of DGM, REGIS II and GeoTOP is described in rasters of top, base and thickness and their associated model uncertainties (standard deviations). In case of REGIS II, the download provides additional raster layers of the hydraulic properties (e.g. k_h, k_v) and the associated uncertainty.

Figure 24.25 shows an example of the set of raster maps of a single geological unit in the DGM model. All 2D raster layers can be viewed and analysed in standard GIS software packages. Borehole data are included in tabular form as well as in GIS point features; fault trajectories are included as line features. The GIS data are accompanied by ArcMap documents that serve as a legend presenting the (hydro)geological layers in the correct stratigraphic order and with an appropriate colouring scheme.

The download of GeoTOP is complemented with the voxel-data in a simple Ascii-format comprising the (x,y,z)-coordinates of each voxel-midpoint and the corresponding attribute values of the voxel. To facilitate the use of the 3D voxel-data in a 2D GIS environment, horizontal slices through the two main attributes of the voxel model (stratigraphy and lithological class) are provided as well. These

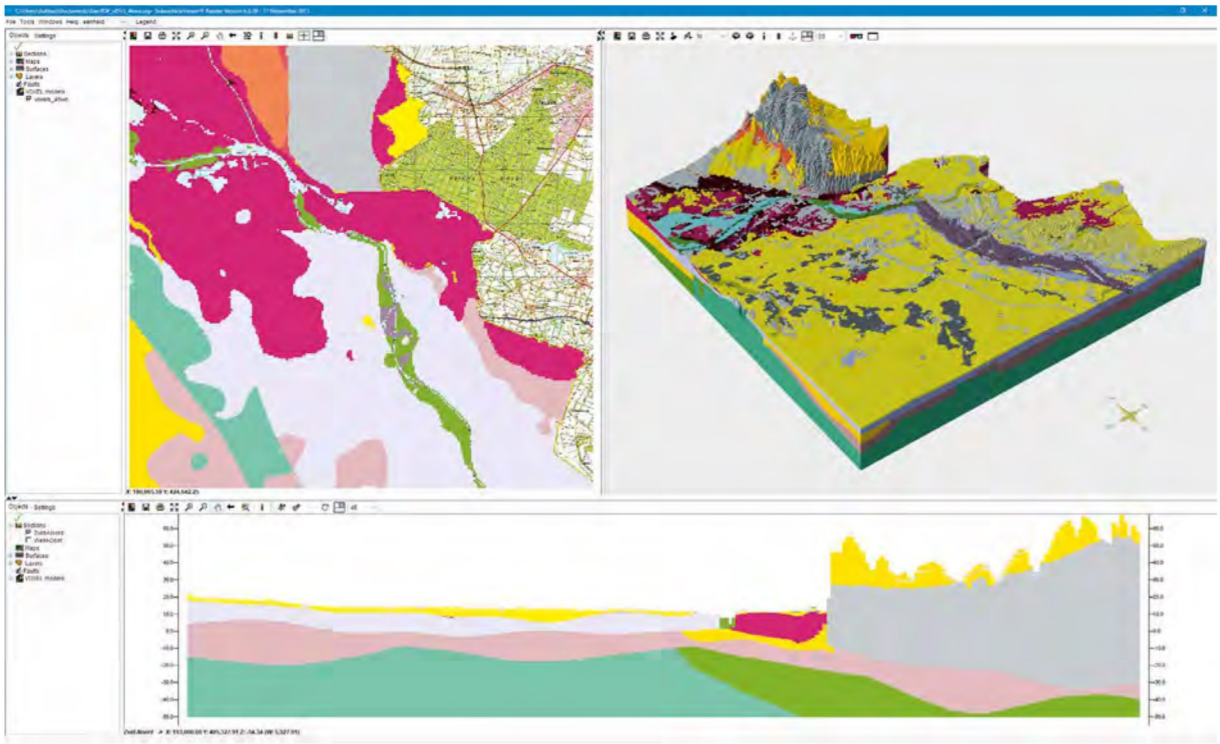


Figure 24.23. *Screenshot of the SubsurfaceViewer® with map view (top left), cross-section view (bottom) and interactive 3D view (top right) of a block of 26 x 25 km cut from the GeoTOP model in the area south of Nijmegen. Colours display the lithostratigraphic units the voxels belong to.*



Figure 24.24. *Part of the GeoTOP voxel model as a NetCDF file visualized in ArcGIS Pro® (Esri, 2020).*

2D slices show the voxels at a certain depth below NAP (Dutch ordnance datum) or below surface level. Figure 24.26 shows an example of slices through the lithological class model at depths of 0, 2, 4, 6, and 8 m below surface level.

The three subsurface models that are part of the key registry of the subsurface (BRO) are accompanied by formal documentation (in Dutch), including extensive descriptions of the modelling procedure (*Totstandkomingsrapport*) as well as the quality control process (*Kwaliteitstoetsingsdocument*). The data structure of each model is formally described in a data catalogue (*Gegevenscatalogus*), including an UML-based class diagram of the objects (e.g. boreholes, layers, voxels) and definitions of these objects as well as their attributes and mutual relationships.

2D maps from vertical voxel-stack analysis

Other 2D raster maps are created by selectively querying the 3D voxel model by using a vertical voxel-stack analysis (Dambrink et al., 2014, 2015; Stafleu et al., 2021a). Maps based on vertical voxel-stack analysis are a step closer to the user's own area of expertise than the geological models themselves. A vertical voxel-stack analysis processes the voxels at a particular (x,y)-location from the uppermost voxel (at land surface) down to the lowermost one (at the bottom of the model), selecting voxels by their attributes like stratigraphy, lithological classes or depth. The result is a single summary value for the (x,y)-location of the stack. By repeating this procedure for all voxel-stacks in the model, a 2D raster map is created with cells measuring 100 x 100 m and attributed with the summary value. Three examples are: a surface geological map (Fig. 24.27a), a map showing the cumulative thickness of peat in the Holocene deposits (Fig. 24.27b), and a generalized soil composition map of the upper 8 m (Fig. 24.27c). The examples given are straightforward and relatively easy to calculate. Maps resulting from more complex voxel-stack analyses include a land subsidence prediction map (Fig. 24.20) and a seismic site-response zonation map (Fig. 24.31).

Innovative modelling methods and case studies

Towed Transient Electro-Magnetic technique (tTEM)

Electromagnetic (EM) techniques map electrical resistivity contrasts in the subsurface in three dimensions (Kirsch, 2009). This geophysical technique allows for rapid surveying of large parts of the subsurface and is extensively used in hydrogeological applications. The collected data are processed to obtain an electrical resistivity model that is subsequently interpreted into geology or groundwater quality. Saline groundwater is a good conductor and in coastal areas it is often an important target in EM mapping. Sediments that contain clay minerals are also good conductors and the distinction between clay and sand can

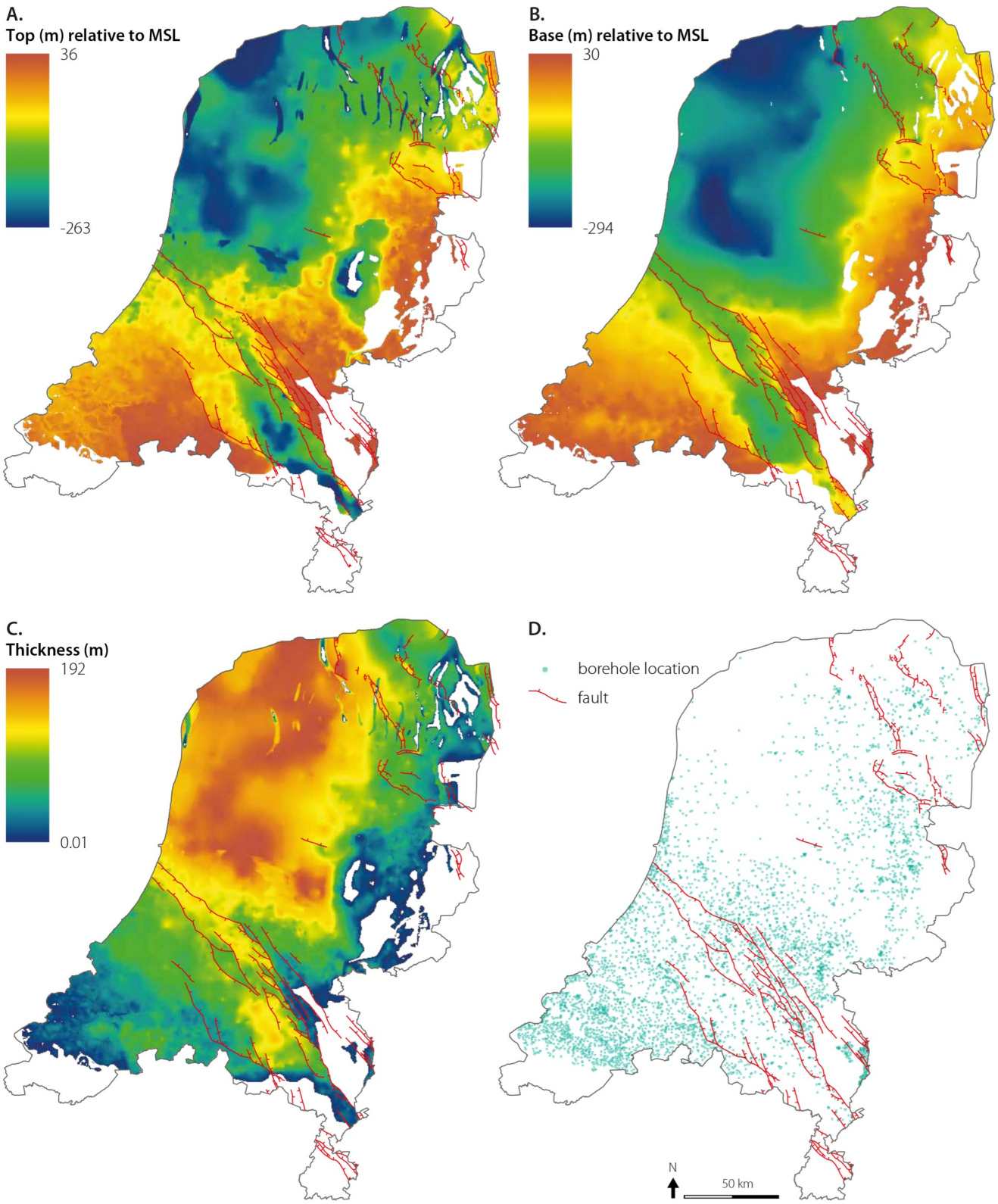


Figure 24.25. *Four raster maps containing the model data of a single geological unit in the DGM model: a) top of the unit; b) base; c) thickness and d) borehole locations where the unit was interpreted. Additional maps of the model uncertainty of top, base and thickness are also available.*

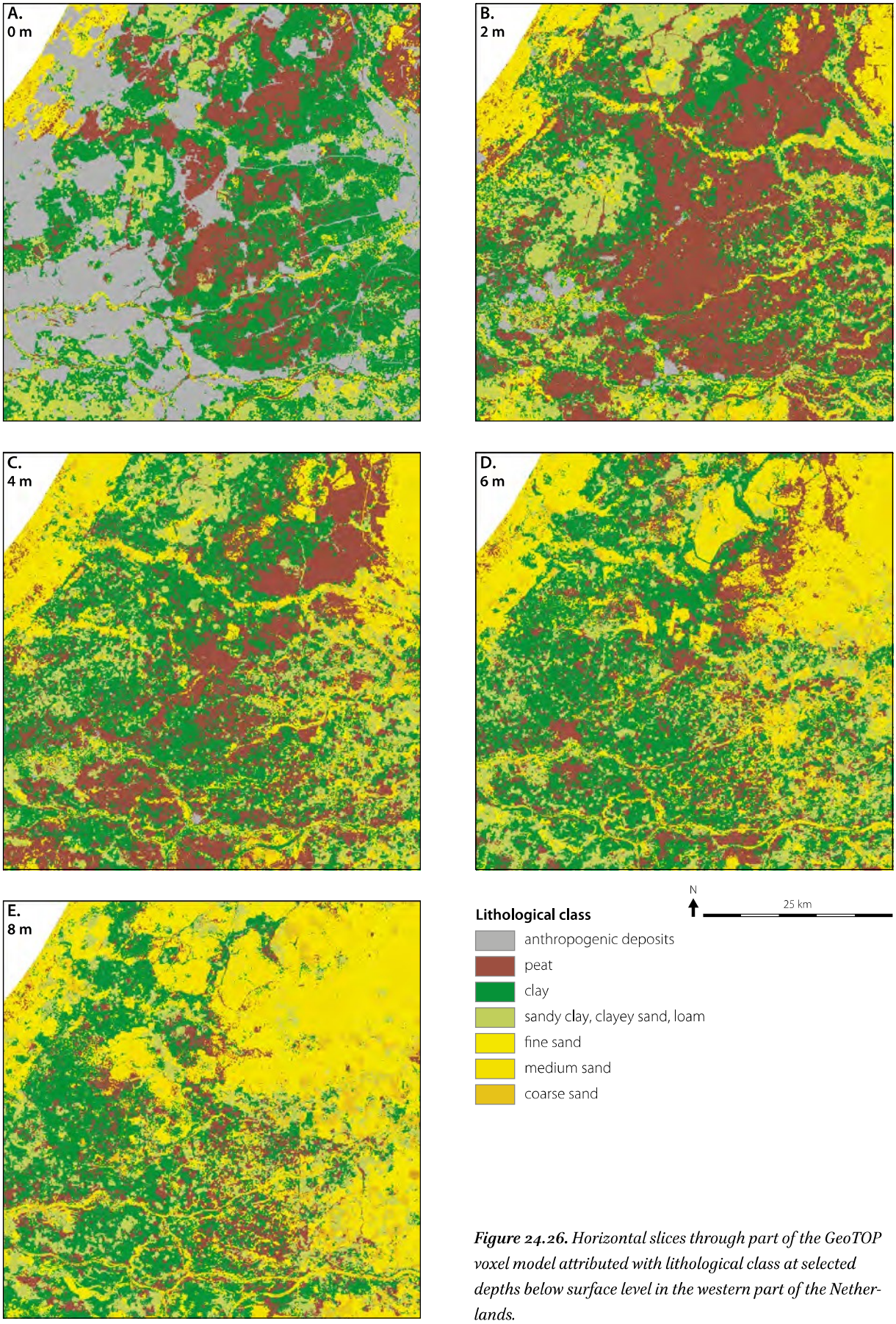


Figure 24.26. *Horizontal slices through part of the GeoTOP voxel model attributed with lithological class at selected depths below surface level in the western part of the Netherlands.*

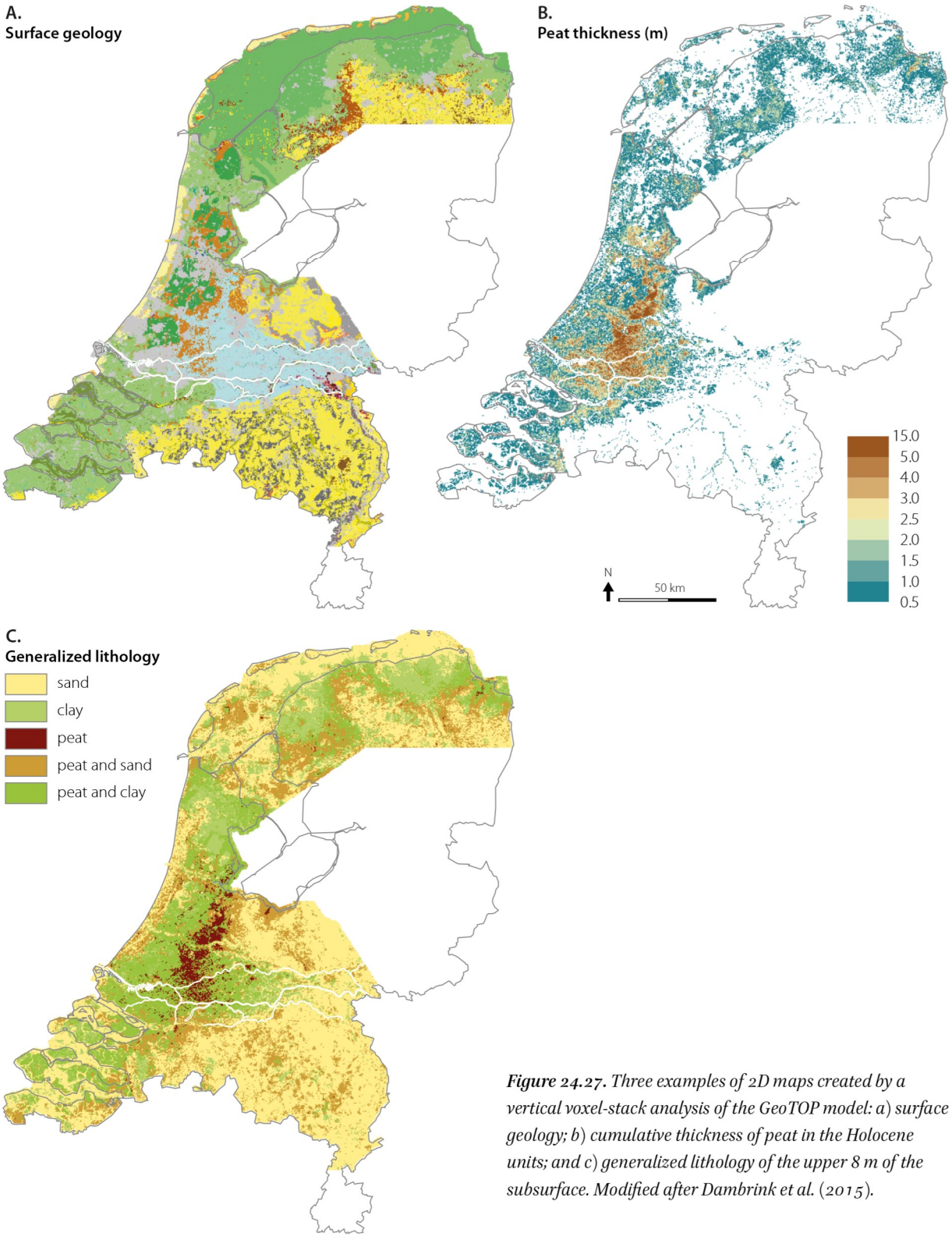


Figure 24.27. *Three examples of 2D maps created by a vertical voxel-stack analysis of the GeoTOP model: a) surface geology; b) cumulative thickness of peat in the Holocene units; and c) generalized lithology of the upper 8 m of the subsurface. Modified after Dambrink et al. (2015).*

often be inferred from the EM signal. The great benefit of the non-invasive EM technique is the ability to measure changes in electrical resistivity (and hence conductivity) with depth, resulting in a 3D model of the subsurface. Expert knowledge of the regional geology and geohydrology, together with existing (borehole) data is of paramount importance for the interpretation. The technique is sensitive to disturbance caused by metal objects (fences, pipelines) and cables that transport electricity, both in the ground and overhead.

The towed Transient Electro-Magnetic technique (tTEM) has been developed to acquire data down to 60-80 m depth by driving the instrument behind an ATV (Sandersen et al., 2021; Fig. 24.28). With a speed of 10-15

km/h, measurements are collected every 5 m. On larger fields, the distance between lines is typically 20 m, resulting in a dense network of data that is inverted into 1D electrical resistivity models, showing the variation of resistivity with depth. Interpolating 1D resistivity models into a 3D model allows for further interpretation in terms of geology and lithology. The tTEM system has been used to map the lateral continuity of clay layers in the province of Drenthe. A field campaign of 2.5 days resulted in almost 40 line-km of data in four different areas. In the results depicted in Figure 24.29 a semi-continuous layer of low resistivity (blue colours) is present, indicating a clay layer. A gas-pipeline is visible in the results causing an interference in the tTEM measurements.

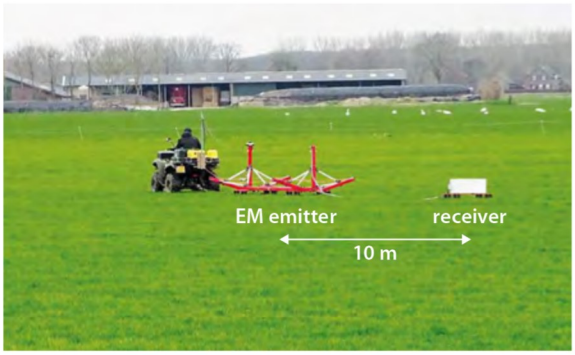


Figure 24.28. A tTEM system, consisting of an EM emitter and receiver towed by an all-terrain vehicle (ATV)..

Site-response assessments

Earthquakes can cause damage to buildings and infrastructure. This holds for natural earthquakes as well as for human-induced earthquakes such as those in the province of Groningen. The composition of the shallow subsurface plays an important role in the extent of the damage caused by earthquakes, because 'weak soils' such as peat, clay and clayey sand/sandy clay can amplify the amplitude of seismic waves. One of the factors related to this 'site-response' is the shear-wave velocity (V_s) of the shallow subsurface, which is often summarized in an average V_s -value for the upper 30 m (V_{s30}).

Kruiver et al. (2017a,b) combined the GeoTOP voxel model of the Groningen area and a set of 60 Seismic Cone Penetration Tests (SCPT's) into a V_s model of the area cov-

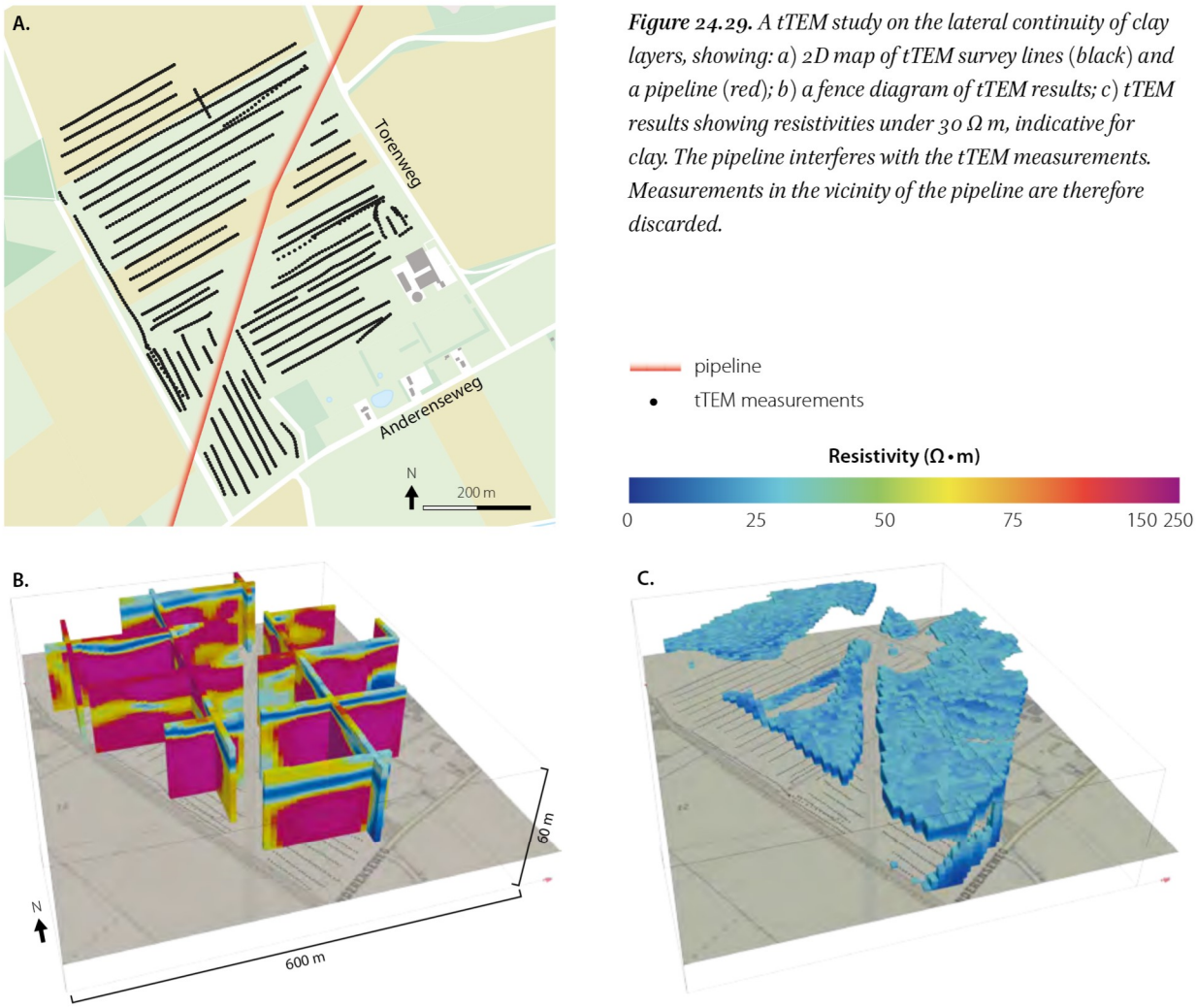


Figure 24.29. A tTEM study on the lateral continuity of clay layers, showing: a) 2D map of tTEM survey lines (black) and a pipeline (red); b) a fence diagram of tTEM results; c) tTEM results showing resistivities under 30 Ω m, indicative for clay. The pipeline interferes with the tTEM measurements. Measurements in the vicinity of the pipeline are therefore discarded.

ering the gas field and a buffer zone of 5 km. The SCPT's were used to establish statistical distributions (with mean and standard deviation) of V_s for each combination of lithostratigraphic unit and lithological class. In a number of combinations, it was possible to quantify a depth-dependent distribution (with slope and intercept). These distributions were used to assign a V_s value to each voxel in the model (Fig. 24.30). The resulting 3D V_s model shows how V_s generally increases with depth and contrasts soft Holocene deposits with low V_s with predominantly stiff Pleistocene deposits with high V_s. Vertical voxel stacks attributed with V_s and other soil properties were used as input for site amplification predictions (Kruiver et al., 2017a,b; Stafleu et al., 2021a).

Natural and induced earthquakes may also occur outside the Groningen area. Stafleu et al. (2022) created a preliminary V_{s30} map of the Netherlands based on the V_s measurements from the Groningen area. Van Ginkel et al. (2022) developed a national seismic site-response zonation map of the Netherlands, designed for low-magnitude induced earthquakes. Sediment profiles typical for the Dutch shallow subsurface were categorized into five classes, each representing a level of expected amplification. The mean amplification for each class, as well as its variability, was quantified using data from 66 sites with measured earthquake amplifications and 115 sites with amplifications estimated from ambient vibrations. The zonation map was subsequently derived from GeoTOP by assigning a sediment class to each vertical voxel stack in the model (Fig. 24.31). In areas where GeoTOP is not yet available, TNO-GDN's voxel model NL3D (Van der Meulen et al., 2013) was used.

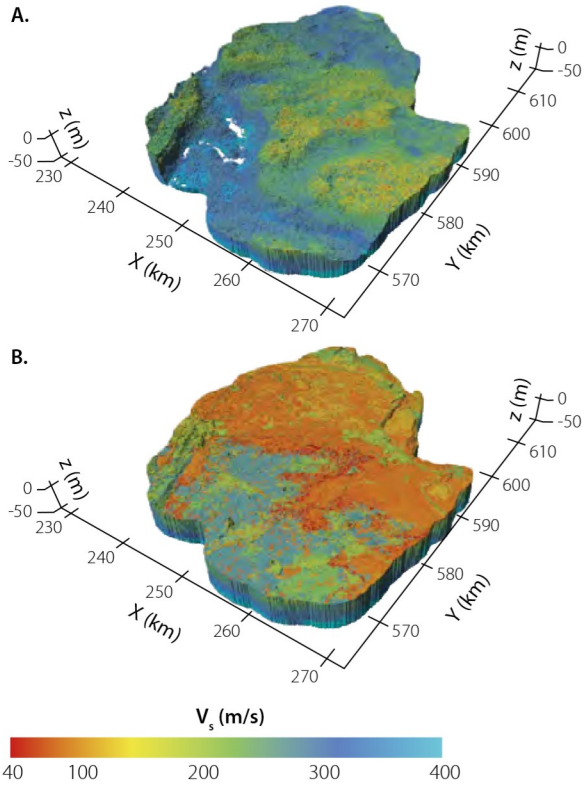


Figure 24.30. *GeoTOP model of the Groningen area covering the gas field and a buffer zone of 5 km. Voxels are attributed with shear wave velocity (V_s) derived from V_s measurements in Seismic Cone Penetration Tests (SCPT's): a) the lower part of the model showing the glacial Peelo Formation with relatively high V_s values; b) the full model revealing Holocene deposits with relatively low V_s values. After Kruiver et al. (2017b).*

ThermoGIS

ThermoGIS (www.thermogis.nl) is a public, web-based geographic information system supporting companies and the government in developing geothermal energy in the Netherlands (ThermoGIS, 2022). ThermoGIS provides depth, thickness, porosity and permeability maps of many potential aquifers in the Netherlands. Geothermal performance maps are calculated with the use of an integrated, stochastic, techno-economic performance module. The most important outputs of ThermoGIS are geothermal potential maps of the Netherlands that can be consulted in a map viewer (Fig. 24.32).

The DGM-deep model is used as basis for the aquifer model for ThermoGIS v2.2. The depth and thickness of the aquifers within the stratigraphic groups of DGM-deep are constructed using information from a maximum of 3855 wells. For most aquifers, this is considerably more than the number of wells used for the calibration (well-tying) of DGM-deep. ThermoGIS v2.2 presents the geothermal potential for 30 individual aquifers, 5 stacked layers which consist of multiple aquifers within a stratigraphic group and an overview layer that integrates all aquifers (see ThermoGIS (2022) for an overview).

For future ThermoGIS updates it is foreseen that the shallow aquifers of the hydrogeological REGIS II model will be incorporated. This model includes aquifers within the Upper North Sea Group and uses the geological DGM-model for the shallow subsurface as a basis. The ThermoGIS workflow consists of numerous steps of which the three most important ones are: (1) modelling aquifer geometry; (2) estimating aquifer properties and a subsurface temperature model; (3) incorporating technical (doublet) and economic parameters.

Aquifer geometry – Modelling aquifer tops, bases and thicknesses in ThermoGIS has many similarities with modelling the geometry of the hydrogeological units in REGIS II. All aquifers within a DGM-deep unit are modelled with respect to the base of that unit, making ThermoGIS and DGM-deep fully consistent. In a reiterating

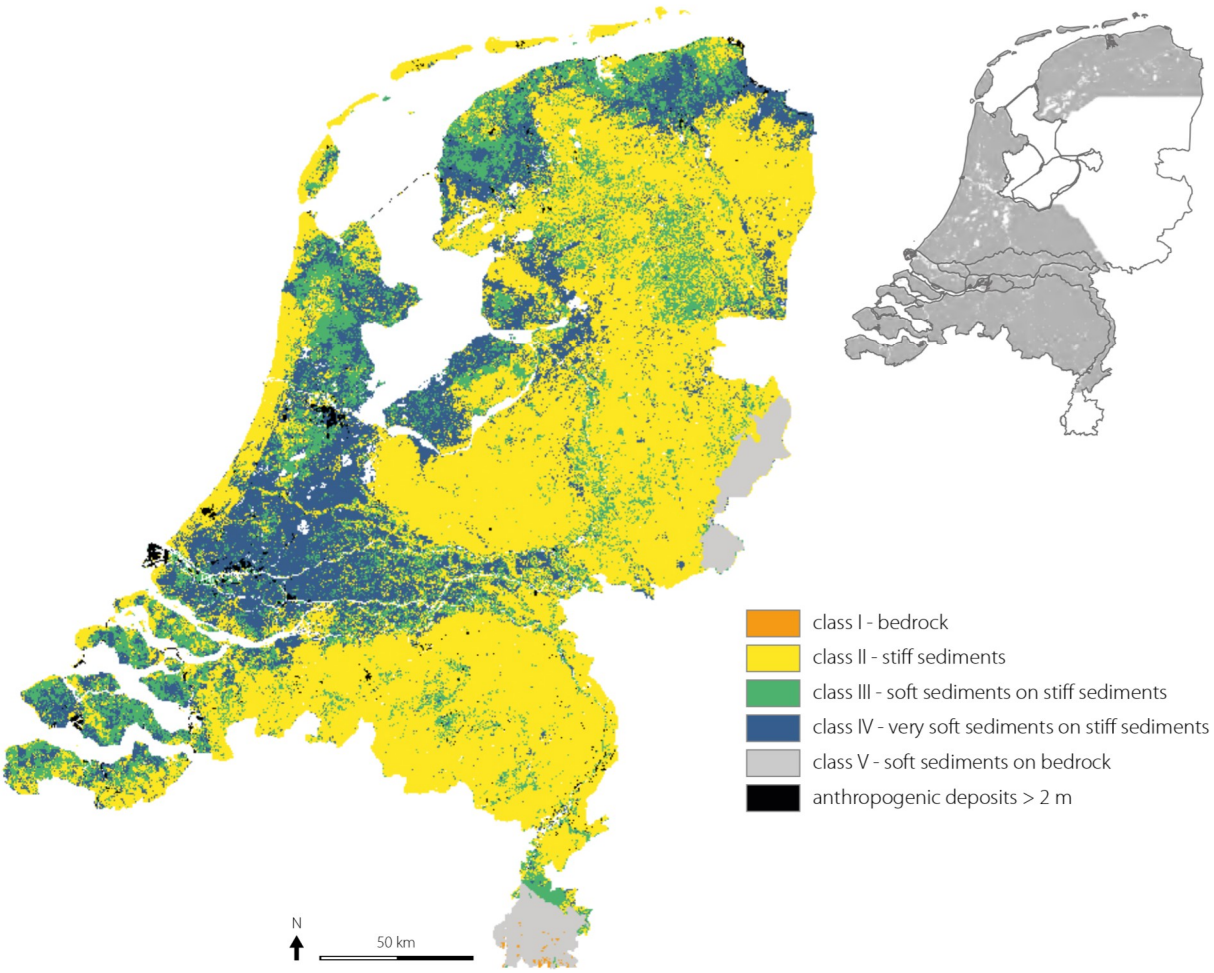


Figure 24.31. *Seismic site-response zonation map for the Netherlands designed for low-magnitude induced earthquakes. Inset map shows the current GeoTOP coverage; areas outside that area are based on the NL3D model. Colours represent the five sediment classes I through V. Areas where anthropogenic deposits exceed 2 m in thickness remain unclassified. After Van Ginkel et al.* (2022).

process, the bases of the aquifers are derived by interpolating the difference between base of the aquifer from well data and the base of the group-level grid and adding it to the latter. Subsequently, the interpolated thickness is added to obtain the top of the aquifer. Multiple aquifers are stacked then between groups' base and top. The interpolation process is assisted by maps with the maximum spatial extent of each aquifer, pinch-out polygons indicating where the thickness converges to zero, and non-pinch-out polygons where the regional thickness trend is retained. In this process, also faults and the overall structural setting of the aquifer are taken into account. For interpolation the convergent gridding algorithm in Petrel® is used. In addition, thicknesses are stochastically modelled using kriging and the resulting variance is subsequently used to calculate P10 and P90 thickness maps. Each aquifer is modelled independently of the position of other aquifers. An integrated and consistent aquifer model is constructed by stacking the aquifers and correcting for intersections.

Aquifer properties and temperature model – For each aquifer, ThermoGIS uses vertically averaged well porosities and permeabilities that are either based on core plug measurements or calculated from petrophysical evaluations and well tests. The porosity-depth relationship is calibrated using burial anomaly maps so as to create country-wide porosity maps. Core-plug derived porosity-permeability relationships (phi-k trends) are used to construct permeability maps and subsequently, the heat in place (HIP) is calculated by using the net thickness, permeability and temperature of the aquifer. The net thickness of the aquifer is determined by multiplying the gross thickness with a net-to-gross ratio. Due to the lack of a reliable and consistent net-to-gross database, a single value was determined for each aquifer based on geological knowledge and available data. The aquifer temperature comes from a 3D temperature model of the Dutch subsurface (Bonté et al., 2012) that was recently updated using new geological and technical results from Békési et al. (2020).

Incorporation of technical (doublet) and economic parameters – In a subsequent step, additional technical (doublet) and economic parameters are incorporated to derive the technical and economic potential and the potential recoverable heat (for more information on these parameters, see Mijnlieff et al., 2025, this volume). The potential maps can be interactively consulted on the ThermoGIS website (ThermoGIS, 2022; Fig. 24.32). The user can either choose for a general overview showing the total potential or a more detailed view where the above-described inputs and outputs of individual aquifers can be considered. In addition, the user can manually alter the technical parameters for site-specific fine-tuning.

High resolution 3D models

Some applications require more detailed information on lithological heterogeneity than is provided by the national subsurface models described in this chapter. An example is the large scale reinforcement by the regional water authority *Hoogheemraadschap De Stichtse Rijnlanden* (HDSR) of the northern Lek River dike. This dike is an important safety measure that keeps a densely populated and economically vital part of the Netherlands safe. The shallow subsurface surrounding the dike consists of a complex alternation of Holocene Rhine sandy channel belt deposits, clayey floodplain deposits and levees or crevasse deposits composed of silt, sand and clays of the Echteld Formation that alternate with peat beds of the Nieuwkoop Formation (Erkens, 2009; Dabekaussen et al., 2019; Fig. 24.33). The Holocene sediments overly a sandy Pleistocene (and locally Early Holocene) substrate of the Kreftenheye Formation with a distinct loam layer at the top (Kreftenheye Formation, Wijchen Member).

Depending on the lithology, different dike-failure mechanisms may play a role. For instance, permeable sand bodies increase the risk of piping, whereas soft soils are prone to macro-instability. Therefore, HDSR needs detailed information on the deposits underneath the dike in order to design location specific and fit-for-purpose reinforcement measures. Incorporating detailed geological information in planning increases confidence in estimating the chance of possible dike failure, potentially leading to an increase of the estimated strength of the dike and thus lower costs by avoiding unnecessary reinforcements.

As more detailed 3D insights into the subsurface below and directly surrounding the dike were needed, the existing GeoTOP dataset was expanded to make a new model with a higher resolution. The required data density was reached by extending the existing GeoTOP dataset (comprising ca. 3600 boreholes) with ca. 1200 additional borehole descriptions from Utrecht University (Cohen, 2017) and by adding ca. 2100 Cone Penetration Test (CPT) results. CPT's, which were not used in the earlier GeoTOP model, are a common geotechnical measurement that determine the strength of the soil. It is a quick and inexpensive measurement that is widely used in soft-sediment

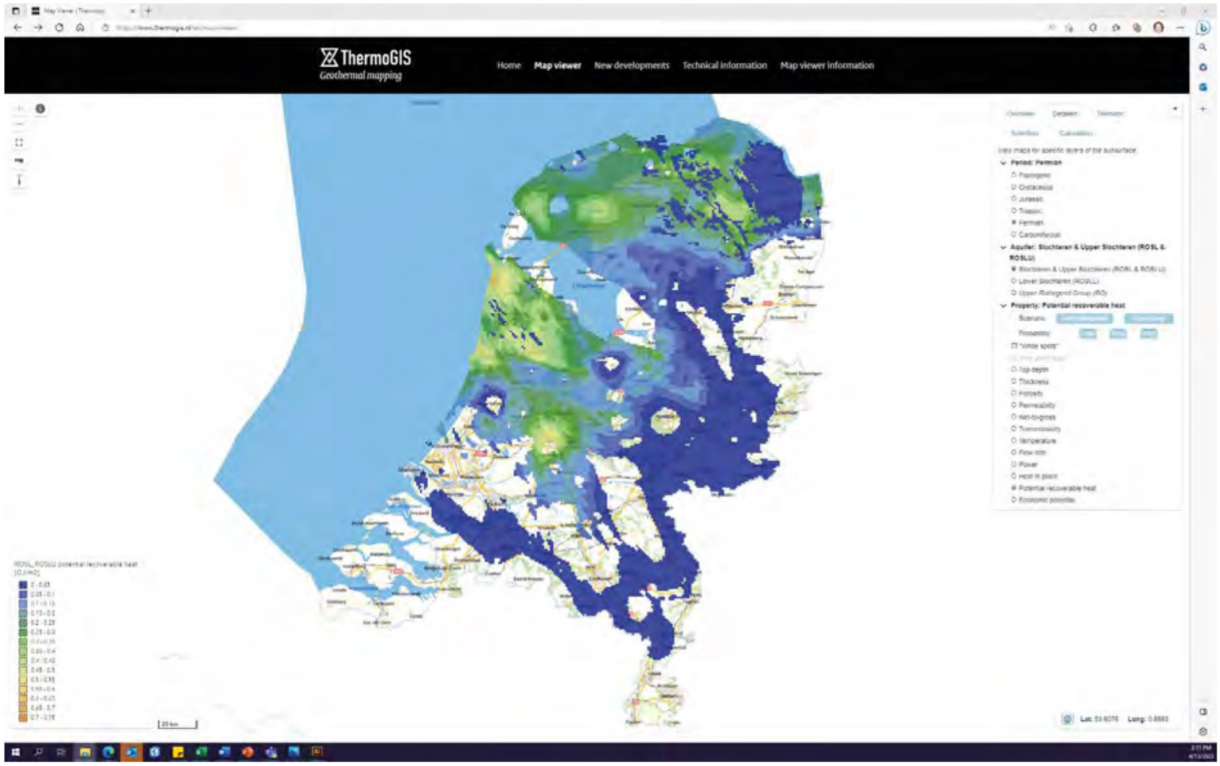


Figure 24.32. *The ThermoGIS Map viewer (ThermoGIS, 2022).*

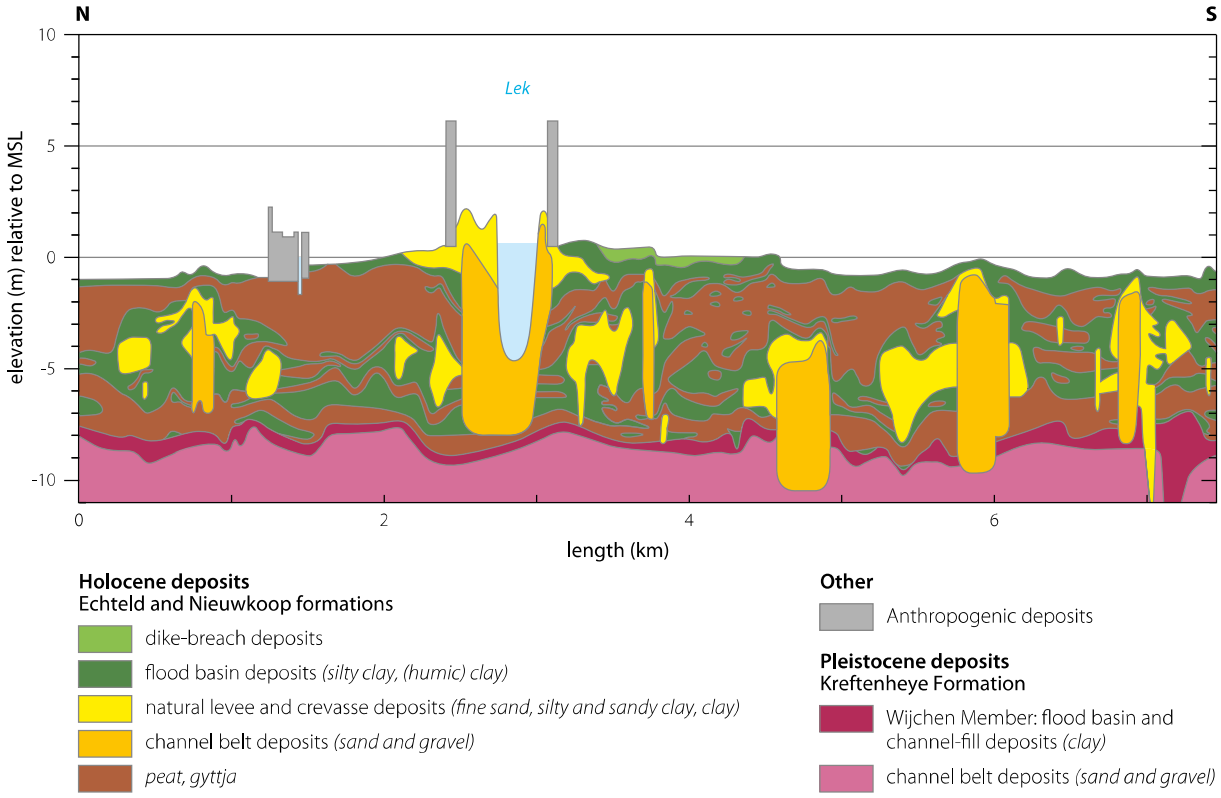


Figure 24.33. *Cross-section through the Holocene and uppermost Pleistocene sediments directly surrounding the dike of the Lek River. Modified after Erkens (2009).*

environments for infrastructural research (roads, railways, dikes) and in the built environment. This combined dataset allowed us to refine the resolution of GeoTOP from 100 x 100 x 0.5 m to 25 x 25 x 0.25 m.

The existing GeoTOP workflow that was followed (Stafleu et al., 2011a, 2021a) allows borehole information to be processed, but not CPT results, which were therefore translated to lithological information. The characteristics of the CPT measurements (cone resistance, sleeve friction, pore water pressure) can be used as proxies for lithology. To establish the relationship between CPT parameters and lithology, there is the classical approach by Robertson (2010) or machine learning approaches. In the case of the Lek River dike, an Artificial Neural Network (ANN) was employed. More than 200 borehole-CPT pairs within the study area (within a distance of 10 m from each other) were used as a training set for the neural network. This allowed for pairing lithological information from the borehole with the CPT parameters at corresponding depths (Fig. 24.34). The trained neural network was used to translate CPT friction ratio and cone resistance to lithological class and so create 'pseudo' borehole-descriptions at all CPT locations. The translated CPT's, together with the borehole-descriptions were used as input for the layer model and the voxel model in a similar way to the national GeoTOP model.

Comparing the high resolution model with the GeoTOP model (Fig. 24.35) clearly shows the level of detail that can be seen in the new high resolution model. Figure 24.35 demonstrates that spatial distribution and correlation of the different lithological classes is improved with higher data density. Furthermore, the higher resolution allows for a better representation of local sediment bodies, e.g. channel belt and crevasse deposits. The increased insight into the spatial distribution of the various lithologies aids the decision-making process of the regional water authority.

High resolution subsurface modelling, as exemplified above, has the potential to form the basis of many other applications. For instance, the voxels could be populated with geotechnical parameters, opening a way forward for 3D calculations of subsurface characteristics. Further development could also be found in methods to quickly update the model with new data, allowing users to add new measurements to the existing model.

Perspectives for systematic subsurface modelling in the Netherlands

From map sheets to projects

Initiated around the turn of the century, subsurface modelling by TNO-GDN has gradually become as mature an

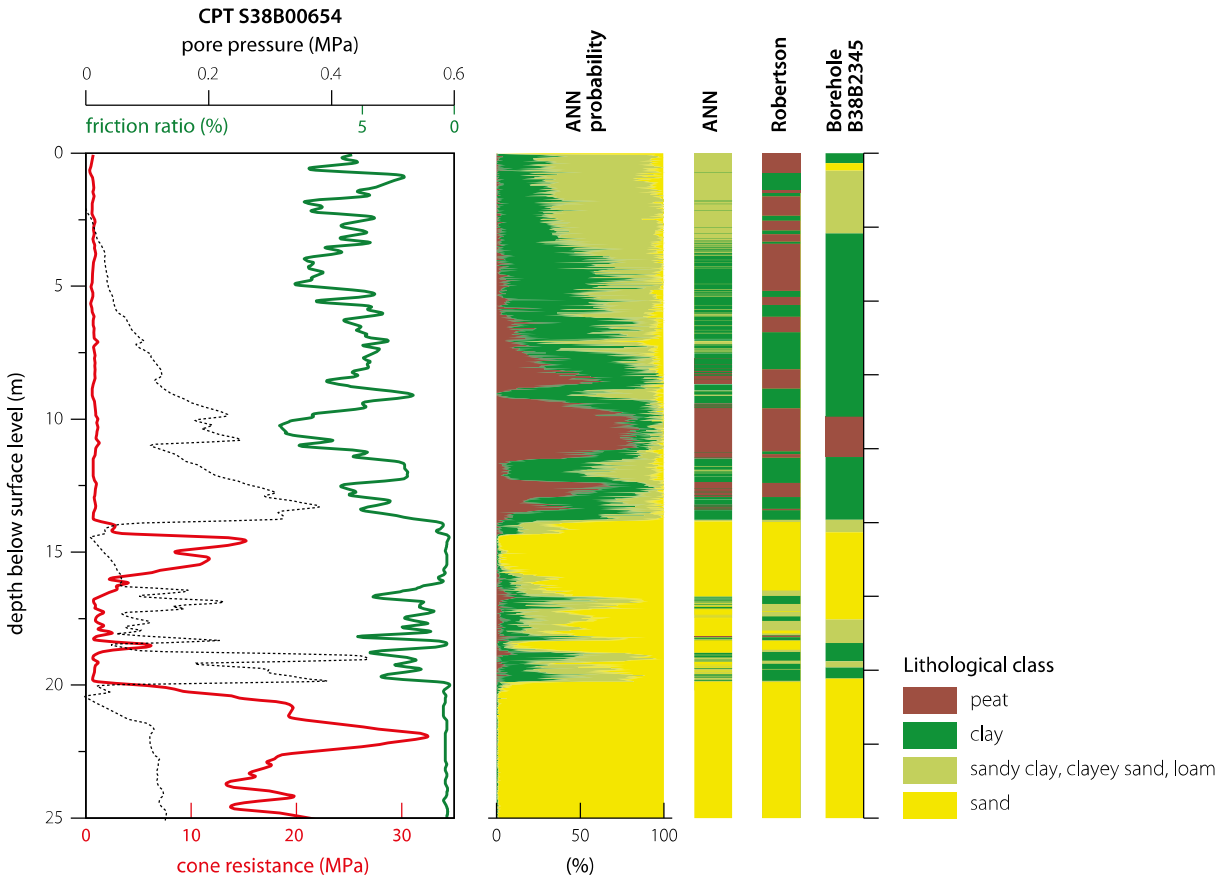


Figure 24.34. *Interpretation of Cone Penetration Test (CPT) measurements (cone resistance, sleeve friction, pore pressure and depth below surface level) into lithological classes using an Artificial Neural Network (ANN). Shown is a CPT-borehole pair not used for training of the ANN. The raw ANN output consists of lithological class probabilities, which are used to determine the most likely lithological class. For comparison both a classic interpretation (Robertson, 2010) and lithology as logged in a nearby borehole are shown. Modified after Dabekaussen et al. (2021).*

effort as the preceding surface geological mapping programmes it replaces (Van der Meulen et al., 2015). A systematic approach, standards and quality control have been developed and implemented in a suite of modelling programmes that each provide a balance between consistency over time and space on the one hand and the need to innovate on the other, as geological understanding and particularly modelling technology evolve continuously.

TNO-GDN is now entering a next stage. The first rounds of shallow subsurface modelling (GeoTOP, DGM and REGIS II) were similar to traditional mapping projects in having a regional focus. In the surface mapping era, data collection, interpretation and actual map sheet production were connected activities, and planned accordingly. In the first twenty years of subsurface modelling, the Geological Survey primarily relied on data collected in the 20th century and, working area by area was the natural continuation of the decades-old practice of working map sheet by map sheet. In the coming years however, our entire data legacy will have been processed in this way, and updates of the individual models will make use of the new data from the key registry for the subsurface (BRO). Even though it is as yet too early to speculate about rates and volumes, two things are already clear: (1) the key registry is already growing much faster than our survey databases did over the past two decades, and (2) subsurface data will never again be generated map sheet by map sheet. Instead, projects – for example public construction and engineering works, soil quality assessments, and assessments of groundwater and other resources – will define the need for, and be the source of, subsurface data and information. This implies that TNO-GDN will have to update and improve their models in much smaller and more irregularly shaped patches than the original model areas. In a project-centred approach it would make sense to eventually work at variable resolutions instead of the currently employed one-size-fits-all specifications.

The energy transition

After the implementation of the key registry for the sub-

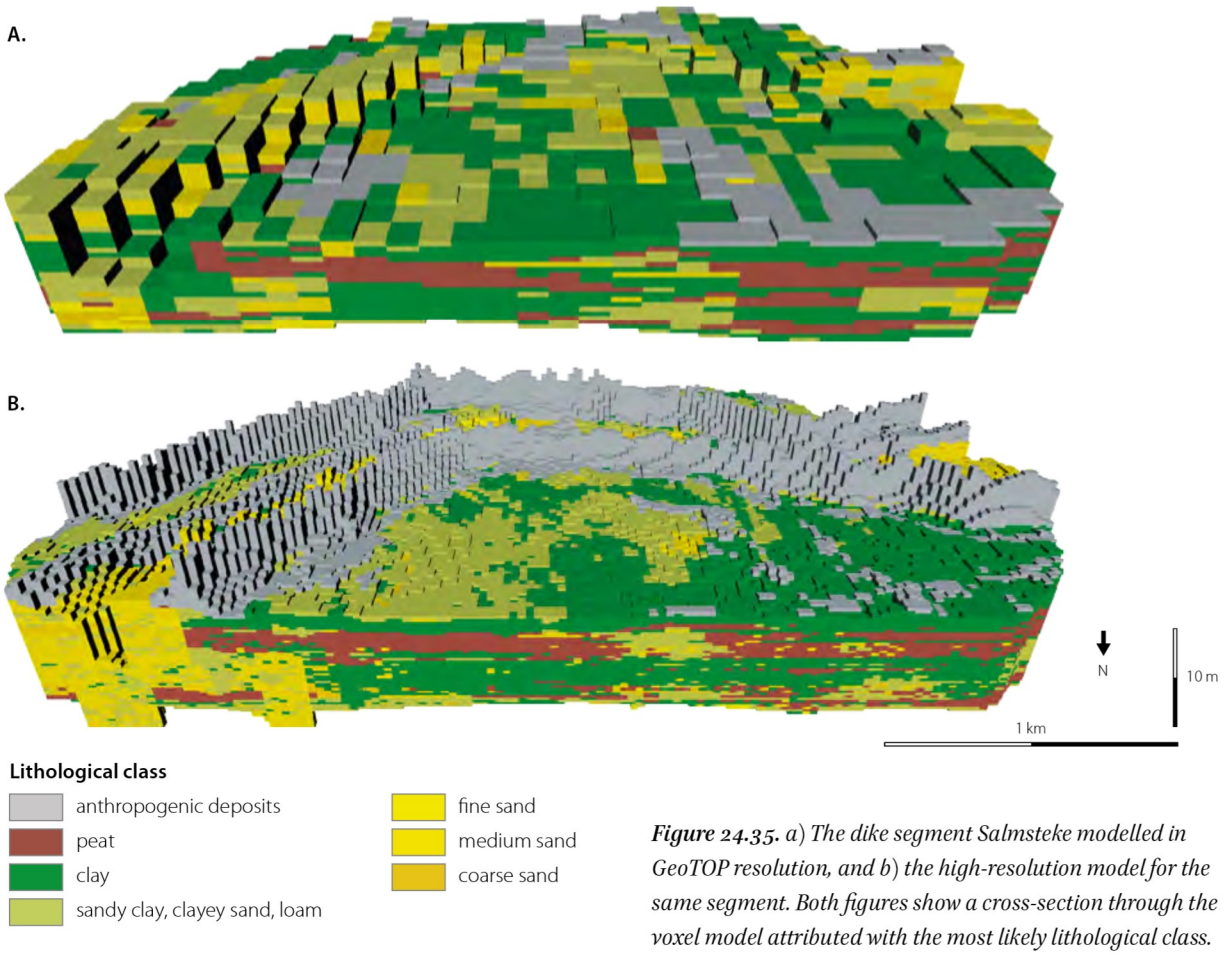


Figure 24.35. *a) The dike segment Salmsteke modelled in GeoTOP resolution, and b) the high-resolution model for the same segment. Both figures show a cross-section through the voxel model attributed with the most likely lithological class.*

surface, TNO-GDN's next major effort will be to attune deep subsurface modelling (DGM-deep) to the needs of the energy transition. The observational support, stratigraphic resolution and overall completeness of the survey's current models is more or less inversely proportional to subsurface use intensity. Figure 24.36 defines an 'energy transition blind spot' that exists, roughly, between 250 m down to which groundwater is abstracted, and the 2.5 to 4 km depth range, where most hydrocarbon extraction has been taking place.

This zone is now being explored for geothermal energy, and CO_2 storage potential, and other new forms of subsurface use. At the same time, groundwater is being abstracted from ever greater depths for environmental reasons. All in all, water and energy related uses of the subsurface, which used to be well-separated vertically, are now beginning to interact and compete for underground space, to the extent that for example the integrity of strategic groundwater reserves has become a concern (Anonymous, 2021). To facilitate optimal use of the subsurface, and to inform the associated public decision making, TNO-GDN has to follow suit and map this hitherto underexplored blind spot. This entails covering a larger volume of subsurface in greater detail, for which purpose the budget of TNO-GDN for mining-related information services has approximately been tripled. Geothermal operators generally have smaller exploration budgets than the hydrocarbon multinationals that are currently leaving the country. A successful Dutch energy transition does not only require a larger geological survey effort, it also presents the challenge to create an investment climate that is as favourable for geothermal energy development as it used to be for the hydrocarbon industry. In order to improve the information baseline the Dutch government initiated the SCAN programme, which consists of acquiring seismic and borehole data in areas that were hitherto underexplored because of a low hydrocarbon potential. It represents the first major public investment in exploration since the search for coal at the beginning of the 20th century (Van Waterschoot van der Gracht, 1918).

Contributing to full virtual representations of the physical environment

Guided by the concept of 'digital twinning', i.e. creating virtual representations of physical objects, the geoscience and geospatial communities currently strive to create more fully-fledged representations of the physical environment, combining the atmosphere, hydrosphere, built envi-

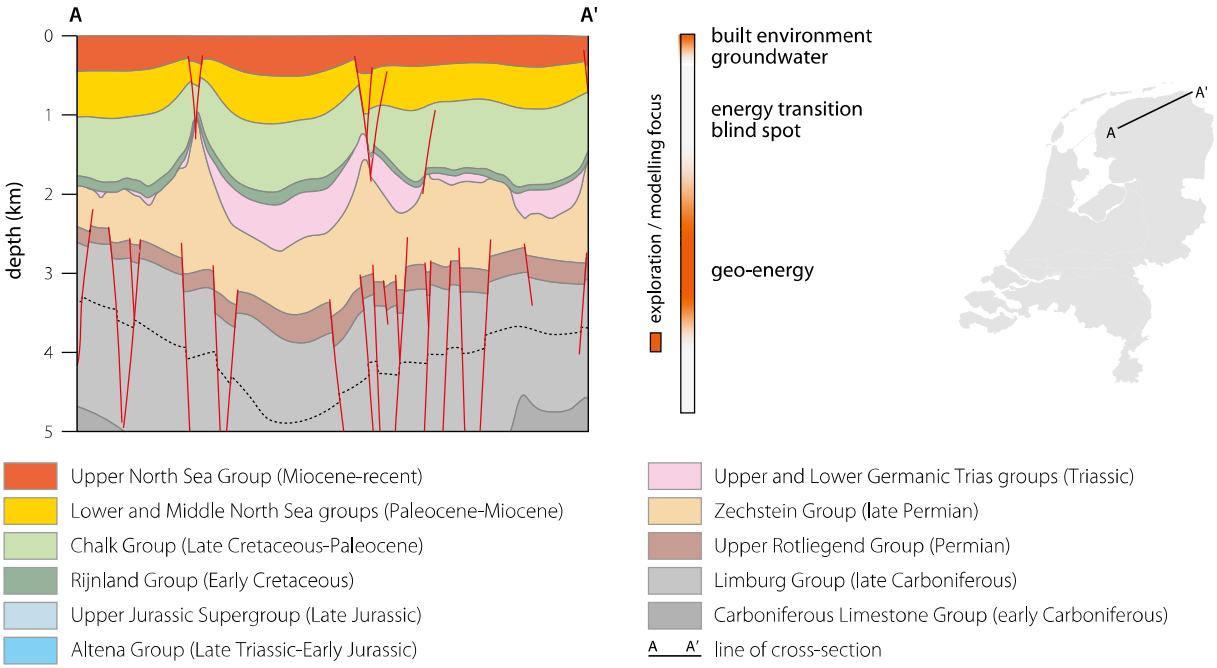


Figure 24.36. *An arbitrary cross-section in the northern Netherlands illustrating the relative depth of shallow (hydrogeological, environmental, geo-engineering) and deep (geo-energy) exploration and modelling, and the gap between the two ('energy transition blind spot'). Reprinted with permission from Van der Meulen et al. (2022).*

ronment and subsurface compartments (Van der Meulen & Bogaard, 2022). Up till now, science has predominantly captured the world in models, i.e. conceptual and/or mathematical representations of selected aspects and processes. In such a paradigm, it has been valid for TNO-GDN to produce individual models of geological strata or properties. However, a digital twin would represent a section of subsurface as an object with everything relevant included, geologically or otherwise. This could start with the integration of subsurface models that have coinciding or overlapping spatial extents, for example a static hydrogeological model such as REGIS II with groundwater flow and transport models. Obvious next steps, from a hydrological point of view, would be to incorporate bodies and streams of surface water, groundwater wells, pollution plumes, sheet pilings, infiltrations, and so forth. The result would then need to be connected to a virtual above-surface world, constrained by live data, and allowing for realistic human observations and interactions. It goes without saying that the current separate 3D models issued by TNO-GDN will be merged, at least at the layer-model level. Sets of geological units or selected depth ranges from the resulting integrated subsurface models could then be populated with parameters associated with the various applications.

Creating digital twins of the subsurface – or, to be more precise, creating digital twins of the physical environment including the subsurface – involves interactions across various disciplines. They would need to be built together with, and interrogated by, non-geoscientists who cannot be expected to use the geoscience data and models at face value. This, in its turn, calls for an increased effort, by TNO-GDN and the geoscience community in general, to inform the public about the subsurface, geological processes and the extent to which society relies on or affects them. As digital twins aspire to 'mirror' reality, they make much better presentations of the information they hold than visualizations of the abstract models that currently support public decision and policy making. In this way, they can bring scientific data and information much closer to the general public, adding legitimacy to, and trust in, decisions and policies based on them.

Acknowledgements

Ronald van Balen, Holger Kessler and Harry Doust are thanked for reviewing earlier drafts of this chapter.

Digital map data

Spatial data of figures in this chapter for use in geographical information systems can be downloaded here: https://doi.org/10.5117/aup.28165088.

References

Anonymous, 2021. Beleidsnota Drinkwater. Ministry of Instructure and Water Management (The Hague): 68 pp.

Békési, E., Struijk, M., Bonté, D., Veldkamp, H., Limberger, J., Fokker, P.A., Vrijlandt, M. & Van Wees, J.-D., 2020. An updated geothermal model of the Dutch subsurface based on inversion of temperature data. Geothermics 88, 101880, DOI: 10.1016/j.geothermics.2020.101880

Bonté, D., Van Wees, J.-D. & Verweij, J.M., 2012. Subsurface temperature of the onshore Netherlands: new temperature dataset and modelling. Netherlands Journal of Geosciences 91 (4): 491-515. DOI: 10.1017/S0016774600000354

Bosch, J.H.A., 2000. Standaard Boor Beschrijvingsmethode, Versie 5.1, TNO (Utrecht), Rapport No. NITG 00-141-A: 134 pp.

CAS, 2022. Climate Impact Atlas. Climate Adaptation Services (CAS). https://www.klimaateffectatlas.nl/en/

Chilès, J.-P. & Delfiner, P., 2012. Geostatistics - Modeling Spatial Uncertainty. Wiley & Sons (Hoboken, New Jersey): 699 pp. DOI: 10.1002/9781118136188

Cohen, K.M., 2017. Laaglandgenese boringendatabase Universiteit Utrecht. DANS. DOI: 10.17026/dans-zcv-knya

Dabekaussen, W., De Bruijn, R., Heerema, C., Kars, R.H., Lourens, A., Schokker, J. & Stafleu, J., 2021. Nieuwe hoge resolutie GeoTOP modellen en update-methodes voor een Sterkere Lekdijk. TNO (Utrecht), Report No. 2021 R12300): 57 pp.

Dabekaussen, W., De Bruijn, R., Kars, R.H., Meijninger, B. & Stafleu, J., 2019. GeoTOP voor Sterke Lekdijk. TNO (Utrecht), Report No. TNO 2019 R11929: 67 pp.

Dabekaussen, W., De Bruijn, R., Kars, R.H., Meijninger, B. & Stafleu, J., 2020. Integrating multiple geotechnical data types with machine learning to construct high-resolution 3D geological models. EGU General Assembly 2020-8500. DOI: 10.5194/egusphere-egu2020-8500

Dabekaussen, W. & Hummelman, H.J., 2021. Uncertainty of the Geological Framework Model of the Netherlands. Workshop Uncertainty Quantification and Visualization in Geological Modelling. Presented at the EAGE Annual conference, Amsterdam, The Netherlands.

Dambrink, R.M., Maljers, D., Schokker, J. & Stafleu, J., 2015. Tailor-made maps generated from 3D geological voxel models (Abstract). 2015 Annual Meeting of the Geological Society of America November 1-4.

Dambrink, R.M., Maljers, D. & Stafleu, J., 2014. Customised geological information derived from multi-purpose 3D voxel models. Presented at 12th Nederlands Aardwetenschappelijk Congres (NAC12) (Veldhoven).

De Jager, J., Van Ojik, K. & Smit, J., 2025. Geological development. In: J.H. Ten Veen, G.-J. Vis, J. De Jager & Th.E. Wong (eds): Geology of the Netherlands, second edition. Amsterdam University Press (Amsterdam): 21-51. DOI: 10.5117/9789463728362_ch01

Dijkstra, J.J., Comans, R.N.J., Schokker, J. & Van der Meulen, M.J., 2019. The geological significance of novel anthropogenic materials: deposits of industrial waste and by-products, Anthropocene 28: 100229. DOI: 10.1016/j.ancene.2019.100229

Duin, E., Doornenbal, J.C., Rijkers, R.H.B., Verbeek, J.W. & Wong, Th.E., 2006. Subsurface structure of the Netherlands; results of recent onshore and offshore mapping. Netherlands Journal of Geosciences 85 (4): 245-276. DOI: 10.1017/S0016774600023064

Erkens, G., 2009. Addendum1. Geological sections across the Lower Rhine valley (Germany) and Rhine-Meuse delta (the Netherlands). In: G. Erkens (ed.): Sediment dynamics in the Rhine catchment - Quantification of fluvial response to climate change and human impact. PhD thesis Utrecht University (the Netherlands), Netherlands Geographical Studies 388: 278 pp.

Feigenbaum, A.V., 1991. Total Quality Control. McGraw-Hill (New York): 3rd ed., Vol. 1, 372 pp.

Goovaerts, P., 1997. Geostatistics for Natural Resources Evaluation. Oxford University Press (New York): 483 pp.

Gunnink, J.L., Maljers, D., Van Gessel, S.F., Menkovic, A. & Hummelman, H.J., 2013a. Digital Geological Model (DGM): a 3D raster model of the subsurface of the Netherlands. Netherlands Journal of Geosciences 92 (1): 33-46. DOI: 10.1017/S0016774600000263

Gunnink, J., Maljers, D. & Hummelman, J., 2010. Quantifying uncertainty of geological 3D layer models, constructed with a-priori geological expertise. Presented at 14th Annual Conference of the International Association for Mathematical Geosciences, IAMG 2010 (Budapest).

Gunnink, J.L., Stafleu, J., Maljers, D. & Hummelman, J., 2013b. Hydraulic parameterization of 3D subsurface models: from measurement-scale to model-scale. In: Russell, H.A.J., Berg, R.C. & Thorleifson, L.H. (eds): Three-Dimensional Geological Mapping, Workshop Extended Abstracts. Annual Meeting of the Geological Society of America (Denver, Colorado): 35-39.

Hademenos, V., Stafleu, J., Missiaen, T., Kint, L. & Van Lancker, V.R.M., 2019. 3D Subsurface characterisation of the Belgian Continenal Shelf: a new voxel modelling approach. Netherlands Journal of Geosciences 98: e1. DOI: 10.1017/njg.2018.18

Hintersberger, E., Iglseder, C., Schuster, R. & Huet, B., 2018. The new database "Tectonic Boundaries" at the Geological Survey of Austria. Jahrbuch Der Geologischen Bundesanstalt 157: 195-207.

Hintersberger, E., Van Ede, R. & Van Gessel, S., 2021. Fault Data Characterization Catalogue. Hazard and Impact Knowledge for Europe Report: 40 pp.

Hummelman, J., Maljers, D., Menkovic, A., Reindersma, R., Stafleu, J. & Vernes, R., 2019. Totstandkomingsrapport Digitaal Geologisch Model (DGM). TNO (Utrecht), Rapport No. R11653: 70 pp. https://www.broloket.nl/sites/default/files/Totstandkomingsrapport-DGM.pdf

Jayasena, R.M., 2020. Graaf- en modderwerk: Een archeologische stadsgeschiedenis van Amsterdam. University of Amsterdam.

pure.uva.nl/ws/files/43045800/11.pdf

Kint, L., Hademenos, V., De Mol, R., Stafleu, J., Van Heteren, S. & Van Lancker, V., 2020. Uncertainty assessment applied to marine subsurface datasets. Quarterly Journal of Engineering Geology and Hydrogeology 54: qjegh2020-028. DOI: 10.1144/qjegh2020-028

Kirsch, R. (ed.), 2009. Groundwater Geophysics – A Tool for Hydrogeology, 2nd ed. Springer Verlag (Berlin – Heidelberg): 548 pp. DOI: 10.1007/978-3-540-88405-7

Kombrink, H., Doornenbal, J.C., Duin, E.J.T., Den Dulk, M., Ten Veen, J.H. & Witmans, N., 2012. New insights into the geological structure of the Netherlands; results of a detailed mapping project. Netherlands Journal of Geosciences 91 (4): 419-446. DOI: 10.1017/S0016774600000329

Koster, K., Stafleu, J. & Stouthamer, E., 2018a. Differential subsidence in the urbanised coastal-deltaic plain of the Netherlands. Netherlands Journal of Geosciences 97 (4): 215-227. DOI: 10.1017/njg.2018.11

Koster, K., Stafleu, J., Cohen, K.M., Stouthamer, E., Busschers, F.S. & Middelkoop, H., 2018b. Three-dimensional distribution of organic matter in coastal-deltaic peat: Implications for subsidence and carbon dioxide emissions by human-induced peat oxidation. Anthropocene 22: 1-9. DOI: 10.1016/j.ancene.2018.03.001

Kruiver, P., Van Dedem, E., Romijn, R., De Lange, G., Korff, M., Stafleu, J., Gunnink, J.L., Rodriguez-Marek, A., Bommer, J.J., Van Elk, J. & Doornhof, D., 2017a. An integrated shear-wave velocity model for the Groningen gas field, The Netherlands. Bulletin of Earthquake Engineering 15: 3555-3580. DOI: 10.1007/s10518-017-0105-y

Kruiver, P.P., Wiersma, A., Kloosterman, F.H., De Lange, G., Korff, M., Stafleu, J., Busschers, F.S., Harting, R., Gunnink, J.L., Green, R.A., Van Elk, J. & Doornhof, D., 2017b. Characterisation of the Groningen subsurface for seismic hazard and risk modelling. Netherlands Journal of Geosciences 96 (5): s215-s233. DOI: 10.1017/njg.2017.11

Maljers - Oosterwijk, D., Vonhögen - Peeters, L., Van Heteren, S., Marges, V., Stafleu, J. & Wiersma, A., 2014. De update van het delfstoffeninformatiesysteem voor het NCP. Deltares (Utrecht), Report No. 1205135-002 (i.o.v Rijkswaterstaat Directie Noordzee): 31 pp.

Maljers, D., Stafleu, J., Van der Meulen, M.J. & Dambrink, R.M., 2015a. Advances in constructing regional geological voxel models, illustrated by their application in aggregate resource assessments. Netherlands Journal of Geosciences 94 (3): 257-270. DOI: 10.1017/njg.2014.46

Maljers, D., Ten Veen, J.H. & Den Dulk, M., 2015b. Description Uncertainty procedure DGM-deep. https://www.dinoloket.nl/en/digital-geological-model-dgm-deep

Pluymaekers, M.P.D., Doornenbal, J.C. & Middelburg, H., 2017. Velmod-3.1. TNO (Utrecht), Report No. 2017 R11014. https://www.nlog.nl/en/velmod-31

Rijksoverheid, 2002. Wet van 31 oktober 2002, houdende regels met betrekking tot het onderzoek naar en het winnen van delfstoffen en met betrekking tot met de mijnbouw verwante activiteiten. (Mining Act, effective May 2022.). wetten.overheid.nl/BWBR0014168/2022-05-01/0

Rijksoverheid, 2015. Wet van 30 september 2015, houdende regels omtrent de basisregistratie ondergrond (Key registry of the subsurface, effective May 2022). Retrieved from wetten.overheid.nl/BWBR0037095/2022-05-01/0

Robertson, P.K., 2010. Soil Behaviour Type from CPT: An Update. 2nd International Symposium on Cone Penetration Testing (Huntington Beach): 575-583.

Russell, H.A.J., Kemp, E.A. & MacCormack, K.E., 2019. Overview of Geological Survey Organizations Contributions on Modelling Approaches. In: K.E. MacCormack, R.C. Berg, H.A.J. Russell, H. Kessler & L.H. Thorleifson (eds): Synopsis of Current Three-Dimensional Geological Mapping and Modelling in Geological Survey Organizations. Alberta Energy Regulator / Alberta Geological Survey (AER/AGS), Special Report 112 (3): 7-18.

Sandersen, P.B.E., Kallesøe, A.J., Møller, I., Høyer, A.-S., Jørgensen, F., Pedersen, J.B. & Christiansen, A.V., 2021. Utilizing the towed Transient ElectroMagnetic method (tTEM) for achieving unprecedented near-surface detail in geological mapping. Engineering Geology 288: 106125. DOI: 10.1016/j.enggeo.2021.106125

Schokker, J., Bakker, M.A.J., Dubelaar, C.W., Dambrink, R.M. & Harting, R., 2015. 3D subsurface modelling reveals the shallow geology of Amsterdam. Netherlands Journal of Geosciences 94 (4): 399-417. DOI: 10.1017/njg.2015.22

Sobisch, H.-G., 2011. One Viewer to Publish 3D Subsurface Models of any Modelling Origin. Abstracts with Programs: GSA Annual Meeting (Minneapolis, Minnesota): 525.

Stafleu, J. & Busschers, F.S., 2017. Analysing Lithological and Grain-Size Trends using a 3D Voxel Model: A Case Study from the Holocene Rhine-Meuse Delta. 79th EAGE Conference & Exhibition, (Paris, France), Workshop Programme: 12-15.

Stafleu, J. & Dubelaar, C.W., 2016. Product Specification Subsurface model GeoTOP. TNO (Utrecht), Report No. 2016 R10133 v1.3: 53 pp.

Stafleu, J., Hummelman, J., De Bruijn, R., Koster, K., Stam, J., Maljers, D. & Schokker, J., 2020. Totstandkomingsrapport GeoTOP - met nieuwe methodiek lagenmodellering, TNO (Utrecht), Report No. 2020 R10758. https://www.broloket.nl/toelichting/geotop

Stafleu, J., Kraaijpoel, D.A. & Osinga, S., 2022. Ideation Challenge 2020: RHINOCEROS: Regional Shear-wave velocity modelling for seismic site Response – Final scientific report. TNO (Utrecht), Report No. 2022 R10324: 21 pp.

Stafleu, J., Maljers, D., Busschers, F.S., Gunnink, J.L. & Vernes, R.W., 2011a. TNO – Geological Survey of the Netherlands: 3-D Geological Modeling of the Upper 500 to 1,000 Meters of the Dutch Subsurface. In: Berg, R.C., Mathers, S.J., Kessler, H. & Keefer, D.A. (eds): Synopsis of Current Three-dimensional Geo-

logical Mapping and Modeling in Geological Survey Organizations. Illinois State Geological Survey Circular 578: 64-68.

Stafleu, J., Maljers, D., Gunnink, J.L. & Busschers, F.S., 2011b. 3D modelling of the shallow subsurface of Zeeland, the Netherlands. Netherlands Journal of Geosciences 90 (4): 293-310. DOI: 10.1017/S0016774600000597

Stafleu, J., Maljers, D., Busschers, F.S., Schokker, J., Gunnink, J.L. & Dambrink, R.M., 2021a. Models Created as 3-D Cellular Voxel Arrays. In: Turner, A.K., Kessler, H. & Meulen, M.J. (eds): Applied Multidimensional Geological Modeling. DOI: 10.1002/9781119163091.ch11

Stafleu, J., Maljers, D. & Gunnink, J.L., 2021b. Visualisation of uncertainty in voxel models of the shallow subsurface of the Netherlands. Workshop Uncertainty Quantification and Visualization in Geological Modelling, Presented at EAGE Annual Conference (Amsterdam, The Netherlands).

Stafleu, J., Sobisch, H.-G., Maljers, D., Hummelman, J., Dambrink, R.M. & Gunnink, J.L., 2013. Visualization and dissemination of 3D geological property models of the Netherlands. Presented at 2013 Annual Meeting of the Geological Society of America (Denver, Colorado, USA).

Stafleu, J., Van der Meulen, M.J., Gunnink, J.L., Maljers, D., Hummelman, J., Busschers, F.S., Schokker, J., Vernes, R.W., Doornenbal, H., Den Dulk, M. & Ten Veen, J.H., 2019. Systematic 3D subsurface mapping in the Netherlands. In: K.E. MacCormack, R.C. Berg, H.A.J. Russell, H. Kessler & L.H. Thorleifson (eds): Synopsis of Current Three-Dimensional Geological Mapping and Modelling in Geological Survey Organizations. Alberta Energy Regulator / Alberta Geological Survey (AER/AGS), Special Report 112 (3): 179-190.

Swierstra, W., Kerckhoffs, T. & Horn, A., 2018. Aanpassingen en kalibratie stationair model IBRAHYM 2.1, Zuid-Limburg. WAT-BF6136R001F01, Royal Haskoning DHV (Maastricht).

Ten Veen, J.H., 2021. Final fault data collection report and database: Annex 1. Hazard and Impact Knowledge for Europe Report: 329 pp.

ThermoGIS., 2022. ThermoGIS V2.1. https://www.thermogis.nl/en

TNO-GDN, 2022a. Delfstoffen Informatie Systeem, TNO – Geologische Dienst Nederland. https://www.dinoloket.nl/dis

TNO-GDN, 2022b. Stratigraphic Nomenclature of the Netherlands, TNO – Geological Survey of the Netherlands. https://www.dinoloket.nl/en/stratigraphic-nomenclature

TNO-NITG, 2004. Geological Atlas of the Subsurface of the Netherlands - onshore. Netherlands Institute of Applied Geoscience TNO (Utrecht): 104 pp.

Unidata, 2022. Network Common Data Form (NetCDF). https://www.unidata.ucar.edu/software/netcdf/

Van Balen, R.T., Bakker, M.A.J., Kasse, C., Wallinga, J. & Woolderink, H.A.G., 2019. A Late Glacial surface rupturing earthquake at the Peel Boundary fault zone, Roer Valley Rift System, the Netherlands. Quaternary Science Reviews 218: 254-266. DOI: 10.1016/j.quascirev.2019.06.033

Van Balen, R.T., Kasse, C., Wallinga, J. & Woolderink, H.A.G., 2021. Middle to Late Pleistocene faulting history of the Heerlerheide fault, Roer Valley Rift System, influenced by glacio-isostasy and mining-induced displacement. Quaternary Science Review 268: 107111. DOI: 10.1016/j.quascirev.2021.107111

Van Dalfsen, W., Mijnlieff, H.A. & Simmelink, E., 2005. Interval velocities of a Triassic claystone: key to burial history and velocity modeling. Poster 178 presented at 67th EAGE Conference & Exhibition (Madrid, Spain).

Van der Meulen, M.J. & Bogaard, P.J.F., 2022. Medium-term Plan 2022-2025 (MLTP25). TNO – Geological Survey of the Netherlands. (Utrecht, Netherlands): 29 pp.

Van der Meulen, M.J., Dijkstra, J.J., Koopmans, T.P.F., Pietersen, H.S., Stam, J. & Maljers, D., 2025. Surface Mineral Resources. In: J.H. Ten Veen, G.-J. Vis, J. De Jager & Th.E. Wong (eds): Geology of the Netherlands, second edition. Amsterdam University Press (Amsterdam): 679-699. DOI: 10.5117/9789463728362_ch18

Van der Meulen, M.J., Doornenbal, J.C., Gunnink, J.L., Stafleu, J., Schokker, J., Vernes, R.W., Van Geer, F.C., Van Gessel, S.F., Van Heteren, S., Van Leeuwen, R.J.W., Bakker, M.A.J., Boogaard, P.J.F., Busschers, F.S., Griffioen, J., Gruijters, S.H.L.L., Kiden, P., Schroot, B.M., Simmelink, H.J., Van Berkel, W.O., Van der Krogt, R.A.A., Westerhoff, W.E. & Van Daalen, T.M., 2013. 3D geology in a 2D country: perspectives for geological surveying in the Netherlands. Netherlands Journal of Geosciences 92 (4): 217-241. DOI: 10.1017/S0016774600000184

Van der Meulen, M.J., Kessler, H., Ten Veen, J.H., Vernes, R.W. & Maljers, D., 2022. Diving into the energy transition. In: Berg, R.C., Thorleifson, L.H. & MacCormack, K.E. (eds): Three-Dimensional Geological Mapping: Workshop Extended Abstracts. Illinois State Geological Survey (Champaign, IL): 51-54.

Van der Meulen, M.J., Kiden, P., Maljers, D., Stafleu, J., Vernes, R.W., Gunnink, J.L., Westerhoff, W.E. & Van Daalen, T.M., 2015. Systematic Geomodeling: What Does It Actually Imply? (MacCormack, K. E., Thorleifson, L. H., Berg, R. C. & Russel, H. A. J. (eds). Alberta Energy Regulator (Edmonton, AL): 83-88.

Van der Meulen, M.J., Van Gessel, S.F. & Veldkamp, J.G., 2005. Aggregate resources in the Netherlands. Netherlands Journal of Geosciences 84: 379-387. DOI: 10.1017/S0016774600021193

Van Ginkel, J., Ruigrok, E., Stafleu, J. & Herber, R., 2022. Development of a seismic site-response zonation map for the Netherlands. Natural Hazards and Earth System Sciences 22: 41-63. DOI: 10.5194/nhess-22-41-2022

Van Lancker, V., Francken, F., Kapel, M., Kint, L., Terseleer, N., Van den Eynde, D., Hademenos, V., Missiaen, T., De Mol, R., De Tré, G., Appleton, R., Van Heteren, S., Van Maanen, P.-P., Stafleu, J., Stam, J., Degrendele, K. & Roche, M., 2019. Transnational and Integrated Long-term Marine Exploitation Strategies (TILES). Final Report. Belgian Science Policy (Brussels): 75- pp.

Van Waterschoot van der Gracht, W.A.J.M., 1918. Eindverslag over de onderzoekingen en uitkomsten van den Dienst der Rijksopsporing van Delfstoffen in Nederland 1903-1916. Martinus

Nijhoff ('s Gravenhage): 664 pp.
Vermeulen, P., Roelofsen, F. & Veldhuizen, A., 2015. Actualisatie en Kalibratie IBRAHYM Beschrijving activiteiten t.b.v IBRAHYM v2.0 (in Dutch), Deltares (Utrecht), Report No. 1206858-000-BGS-0022: 38 pp.
Vermeulen, P., van der Linden, W., Veldhuizen, A., Massop, H., Vermulst, H. & Swierstra, W., 2007. IBRAHYM Grondwater Modelinstrumentarium Limburg. TNO (Utrecht), Report No. 2007-U-R0193/B: 126 pp.
Vernes, R.W., Dabekaussen, W., Gunnink, J.L., Harting, R., De Heer, E., Hummelman, J.H., Menkovic, A., Reindersma, R. & Van der Ven, T.J.M., 2021. Application Theme 2 – Groundwater Evaluations – Case Study 19.4: REGIS II – A 3-D Hydrogeological Model of the Netherlands. In: Turner, A.K., Kessler, H. & Meulen, M.J. (eds): Applied Multidimensional Geological Modeling. DOI: 10.1002/9781119163091.ch19
Vernes, R.W. & Van Doorn, Th.H.M., 2005. Van Gidslaag naar Hydrogeologische Eenheid – Toelichting op de totstandkoming van de dataset REGIS II. TNO (Utrecht), Report NITG 05-038-B: 105 pp.
Verweij, H., Zaadnoordijk, W.J., Oude Essink, G.H.P. & Hartog, N., 2025. Hydrogeology. In: Ten Veen, J.H., Vis, G.-J., De Jager, J. & Wong, Th.E. (eds): Geology of the Netherlands, second edition. Amsterdam University Press (Amsterdam): 627-677. DOI: 10.5117/9789463728362_ch17
Wellmann, J.F. & Regenauer-Lieb, K., 2012. Uncertainties have a Meaning: Information Entropy as a Quality Measure for 3-D Geological Models. Tectonophysics 526-529: 207-216. DOI: 10.1016/j.tecto.2011.05.001
Westerhoff, W.E., Wong, Th.E. & De Mulder, E.F.J., 2003. Opbouw van de ondergrond. In: De Mulder, E.F.J., Geluk, M.C., Ritsema, I.L., Westerhoff, W.E. & Wong, Th.E. (eds): De ondergrond van Nederland. Wolters-Noordhoff (Groningen/Houten): 247-352.
Zehner, B., Ayala, C., Bense, F., Dabekaussen, W., Den Dulk, M., Franek, J., Pueyo, E.L., Malz, A., Müller, C.O. & Stück, H., 2021. Sources of uncertainty in 3D geomodels. 3D Geomodeling for Europe Report (Project number GeoE.171.005). 64 pp.